MICROBIOLOGICALLY INFLUENCED CORROSION OF 1018 CARBON STEEL IN STATIC SEAWATER/FUEL (PETROLEUM-BASED AND RENEWABLE) MIXTURES

A THESIS SUBMITTED TO THE GRADUATE DIVISION OF THE
UNIVERSITY OF HAWAIʻI AT MĀNOA IN PARTIAL FULFILLMENT
OF THE REQUIREMENTS FOR THE DEGREE OF

MASTER OF SCIENCE

IN

MICROBIOLOGY

AUGUST 2017

By

Jan A. N. Kealoha

Thesis Committee:

Stuart Donachie, Chairperson
Lloyd Hihara
Anne Alvarez

Keywords: Microbiologically-Influenced Corrosion (MIC), 1018 carbon steel, Diesel, F-76, HRD, Tubercle

Acknowledgements

I am extremely grateful for…

… the support of the Hawai‘i Natural Energy Institute (HNEI) for funding this project though the Asia Pacific Research Initiative for Sustainable Energy Systems (APRISES), which is a grant from the U.S. Naval Research Laboratory (award number N00014-13-1-0463), particularly Dr. Scott Turn of HNEI.

... Dr. Shengxi Li for the long hours/days/months of corrosion analysis (XRD, Raman, FTIR, SEM, and EDXA).

… Drs. Anthony Amend and Richard O'Rorke for their guidance with Illumina sequencing.

… Hawai‘i Ocean Time-series Program, especially Susan Curless and Brett Updyke

… Aaron Toyama and Gavin Taketa of the UH College of Engineering Machine Shop for cutting over 700 steel coupons and moving my samples around with the forklift.

… The Hawai‘i Corrosion Lab members for their support; especially Ryan Sugamoto, Daniel Hong, Jeff Nelson, Raghu Srinivasan and Corey Kaneshiro for all the extra helping hands and advice to keep me sane.

… Undergraduate students: Alex Park, Andrew Rogitz, Kate Quiambao, Justin Shortell, James Miller, Shekinah Eugenio, Jenna Maligro, Ashlyn Tanaka who helped process my samples.

…My Thesis committee, Drs. Stuart Donachie, Lloyd Hihara and Anne Alvarez, for their guidance, patience and enthusiasm that got me though the massive undertaking of this project.

I would also like to thank my friends and family for all their love, encouragement and patience. Sorry everyone, clearly, I was on Hawaiian time.

Lastly, I couldn’t have done it without my husband Ko. Thank you for all the delivered meals, late night pickups, long minutes waiting for me outside the building while I finished up at my desk even though you called me 45 minutes ago to tell me you were coming to get me.

Abstract

Microbiologically influenced corrosion of steel was compared to electrochemical corrosion in multiple fuel and seawater combinations. Corrosion rates were higher in Hydro-processed Renewable Diesel (HRD) compared to petroleum-based F-76 (0.035 vs. 0.016 mm/year, respectively) and were higher under aerobic than anaerobic conditions. No significant differences in types of corrosion products, oxygen diffusion, or pH, were observed when comparing natural vs filtered seawater. White carbonates and magnesium hydroxide precipitates were predominantly formed in HRD, whereas red goethite formed in F-76. In the seawater phase, magnetite (black) formed, typically under a layer of orange lepidocrocite. Rust tubercles formed on steel surfaces in the fuel phase of 59% of all samples resulting in corrosion pits on the underlying metal. The HRD and blended fuel contained more rust tubercles, regardless of exposure time. Microbes associated with accelerated corrosion rates were taxonomically assigned on the basis of their partial 16S or ITS1 rRNA gene sequences.

Table of Contents

List of Tables

List of Figures

List of Abbreviations & Symbols

In order of appearance in text

MIC	**M**icrobiologically **I**nfluenced **C**orrosion
1018	UNS G**1018**0 (Unified Numbering System) G carbon & alloyed steels
F-76	Marine Diesel NATO **F-76**, naval distillate **F-76**
HRD	**H**ydro-treated **R**enewable **D**iesel
Blend	50:50 v/v **blend** of F-76: HRD
RIMPAC	"**Rim** of the **Pac**ific" International Naval exercise
ASTM	**A**merican **S**ociety for **T**esting and **M**aterials
FAME	**F**atty **A**cid **M**ethyl **E**sters
CDT	**C**athodic **D**epolarization **T**heory
EPS	**E**xtracellular **P**olymeric **S**ubstances
IOB	**I**ron-**O**xidizing **B**acteria
SRB	**S**ulfate-**R**educing **B**acteria
MCE	**M**ixed **C**ellulose **E**ster
SW	**S**ea **W**ater
ALOHA	**A L**ong-**T**erm **O**ligotrophic **H**abitat **A**ssessment
HOT	**H**awai'i **O**cean **T**ime-series
N	**N**atural, unaltered from time of collection
S	**S**terile filtered through 0.22µm membrane filter
V	**V**ented, aerobic filtered through 0.22 µm membrane in grey cap
T	**T**ightened, anaerobic, solid orange cap
O	**O**pen, aerobic, uncapped bottle
NCB	**N**egative **C**ontrol **B**ottle
DO	**D**issolved **O**xygen
TAN	**T**otal **A**cid **N**umber
ISO	**I**nternational **O**rganization for **S**tandardization
CR	**C**orrosion **R**ate
XRD	**X**-**R**ay **D**iffraction

FTIR	**F**ourier **T**ransform **I**nfrared **S**pectroscopy
ESEM	**E**nvironmental **S**canning **E**lectron **M**icroscopy
EDXA	**E**nergy **D**ispersive **X**-**R**ay **A**nalysis
MA	**M**arine **A**gar 2216 culture medium
TSA	**T**rypticase **S**oy **A**gar culture medium
R2A	**R**easoner's **2** **A**gar culture medium
SAPI	**S**ulfate **A**merican **P**etroleum **I**ndustry culture medium
BH	**B**ushnell **H**aas culture medium
PDA	**P**otato **D**extrose **A**gar culture medium
DNA	**D**eoxyribo**n**ucleic **A**cid
PCR	**P**olymerase **C**hain **R**eaction
RNA	**R**ibonucleic **A**cid
18S	A component of the 40S small ribosomal subunit in eukaryotes
16S	A component of the 30S small ribosomal subunit in prokaryotes
BLAST	**B**asic **L**ocal **A**lignment **S**earch **T**ool
ITS-1	**I**nternal **T**ranscribed **S**pacer region 1. Between the 18S and 5.8S rRNA genes in eukaryotes
OTU	**O**perational **T**axonomic **U**nit

Chapter 1. Introduction

1.1 Objectives of this study

The proposed utilization of biofuels in Navy ships requires that we not only understand how safe biofuels are in terms of security of supply and storage, but also how they might affect plain carbon steels used in ship ballast tanks and fuel lines (*Diesel fuel storage and handling guide*, 2014). For example, could the replacement of conventional petroleum-based fuels with alternative biofuels result in unexpected corrosion-induced failures? Hence, any significant differences in performance of storage systems that may occur when replacing petroleum-based fuels with pure biofuels or blended bio-petroleum fuels should be determined. This is a matter of national security, given how the reliability of fuel supplies and storage systems for the military may be affected, as well as the potential impacts on the integrity and safety of the nation's energy supplies.

Electrochemical (or abiotic) corrosion plays a leading role in metal deterioration, especially in a marine or other high-salt environment. However, corrosion can also be caused, enhanced or accelerated by biological processes. This is known in industry as microbiologically-influenced corrosion (MIC), or biocorrosion. Here, MIC of steel was compared to electrochemical corrosion in an alternative fuel and seawater combination. The corrosion behavior of UNS G10180 plain-carbon steel in blended seawater-fuel mixtures was thus evaluated at various intervals for one year, as follows: i) in natural and synthetic seawaters; ii) under aerobic and anaerobic conditions; and iii) with and without naturally-occurring microbes. Fuels investigated were petroleum-diesel naval distillate F-76, green-diesel HRD, and a 50%-50% blend of F-76 and HRD. In addition to physical analysis of corrosion products, both molecular, *i.e.*, DNA-based, and cultivation methods were used to gain insight into how microbial diversity may impact diesel fuels and fuel system infrastructure.

1.2 Background

The increased production of fuels from non-traditional sources in recent decades rests in the strategic value of lowering the reliance of the United States upon foreign oil sources (Bartis & Lawrence Van Bibber, 2011). In fiscal year 2011, the Department of Defense spent $17.3 billion

on petroleum-based fuels, 28% of which was used by the U.S. Navy (Craig, 2011; Schwartz, et.al., 2012). In 2009, Secretary of the Navy Ray Mabus presented five energy goals to reduce the Department of the Navy's energy consumption by off-setting reliance on foreign sourced oil with alternative energy (ONR, 2012). One of the goals included demonstrating (during the "Rim of the Pacific" [RIMPAC] 2012 exercise) and deploying a "Great Green Fleet" in 2016. This fleet would comprise ships and aircraft using alternative energy. Navy surface ships in the RIMPAC demonstration thus used an advanced biofuel, specifically Hydro-processed Renewable Diesel (HRD) blended in equal parts with NATO Fuel-76 (F-76). Operations using this 50/50 diesel blend were comparable to traditional F-76 during RIMPAC-2012. However, studies must be conducted to examine the effects any alternative fuel or blend will have on industrial infrastructure, especially if the fuel is to be used as a "drop in" replacement (ONR, 2012), as HRD is meant to be.

Compensated fuel ballast systems are common aboard large ships because they allow for better utilization of the limited space below deck (Craig, 2011). In these systems, natural seawater replaces fuel consumed to help maintain vessel stability, but in doing so introduces chlorides and marine microbes, either of which can have severe effects on fuel, such as degradation, and accelerate corrosion of the fuel system (Craig, 2011). Depending on ship size, ballast tanks can range between 1 and 200,000 m^3, with inner surface areas up to 1.5 million to 7 million m^2 (Heyer et al., 2013). The use of natural seawater introduces nutrients, chlorides and live organisms, which can adversely affect the inner surfaces of the fuel tanks. Although, most shipboard metal is treated for mitigation of corrosion, usually with some type of environmentally-protective coating, no coating or treatment will work indefinitely. Coating imperfections or deterioration, premature or not, will eventually expose the base metal to corrosive environmental conditions. Typical corrosion rates for carbon steel can range from 0.01 to 0.1 mm/year in a marine atmosphere, *i.e.*, one with a significant concentration of chlorides in the air, but without water acting as a direct electrolyte, ~0.1 mm/year in quiescent seawater, and ~0.8 mm/year with seawater at a flow rate of 4 m/sec (Francis, 2012).

Chapter 2. Literature Review

2.1 Diesel fuel

2.1.1 Petroleum diesel

Petroleum diesel, a.k.a. petrodiesel, diesel fuel, or diesel, is the product of the fractional distillation of crude oil between 200°C and 350°C (392-662°F) at atmospheric pressure, resulting in a mixture of carbon chains of 8-21 carbon atoms long (Yoon, 2009). The "Standard Specification for Diesel Fuel Oils" is defined in American Society for Testing and Materials (ASTM) standard D975 (https://www.astm.org/Standards/D975.htm).

2.1.2 Biodiesel

Biodiesels are fatty acid methyl esters (FAME) produced in a transesterification process, that in which vegetable oils or animal fats catalytically react with short-chained aliphatic alcohols, typically methanol or ethanol (Knothe, 2010; Yoon, 2009). Biodiesel is defined in ASTM standard D6751 (https://www.astm.org/Standards/D6751) as a fuel that is comprised of mono-alkyl esters of long-chain fatty acids. The presence of oxygen and the carbon-carbon double bond categorizes biodiesels as chemically different from regular diesel.

2.1.3 Petrodiesel-like fuel

Petrodiesel-like fuel, often called "green diesel" or "renewable diesel", is produced from vegetable oils and/or animal fats using a hydrodeoxygenation process that uses hydrogen to remove oxygen and saturate the carbon-carbon double bonds, making it chemically similar to petroleum diesel. Petrodiesel-like fuel can also be derived from recently living biomass (Knothe, 2010; Yoon, 2009).

2.2 Seawater

Iron is essential for life in the ocean, as a component of cytochromes in the electron transport chain, as well as components of nitrate reductase and nitrogenase in the nitrogen cycle (Weinberg, 1989). In oligotrophic areas in which large ships often take on ballast water, iron is considered a limiting micronutrient only available to the surface water through atmospheric deposition and/or upwelling (Duce & Tindale, 1991). Therefore, any organism introduced into a

poorly maintained ballast tank may be able to scavenge the iron from the steel, which could ultimately result in failure of the tank through corrosion.

2.3 Mild steel

Low carbon steel offers the appropriate range of desirable properties for use in large scale industrial applications, such as strength, toughness, ductility, and weldability (Trench & Kiefner, 2001). The wide availability and low-initial cost of mild steel has made it a widely used material in global infrastructure (Suflita, 2013). Mild steel is considered a low-initial cost alloy because it is inexpensive and relatively easy to use in construction, although without the proper protections it can become very costly to maintain. High quality coatings and/or cathodic protection are typical ways to prevent premature failure (Francis, 2012). Mild steel also permits adhesion of greater numbers of microbial cells than do high-priced stainless steels (Gaylarde & Beech, 1988; Usher, Kaksonen, Cole, & Marney, 2014).

2.4 Corrosion

Corrosion causes significant direct and indirect losses to industry worldwide (Hays, 2013; Welikala, Singh, Gates, & Panter, 2012). It has been estimated that the direct cost of corrosion in the United States exceeds 3% of the country's gross domestic product, or $276 billion annually (Koch, Brongers, Thompson, Payer, & Virmani, 2002). As of 2014, however, the World Bank listed the USA's gross domestic product as $17.4 trillion, of which 3% is $522 billion in direct costs alone. Not taken into account are the indirect costs of corrosion, such as environmental damage and clean up, waste of resources, loss of production, or personal injury as a result of failure due to corrosion (Hays, 2013).

Typical electrochemical (abiotic) corrosion involves an electrode immersed in an electrolyte and the movement of electrons from anodic to cathodic sites which degrades the metal electrode. Due to localized variations, anodic and cathodic regions are always present on the steel surface (Witherby & Co. Ltd., 2002). In an aerated environment, oxygen can be reduced at the cathode (1), causing iron dissolution at the anode (2) (Revie & Uhlig, 2008). If chlorides are present in the electrolyte, the positively charged iron released into solution can form a highly soluble salt, $FeCl_2$ (3) that will precipitate on the metals' surface.

$$O_2 + 2H_2O + 4e^- \rightarrow 4OH^- \quad (1)$$

$$2e \rightarrow Fe^{2+} + 2e^- \quad (2)$$

$$Fe^{2+} + 2Cl^- \rightarrow FeCl_{2(aq)} \leftrightarrow FeCl_{2(s)} \quad (3)$$

In an oxygen-free/anoxic environment, hydrogen evolution at the cathode (4) can occur, creating excess hydrogen that can react with chloride ions to form hydrochloric acid (5), which in turn can further corrode the metal surface.

$$2H_2O + 2e^- \rightarrow H_2 + 2OH^- \quad (4)$$

$$H_2 + 2Cl^- \rightarrow 2HCl \quad (5)$$

Uniform and localized corrosion are the typical types of corrosion that affect mild steel (Revie & Uhlig, 2008). The former causes a gradual decrease in the metal's strength as the entire surface corrodes at a uniform rate, whereas localized corrosion (*i.e.*, pitting) will cause a penetrating pit in the metal due to higher corrosion rates at a localized site. Corrosion rates of iron are typically controlled by the cathodic reaction, and are in general much slower (Revie & Uhlig, 2008). Anodic dissolution of metal is spurred on by the cathodic consumption of electrons, most notably by either oxygen reduction by hydrogen in aerated conditions (1), or hydrogen evolution in anaerobic conditions (4).

2.5 Scaling

The formation of various precipitates in liquid media or on surfaces can enhance or retard corrosion. However, iron oxides will typically form on the metal surface and provide a buffer zone, or passivation layer, within pH range of the electrolyte being about 4-10, thereby limiting further corrosion (Revie & Uhlig, 2008). If the electrolyte (*i.e.*, seawater) was originally nearly saturated with carbonates, the corrosion process can supersaturate the water to cause excessive carbonate deposition (Olsen & Szybalski, 1949). This deposition is known as scaling. Carbonate scales therefore can limit corrosion by acting as a passivation layer (Nergaard & Grimholt, 2010). Examples of scale constituents in deposition reactions include:

Carbonic acid:

$$CO_2 + H_2O \leftrightarrow H_2CO_3 \quad (6)$$

$$H_2CO_3 + H_2O \leftrightarrow HCO_3^- + H^+ \quad (7)$$

$$HCO_3^- \leftrightarrow CO_3^{2-} + H^+ \quad (8)$$

Iron carbonate:

$$Fe + H_2CO_3 \leftrightarrow FeCO_3 + H_2 \quad (9)$$

Calcium carbonate at the cathode:

$$Ca^{2+} + HCO_3^- + OH^- \rightarrow H_2O + CaCO_3 \quad (10)$$

Sodium carbonate at the cathode:

$$2Na^{2+} + HCO_3^- + OH^- \rightarrow H_2O + Na_2CO_3 \quad (11)$$

Magnesium hydroxide at the cathode:

$$Mg^{2+} + 2OH^- \rightarrow 2MgOH \quad (12)$$

$$2MgOH \rightarrow 2MgO + H_2 \quad (13)$$

2.6 MIC / Biocorrosion

It is estimated that about 50% of the costs resulting from corrosion are due to MIC (Javed et al., 2012; Passman, 2013). MIC involves the corrosion of materials, usually metallic, caused directly or promoted by microorganisms (Little & Lee, 2007). More specifically, it is any biological process that either facilitates or impedes one of the anodic or cathodic reactions, or that permanently separates the anodic/cathodic sites on a material surface, thus increasing or inhibiting corrosion (Videla & Herrera, 2005). Many studies have implicated MIC as the source of localized corrosion *via* pitting, de-alloying, erosion corrosion, enhanced galvanic corrosion, stress corrosion cracking and hydrogen embrittlement (Javed et al., 2012; Patil, Choudhary, & Singh, 2012). High biocorrosion rates on stainless steel in the range of mm/year have been observed, which is much higher than that expected by abiotic corrosion, which are typically 100 times less per year (Javed et al., 2012).

Many microorganisms are able to utilize hydrocarbons, including over 75 *Bacteria* genera, and 100 fungal genera (Prince, 2005). Fungi are capable of excreting extracellular enzymes or proteins that could aid the initial metabolism of hydrocarbons (van Beilen & Witholt, 2005). In oil field water reservoirs, microbial cell densities can range from a few cells to 10^6 cells per milliliter (Magot, 2005).

The Cathodic Depolarization Theory (CDT) was proposed in 1934 by von Wolzogen Kuhr and van der Flugt which focused on the conversion of the cathodic hydrogen to H^+ in solution,

equation (20) (Javed et al., 2012; Majumder & Singh, 2012; Videla & Herrera, 2005; von Wolzogen Kuhr & van der Vlugt, 1934). Equations (14) through (19), listed below, shows how the freed H^+ ion (14)would then reduce the sulphate (SO^{-4}) to sulphide (S^-) allowing iron (II) sulphide (FeS) to form (Singh, Sharma, & Lata, 2008):

$$8H_2O \rightarrow 8OH^- + 8H^+ \quad (14)$$

$$4Fe \rightarrow 4Fe^{2+} + 8e \text{ (anode)} \quad (15)$$

$$8H^+ + 8e \rightarrow 8\,H \text{ (cathode)} \quad (16)$$

$$SO_4^{2-} + 8H \xrightarrow{(bacteria)} S^{2-} + 4H_2O \text{ (cathodic deploarization)} \quad (17)$$

$$Fe^{2+} + S^{2-} \rightarrow FeS \text{ (anode)} \quad (18)$$

$$3Fe^{2+} + 6OH^- \rightarrow 3Fe(OH)_2 \text{ (anode)} \quad (19)$$

$$4Fe + SO_4^- + 4H_2O \rightarrow FeS + 3Fe(OH)_2 + 2OH^- \quad (20)$$

Many amendments to the CDT were proposed as biocorrosion research progressed in the 1960s. Since the 1980s especially, it has become widely accepted that any metal in contact with an environment in which there is microbial growth will corrode to some degree, either by direct microbial action, or indirectly through the release of corrosive metabolites (Eidsa, 1988). Microbes such as *Bacteria*, *Archaea*, *Fungi* and eukaryotic photoautotrophs, cf. algae, can decrease or increase electrochemical corrosion rates (Javed et al., 2012). For example, microbially mediated iron dissolution rates can be as much as 6-8 times greater than abiotic reactions alone (Edwards et al., 2004). The most widely accepted theory about the mechanism of MIC is based on the role that extracellular polymeric substances (EPS) produced by bacteria in biofilms have on creating metal complexes with byproducts of oxidation reactions (Singh et al., 2008; Patil et al., 2012; Welikala et al., 2012).

The first step in understanding the roles that microbes play in corrosion is to identify those responsible for changes in both the type and concentration of ions present in the medium, and for changes in pH and oxidation-reduction potentials on a corroding surface. In the establishment of a corrosive biofilm, iron-oxidizing bacteria (IOB) colonize the surface with other EPS-producing microbes. IOB are microaerophilic, occupying the transition zone between aerobic and anaerobic regions (Figure 1a), and obtaining energy directly through the oxidation of ferrous iron (Fe^{2+}) to ferric iron (Fe^{3+}), often leading to the formation of thick layers of iron oxides (Little, Lee, & Ray, 2011; Obuekwe, Donald, Cook, & William, 1981). Metal dissolution occurs at an

anodic site on the metal surface coupled to electron uptake by an acceptor at a cathodic site (Hamilton, 1998). The localized anodic region where the iron is being oxidized, called a corrosion pit, releases metal cations into the seawater typically forming or adding to insoluble iron oxide layers over the metal surface (Ray, Lee, & Little, 2010). These deposits can accumulate into a structurally complex rust tubercle (Figure 1b) which is fundamentally caused by a differential aeration cell (Eidsa, 1988; Herro, 1998; Olsen & Szybalski, 1949; Usher, Kaksonen, Cole, et al., 2014). Oxygen gradients form as the iron oxides slow the rate of oxygen diffusion from the outter to inner corrosion product layers of the tubercle wall (Usher, Kaksonen, & MacLeod, 2014). These anaerobic pockets become ideal habitat for sulfate-reducing bacteria (SRB) colonization (Figure 1b). SRB are anaerobic *Bacteria* and *Archaea* that use sulfate as a terminal electron acceptor in the dissimilatory reduction to sulfide (Muyzer & Stams, 2008). They have an indirect role in MIC because it is their production of intermediate metabolites such as thiosulfates, polythionates and of the final metabolites such as sulfides, bisulfides, and hydrogen sulfide, that is corrosive to mild steel (Videla & Herrera, 2005). For example, hydrogen sulfide reacts with Fe(II) to generate FeS, which then goes on to form pyrite (FeS_2) which can be oxidized (Varnam & Malcolm, 2000). In addition to microbial metabolites, charged ions such as chlorides, sulfates and carbonates from the surrounding seawater also migrate toward the anodic pit to neutralize the built up charge, forming extremely corrosive acids (*e.g.*, iron(III) chloride [which is acidic when dissolved in water] and hydrochloric acid), which lower the pH in the tubercule (Figure 1c) and further corrode the steel (Ray et al., 2010).

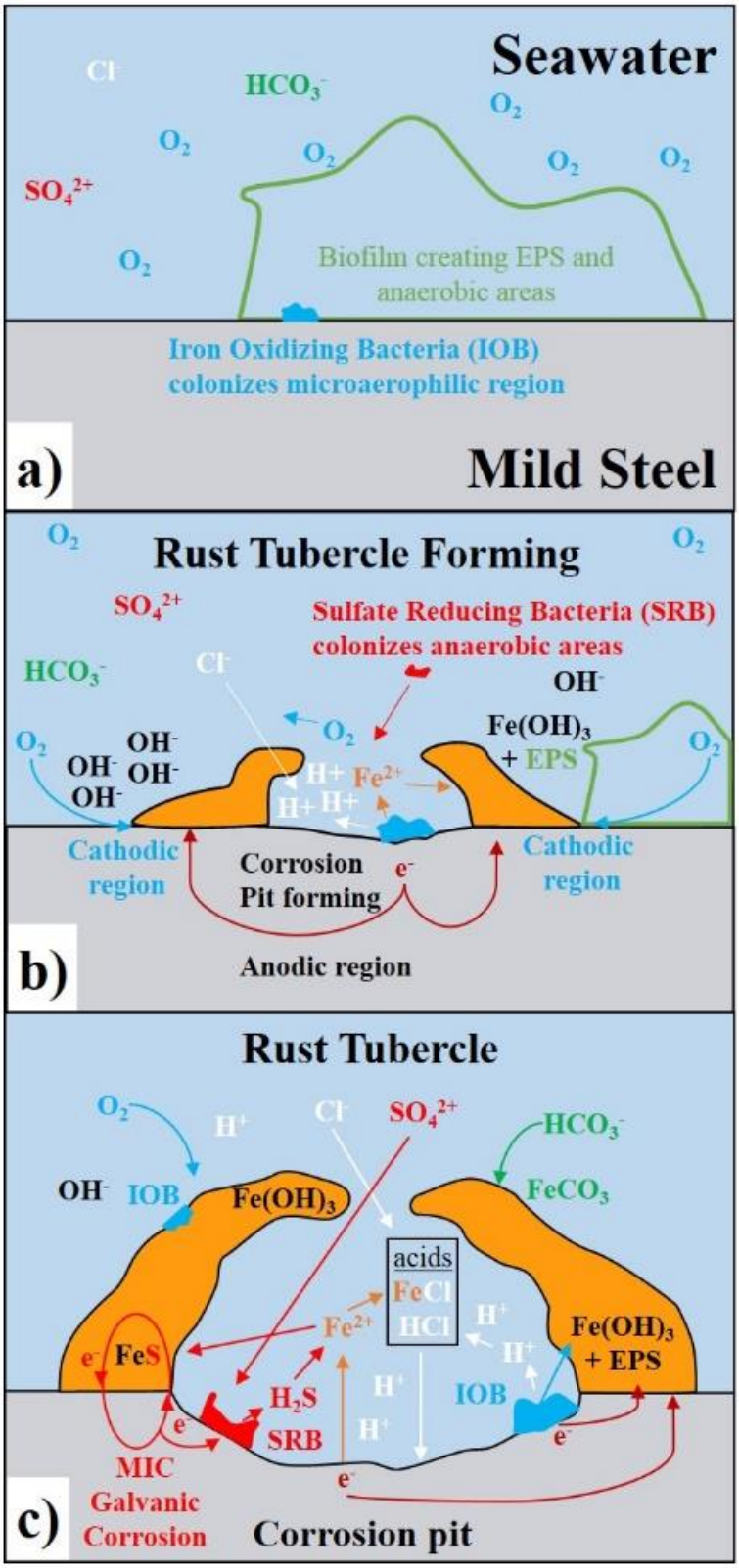

Figure 1. Rust tubercle formation (a-c) on mild carbon steel immersed in seawater via electrochemical and microbial corrosion. Modified from (Advanced Materials Association, n.d.; Herro, 1998).

Chapter 3. Materials and Methods

3.1 Sample material selection

3.1.1 Fuel selection

The fuels used in this study was selected on the basis of need by the United States Navy, and because they satisfied the specifications defined in MIL-DLT-16884L ("Fuel, Naval Distillate," 2006) for NATO F-76 (Fu & Turn, 2015). Two such diesel fuels were provided by the U.S. Navy Supply Center at Patuxent River, MD through Dr. Scott Turn of the Hawai'i Natural Energy Institute at the University of Hawai'i at Mānoa. Three fuels were used: F-76, HRD, and a 50:50 blend of F-76 and HRD. To compare biotic and abiotic effects of the fuels on corrosion, 50% of each fuel type was passed through mixed cellulose ester (MCE) 0.22µm Millipore membrane filters before distribution to experimental containers.

3.1.2 Seawater selection

Seawater (SW) was collected between the surface and 10 m deep at Station ALOHA (A Long-Term Oligotrophic Habitat Assessment; 22° 45'N, 158° 00'W), located 100 km north of O'ahu, Hawai'i. Physical and chemical characteristics of seawater at this oceanographic station have been determined regularly since 1988 (Bingham & Lukas, 1996; Brown et al., 2009; Chavez, Messié, & Pennington, 2011; Riser & Johnson, 2008). Water at the site is also considered representative of the type of water a ship would pick up as ballast to offset fuel consumed while underway. Seawater was collected on July 31, 2012 to 10 m depth during Hawai'i Ocean Time-series (HOT) cruise 244. According to HOT, heterotrophic bacterial numbers in the upper 10 m here typically range from 3 to $7x10^5$ cells/ml, and picoeukaryotes typically range from 1 to $3x10^3$ cells/ml ("Hawaii Ocean Time-series (HOT)," 2015). Basic parameters of the collected seawater were determined (Table 1).

Table 1. Chemical and biological parameters of seawater collected at ~10 m depth at Station ALOHA during HOT 244 (08/01/2012) based on bottle measurements. http://hahana.soest.hawaii.edu/hot/hot-dogs/interface.html.

Temp °C	**Salinity**	**Oxygen** µmol/kg	**pH**	**Alkalinity** µeq/kg	**Nitrate** µmol/kg	**Heterotrophic bacteria** $x10^5$/ml	**Eukaryotes** $x10^5$/ml
25.044	35.152	208.675	8.065	2318.0	0.030	4.810	0.007

To compare the effects on the fuels and steel of biotic and abiotic aspects of the natural seawater, half of the seawater was passed through 0.22 µm MCE membrane filters, which presumably removed $4.817x10^5$ microbes per ml of seawater (the sum of heterotrophic bacteria and eukaryotes) before the water was distributed to the experimental containers.
Artificial seawater replaced natural seawater in a concurrent series of experiments (ASTM D1141-98).

3.1.3 Metal selection

Unified Numbering System for Metals and Alloys (UNS) G10180 (1018) steel was used throughout this study because its specifications match those of steels used in pipelines and fuel tanks. Chemical composition of 1018 steel reported by the UNS specification was 0.15-0.20% carbon, 0.60-0.90% manganese, 0.04% max. phosphorus, 0.05% max. sulfur, with the balance percent as iron.

3.2 Experimental design

Sheets of 1018 steel were machined into 648 coupons (5.715 x 2.54 x 0.3175 cm). A BenchMark 320 dot-peen marking system pin-stamped each coupon with a unique identifier. Coupons were then acetone-washed to remove oil residue and stored in a dry box (<1% relative humidity) to prevent oxidation. Each coupon's initial mass was determined to the fourth decimal place. All 100 ml Pyrex sample bottles were pre-cleaned with a 1% Liquinox solution, rinsed with deionized water and dried. Coupons were placed in the sample bottles and sterilized by autoclaving at 132°C for 15 min, with their loosely placed solid orange caps tightened after the bottles cooled.
Three fuels (F-76, the 50:50 v/v blend of F-76 and HRD, and HRD) were tested as "Natural" (N) or "Sterile" (S) samples in natural, sterile and ASTM seawater (Table 2). Unfiltered fuels and natural seawater were considered to contain representative, naturally occurring microbial communities. All microbes larger than 0.22 µm were presumed to be removed upon passage through 0.22 µm pore size filter. The seawater was distributed to experimental bottles two days after collection. Coupons were positioned in each bottle at a 45° angle to expose the bottom half of the coupon to the water phase and the top half to the fuel phase (Figure 2c-e).

Table 2. Fuel/water/cap type combinations of sample triplicates for each of the 5 exposure periods. Sample names pin-stamped to each steel coupon shown for each of the 648 samples

Fuel	Water	C	EC	3 Day			10 Day			30 Day			6 Month			12 Month		
N F-76	N SW	O	1	1A01	2A01	3A01	1B01	2B01	3B01	1C01	2C01	3C01	1D01	2D01	3D01	1E01	2E01	3E01
		V	2	1A02	2A02	3A02	1B02	2B02	3B02	1C02	2C02	3C02	1D02	2D02	3D02	1E02	2E02	3E02
		T	3	1A03	2A03	3A03	1B03	2B03	3B03	1C03	2C03	3C03	1D03	2D03	3D03	1E03	2E03	3E03
S F-76		O	4	1A04	2A04	3A04	1B04	2B04	3B04	1C04	2C04	3C04	1D04	2D04	3D04	1E04	2E04	3E04
		V	5	1A05	2A05	3A05	1B05	2B05	3B05	1C05	2C05	3C05	1D05	2D05	3D05	1E05	2E05	3E05
		T	6	1A06	2A06	3A06	1B06	2B06	3B06	1C06	2C06	3C06	1D06	2D06	3D06	1E06	2E06	3E06
N F-76	S SW	O	7	1A07	2A07	3A07	1B07	2B07	3B07	1C07	2C07	3C07	1D07	2D07	3D07	1E07	2E07	3E07
		V	8	1A08	2A08	3A08	1B08	2B08	3B08	1C08	2C08	3C08	1D08	2D08	3D08	1E08	2E08	3E08
		T	9	1A09	2A09	3A09	1B09	2B09	3B09	1C09	2C09	3C09	1D09	2D09	3D09	1E09	2E09	3E09
S F-76		O	10	1A10	2A10	3A10	1B10	2B10	3B10	1C10	2C10	3C10	1D10	2D10	3D10	1E10	2E10	3E10
		V	11	1A11	2A11	3A11	1B11	2B11	3B11	1C11	2C11	3C11	1D11	2D11	3D11	1E11	2E11	3E11
		T	12	1A12	2A12	3A12	1B12	2B12	3B12	1C12	2C12	3C12	1D12	2D12	3D12	1E12	2E12	3E12
N Blend	N SW	O	13	1A13	2A13	3A13	1B13	2B13	3B13	1C13	2C13	3C13	1D13	2D13	3D13	1E13	2E13	3E13
		V	14	1A14	2A14	3A14	1B14	2B14	3B14	1C14	2C14	3C14	1D14	2D14	3D14	1E14	2E14	3E14
		T	15	1A15	2A15	3A15	1B15	2B15	3B15	1C15	2C15	3C15	1D15	2D15	3D15	1E15	2E15	3E15
S Blend		O	16	1A16	2A16	3A16	1B16	2B16	3B16	1C16	2C16	3C16	1D16	2D16	3D16	1E16	2E16	3E16
		V	17	1A17	2A17	3A17	1B17	2B17	3B17	1C17	2C17	3C17	1D17	2D17	3D17	1E17	2E17	3E17
		T	18	1A18	2A18	3A18	1B18	2B18	3B18	1C18	2C18	3C18	1D18	2D18	3D18	1E18	2E18	3E18
N Blend	S SW	O	19	1A19	2A19	3A19	1B19	2B19	3B19	1C19	2C19	3C19	1D19	2D19	3D19	1E19	2E19	3E19
		V	20	1A20	2A20	3A20	1B20	2B20	3B20	1C20	2C20	3C20	1D20	2D20	3D20	1E20	2E20	3E20
		T	21	1A21	2A21	3A21	1B21	2B21	3B21	1C21	2C21	3C21	1D21	2D21	3D21	1E21	2E21	3E21
S Blend		O	22	1A22	2A22	3A22	1B22	2B22	3B22	1C22	2C22	3C22	1D22	2D22	3D22	1E22	2E22	3E22
		V	23	1A23	2A23	3A23	1B23	2B23	3B23	1C23	2C23	3C23	1D23	2D23	3D23	1E23	2E23	3E23
		T	24	1A24	2A24	3A24	1B24	2B24	3B24	1C24	2C24	3C24	1D24	2D24	3D24	1E24	2E24	3E24
N HRD	N SW	O	25	1A25	2A25	3A25	1B25	2B25	3B25	1C25	2C25	3C25	1D25	2D25	3D25	1E25	2E25	3E25
		V	26	1A26	2A26	3A26	1B26	2B26	3B26	1C26	2C26	3C26	1D26	2D26	3D26	1E26	2E26	3E26
		T	27	1A27	2A27	3A27	1B27	2B27	3B27	1C27	2C27	3C27	1D27	2D27	3D27	1E27	2E27	3E27
S HRD		O	28	1A28	2A28	3A28	1B28	2B28	3B28	1C28	2C28	3C28	1D28	2D28	3D28	1E28	2E28	3E28
		V	29	1A29	2A29	3A29	1B29	2B29	3B29	1C29	2C29	3C29	1D29	2D29	3D29	1E29	2E29	3E29
		T	30	1A30	2A30	3A30	1B30	2B30	3B30	1C30	2C30	3C30	1D30	2D30	3D30	1E30	2E30	3E30
N HRD	S SW	O	31	1A31	2A31	3A31	1B31	2B31	3B31	1C31	2C31	3C31	1D31	2D31	3D31	1E31	2E31	3E31
		V	32	1A32	2A32	3A32	1B32	2B32	3B32	1C32	2C32	3C32	1D32	2D32	3D32	1E32	2E32	3E32
		T	33	1A33	2A33	3A33	1B33	2B33	3B33	1C33	2C33	3C33	1D33	2D33	3D33	1E33	2E33	3E33
S HRD		O	34	1A34	2A34	3A34	1B34	2B34	3B34	1C34	2C34	3C34	1D34	2D34	3D34	1E34	2E34	3E34
		V	35	1A35	2A35	3A35	1B35	2B35	3B35	1C35	2C35	3C35	1D35	2D35	3D35	1E35	2E35	3E35
		T	36	1A36	2A36	3A36	1B36	2B36	3B36	1C36	2C36	3C36	1D36	2D36	3D36	1E36	2E36	3E36
N F-76	ASTM SW	O	37	N/A			N/A			N/A			1D37	2D37	3D37	1E37	2E37	3E37
		V	38										1D38	2D38	3D38	1E38	2E38	3E38
		T	39										1D39	2D39	3D39	1E39	2E39	3E39
S F-76		O	40										1D40	2D40	3D40	1E40	2E40	3E40
		V	41										1D41	2D41	3D41	1E41	2E41	3E41
		T	42										1D42	2D42	3D42	1E42	2E42	3E42
N Blend		O	43										1D43	2D43	3D43	1E43	2E43	3E43
		V	44										1D44	2D44	3D44	1E44	2E44	3E44
		T	45										1D45	2D45	3D45	1E45	2E45	3E45
S Blend		O	46										1D46	2D46	3D46	1E46	2E46	3E46
		V	47										1D47	2D47	3D47	1E47	2E47	3E47
		T	48										1D48	2D48	3D48	1E48	2E48	3E48
N HRD		O	49										1D49	2D49	3D49	1E49	2E49	3E49
		V	50										1D50	2D50	3D50	1E50	2E50	3E50
		T	51										1D51	2D51	3D51	1E51	2E51	3E51
S HRD		O	52										1D52	2D52	3D52	1E52	2E52	3E52
		V	53										1D53	2D53	3D53	1E53	2E53	3E53
		T	54										1D54	2D54	3D54	1E54	2E54	3E54

Abbreviations: C - Cap type; EC - Environmental Condition 1-54; N - "Natural" unfiltered; S - "Sterile" filtered (0.22 µm);
Blend - 50:50 F-76 and HRD-76 diesel mixture; SW - Seawater; ASTM - American Standard Testing Method D1141-98 seawater;
O – "Open" aerobic condition; V – "Vented" 0.22 µm filtered aerobic; T – "Tightened" anaerobic; N/A – not applicable

Triplicate fuel-seawater mixtures (40 mL fuel + 40 mL seawater) were prepared and incubated under three different environmental conditions (Table 2): V – "Vented", aerobic, air filtered through 0.22 µm membrane in grey cap (Corning, Figure 2a & 2d); T – "Tightened (cf. non-vented)" anaerobic (solid orange cap, Figure 2b & 2e); O – "Open" aerobic (uncapped bottle, Figure 2c, Table 2).

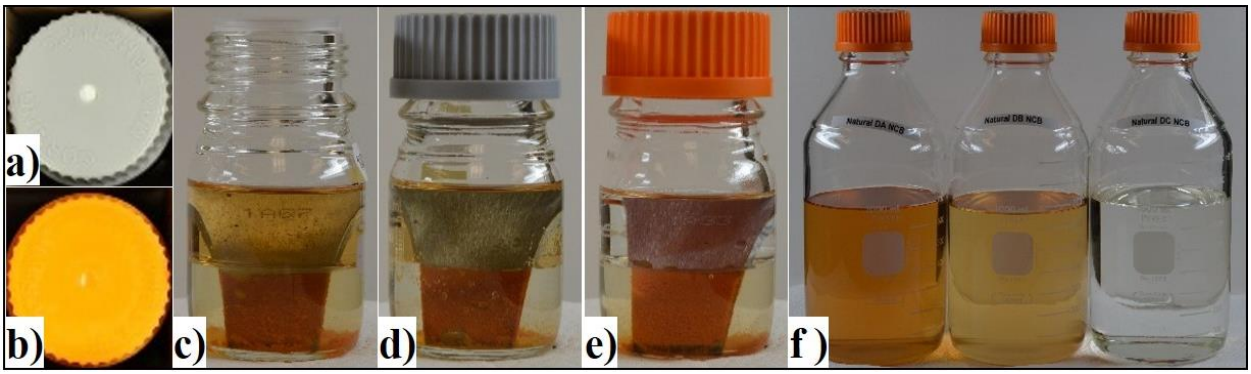

Figure 2. Sample bottle design a) Grey cap with filter (vented); b) Solid orange cap (non-vented); c) Open/uncapped sample bottle with F-76/natural seawater; d) Vented grey cap on sample bottle with blended fuel/seawater; e) Tightened orange cap on sample bottle with HRD /seawater; f) Negative control bottles containing (left to right) F-76; blend; HRD.

Negative-control bottles (NCB) separately contained the 9 liquid types with no steel coupon, and only tightened orange caps (Figure 2f, Figure 3c). These NCB and 648 experimental bottles were incubated outdoors in UV-shaded boxes under a rain-protective alcove (Figure 3a-b), and retrieved after five different exposure periods: 3, 10, 30, 182, 365 days (Figure 3c-d). Long-term corrosion tests (1 year or more) tend to yield lower corrosion rates than short-term tests because corrosion products restrict diffusion of fresh seawater and oxygen to the metal surface (Francis, 2012).

Precautions were taken to minimize temperature variations caused by spatial distribution of the samples. Cardboard flaps were taped in a vertical position to shade bottles from direct sun exposure, and to block wind (Figure 3a). Boxes were arranged on wire shelving to permit even distribution of air throughout the day (Figure 3c). Contents of sample bottles were all created from seawater collected July 31, 2012, and lot-numbered fuel barrels to minimize batch effect. All samples from every exposure period were processed within hours from start to finish.

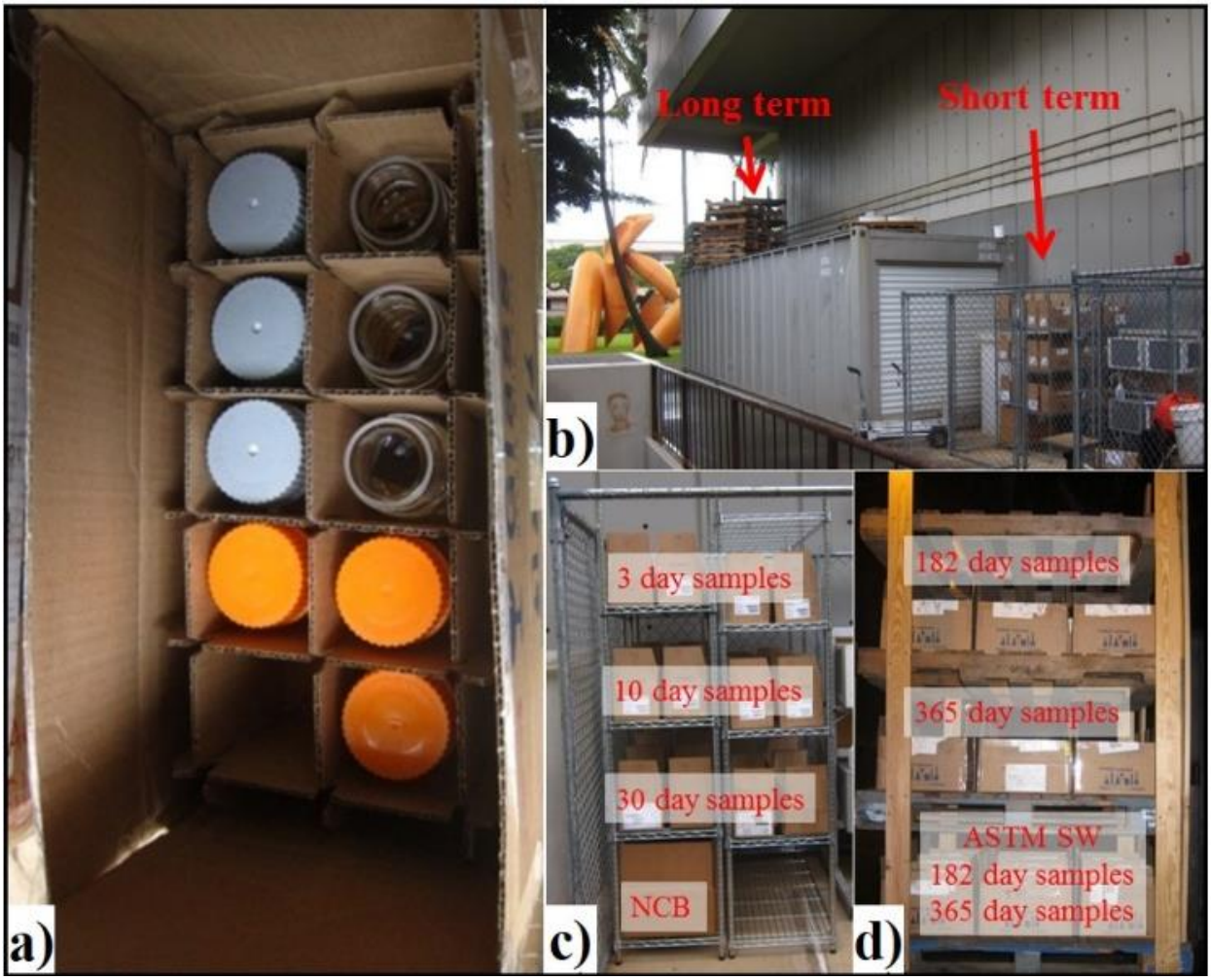

Figure 3. Exposure environment of sample bottles a) One set of triplicate sample bottles in UV-protective box; b) Outdoor exposure site under rain-protective alcove; c) Boxes of short exposure time sample bottles and negative control bottles stored at ground level in locked cage; d) Boxes of long exposure sample bottles arranged on a stand and stored on top of a shipping container.

3.3 Measurements

3.3.1 Temperature and relative humidity

Relative humidity & temperature sensors (RHTemp1000IS, MadgeTech, Warner, NH, USA) were placed among the long-term and short-term sample bottle boxes for the duration of the outdoor incubation (Figure 3b). The long-term sensor was replaced with a new one during the 6-month sample collection to ensure full coverage of the one-year exposure. Environmental parameters were recorded every 15 minutes.

3.3.2 pH

Seawater pH was measured in each sample bottle using pH indicator strips (0-14, VWR, Radnor, PA, USA) after withdrawal of liquid sub-samples for microbial analyses and removal of steel coupon for corrosion analyses. Indicator strips were used because loose corrosion products in the seawater layer interfered with pH meter measurements. The pH of the diesel was not recorded because test strips all read 4.0, regardless of fuel and exposure period, while it took 30-45 min for the pH meter to stabilize in each sample.

An additional experiment was run to determine what happens to the pH of seawater overlain with diesel in the absence of corroding steel. Triplicate bottles containing 18 ml ASTM seawater and 18 ml of each of the 3 fuels were incubated through the same time intervals used in the initial experiment, *i.e.*, 3, 10, 30, 182, and 365 days. Caps were left in place to prevent contamination, but they were not tightened completely, so gas exchange could occur. No metal coupons were placed in these bottles, and they were incubated in a chemical fume hood instead of outdoors. At the conclusion of the incubation period, the fuel layer was removed from each sample bottle and the pH of the underlying seawater was determined with a Low Maintenance Gel-Filled pH Electrode connected to an Orion 4 Star pH/DO portable meter (Thermo Scientific, Waltham, MA, USA), and pH indicator strips.

A one-way analysis of variance (ANOVA) determined whether or not the pH of ASTM seawater changed significantly over the duration of the experiment when overlain with either F-76 or HRD fuel. Significance of variation was calculated as statistical F and *p* values.

3.3.3 Dissolved oxygen (DO)

Oxygen saturation in the fuel overlain with seawater was measured every 30 seconds with an RDO® Optical Dissolved Oxygen Sensor connected to a portable Orion 4 Star pH/DO meter (Thermo Scientific, Waltham, MA, USA); the sensor was mounted through a hole drilled in the bottom of a 100 ml sample bottle (Figure 4). The bottle was wrapped with plastic tubing that carried heated water circulated through an Isotemp recirculating water bath, creating a “thermal jacket” that maintained the fuel/seawater sample at 30 °C for the duration of the experiment. The DO probe was overlain to a depth of ~1 cm with ASTM seawater (which equated to ~18 ml in a 100 ml bottle), and a ~1 cm deep layer of one of the three diesel fuels per trial (also equal to

~18 ml of the respective fuel). Two holes in the cap allowed gas to be pumped into the bottle and vented out through a gas trap. The allowable oxygen concentration in cold water for corrosion control in steel systems, as reported in Table 18.1 in *Corrosion and Corrosion Control* (Revie & Uhlig, 2008), for water is 0.3 ppm, or 0.2 mL/L (about 3% oxygen saturation). Nitrogen gas (99.9% purity) was bubbled into both liquids (Figure 4b) at 3 psi until the oxygen saturation detected through 15min was <3.5%. The tube supplying nitrogen gas was then pulled into the headspace of the bottle (Figure 4c) and the source nitrogen gas was switched to compressed air. Air was then pumped into the headspace at ~3 psi until the oxygen saturation was 100% (>6.46 mg/L oxygen). The oxygen saturation was determined in each of the three fuel/ASTM seawater combinations in three independent tests.

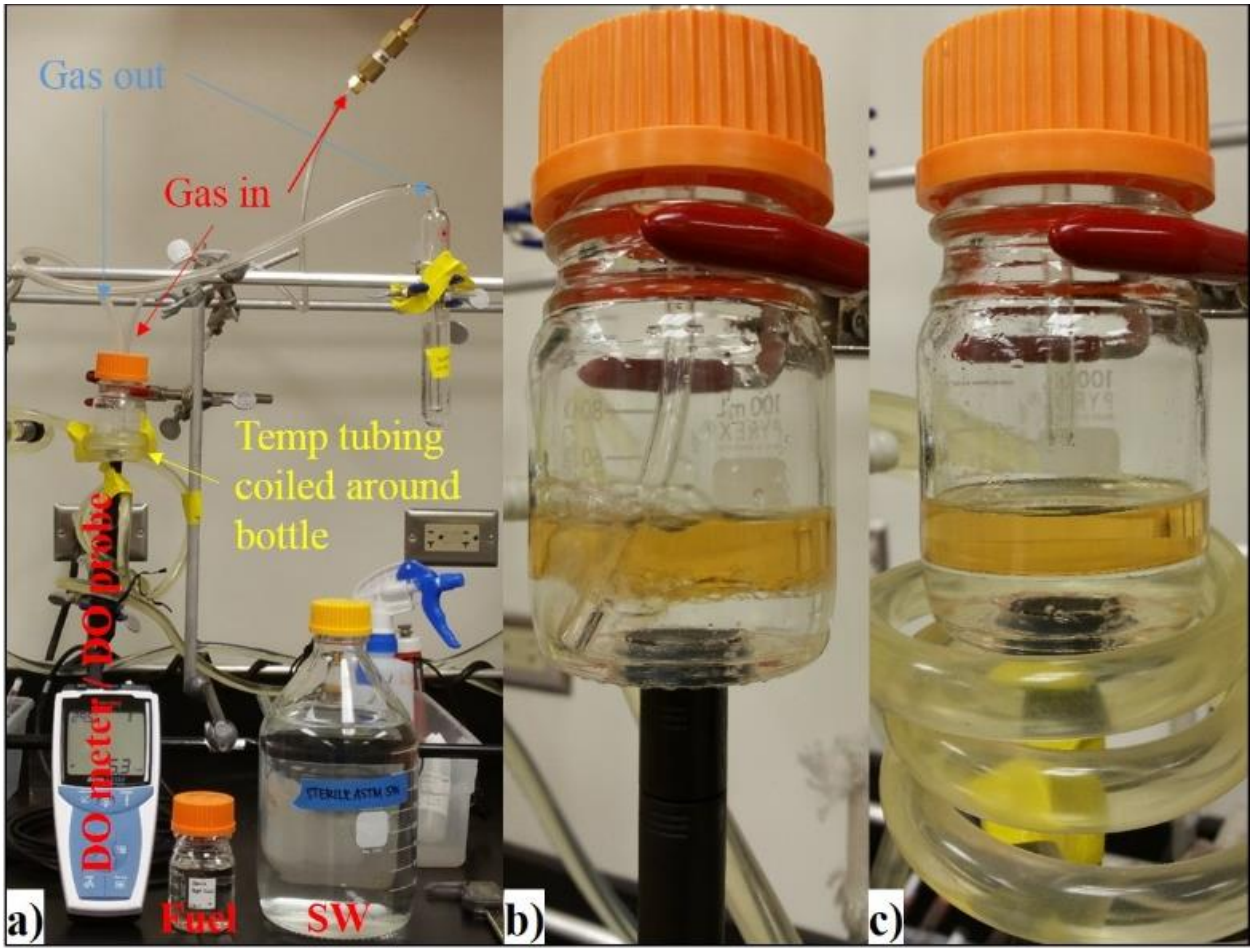

Figure 4. a) Dissolved oxygen bottle set up; b) enlarged area of Figure 4a showing coil removed; nitrogen gas bubbling through a 1cm seawater and 1cm fuel layer to remove O_2 from both liquids at 1 atm and 30°C; c) measurement of oxygen concentration in bottom layer while compressed air is pumped into bottle's headspace after removal of oxygen.

3.3.4 Total acid number (TAN)

Titra-Lube TAN kits (Dexsil, Hamdem, CT, USA), similar to ASTM D-664[1], were used to determine TAN values of the fuels per the manufacturer's instructions. Results were used to determine the degree of oxidation as a function of acid buildup of oils, and are read as TAN units, where 1 TAN = 1 mg KOH/g of sample. TAN is essentially defined as the number of milligrams of potassium hydroxide required to neutralize the acidity in one gram of oil. Test kit precision, according to the manufacturer, is +/- 0.02 TAN units, with a detection limit of 0.05 TAN units. Oil with high TAN values, *i.e.*, >0.5, are less desirable since they have been known to cause problems with corrosion and refinery processes, according to the manufacturer's website. TAN values were determined in samples from the 1 month, 6 month and 12 month incubations.

3.3.5 Percentage of water in fuel determined by HydroSCOUT

The HydroSCOUT Analyzer System (Dexsil, Hamdem, CT, USA) is a field test kit for quantifying the percentage of water (between 2 and 85%) in used oil (USEPA 9001[2]) by measuring the resulting pressure of hydrogen gas production when reacting the sample hydrocarbon with calcium hydride in a closed container (21). Using the Ideal Gas Law, the internal pressure of the reaction tube is converted to the amount of water present in the sample.

$$CaH_2 + H_2O \rightarrow Ca(OH)_2 + 2H_2 \text{ (1 mole } H_2 \text{ for every mole of } H_2O \text{ present)} \qquad (21)$$

Program C (Light Oil/Liquid) was used per the manufacturer's instructions with the result reported in ppm water in oil. The method detection limit is 50 ppm. The percentage of water in the diesel samples were determined from the 1 month, 6 month and 12 month samples.

3.3.6 Mass loss / corrosion rate

Once characterization of the corrosion product was completed, loose corrosion products were removed from each coupon with paper towels. These mechanically cleaned coupons were then

[1] ASTM D664 11a, "American Standard Test Method for Acid Number of Petroleum Products by Potentiometric Titration"

[2] U.S. EPA SW-846 Draft Method 9001 "Diagnostic Test For Water in Oil"

chemically cleaned per ISO 8407[3] C.3.5, after which they were sonicated in distilled water, the excess water was removed with paper towels, and cleaned coupons were stored with desiccant for at least 1 hour before being weighed in order to determine mass loss. Differences in sample coupon weights between cleaning cycles were compared to the mass loss of virgin steel coupons of the same size and cleaning cycle count to determine the point at which base metal was being removed instead of corrosion product. Three to six cleaning cycles were completed on each coupon, depending on mass loss comparisons to virgin steel mass loss. The total mass loss from each coupon was determined by subtracting the final weight of each cleaned coupon from the initial weight. Corrosion rates (CR) were calculated (22) for each coupon and each triplicate of the 36 environmental conditions at 3, 10, and 30 days and 54 environmental conditions at 6 and 12 months were averaged.

Corrosion rate in mm/year by ASTM G1:1999 (ASTM International, 1999):

$$\text{Corrosion Rate } (\frac{\text{mm}}{\text{yr}}) = \frac{\text{K} * \text{W}}{\text{A} * \text{T} * \text{D}} \tag{22}$$

K = a constant (8.76 x 10^4 = conversion factor of $\frac{cm}{hour}$ to $\frac{mm}{year}$ via ASTM G1.8.1.2)

T = time of exposure in hours (actual hours = 97h, 262h, 736h, 4354h, 8717h)

A = Surface area in cm^2 based on average coupon size
($2 \times [5.715 \times 0.3175 + 5.715 \times 2.54 + 0.3175 \times 2.54] = 34.27\ cm^2$)

W = mass lost in grams

D = density of steel in g/cm^3 ($7.86 g/cm^3$ chosen from ASTM G1 Appendix X1.1)

One-way ANOVA was used to determine which environmental variable tested significantly affected the corrosion rate of 1018 steel. Significance of variation was calculated as statistical F and *p* values.

High resolution (12000 bpi) scans of both sides of the cleaned coupons were acquired with a Cannon CanoScan LiDE700F flatbed scanner.

[3] ISO 8407:1991 International Organization for Standardization "Corrosion of Metal and Alloys - Removal of Corrosion Products from Corrosion Test Specimens"

3.4 Corrosion product characterization

3.4.1 Visual observations

Notations were based on general color of corrosion products present on each coupon and the relative percent of coverage of the coupon by each color of corrosion product, observed on the front side of each coupon after their removal from the sample bottles. Categories 0-3 were distinguished by: 0 = No particular colored product observed in the specified coupon region; 1 = >0 to 25% specified region covered; 2 = 25-75% coverage; 3 = >75% coverage. A Nikon D700 DSLR camera with an AF Micro-NIKKOR 60 mm f/2.8D recorded images of both the front and back of each sample coupon.

3.4.2 X-ray diffraction (XRD)

This non-destructive analytical technique enabled the chemical composition of a 2x2 cm area of the coupon's surface to be determined by measuring the intensity of X-ray scatter as a function of incidence and scattering angles, polarization, and wavelength. Resulting spectra were compared to those in the International Centre for Diffraction Data database to identify likely corrosion species on the coupon.

X-ray diffraction spectra of the corroded steel coupon surfaces were determined in a Rigaku MiniFlex™ II benchtop XRD system equipped with Cu (Kα) radiation. Scans were conducted in the range of 3 – 90° (2(θ)) with a scan speed of 1° (2θ)/min. Crystalline phase identification was completed on the basis of comparison of peak position and peak intensity using the International Center for Diffraction Data 2008 PDF-2.

3.4.3 Raman spectroscopy

Raman spectroscopy focuses a green or red laser at a single point on the corroded surface in order to generate a spectral "fingerprint" of the material at that point. Its use here refined corrosion product identifications determined by XRD analysis.

Raman spectroscopy was performed in a Nicolet Almega XR dispersive Raman spectrometer (Thermo Scientific, Waltham, MA, USA) equipped with multiple Olympus† objectives and a Peltier-cold charge-coupled device detector. The instruments were operated with a 532 nm

excitation Nd:YAG green laser and an infrared diode 780 nm laser, with an accumulation time of 120 seconds.

3.4.4 Scanning electron microscopy with energy dispersive x-ray analysis

A Hitachi S-3400N II scanning electron microscope equipped with an Oxford Instruments energy dispersive x-ray spectrometer INCA-350 characterized morphological and quantitative elemental analysis of corroded regions on sample coupons.

3.5 Identification of cultivated microorganisms

3.5.1 General & selective media

Subsamples (0.25-0.75 ml) of the 12-15 ml of fuel/seawater interface layers stored at -20°C, were transferred to each of 6 different enrichment media (Table 3) per sample bottle. Inoculated plates were wrapped with Parafilm (Bemis NA, WI, USA) and incubated at room temperature 25°C +/- 5°C, the mean temperature of surface waters around Station ALOHA where the seawater was collected. Each of the 3882 inoculated plates were checked for growth every 1-3 days for 4 weeks. During this period, representative colony types were transferred by streaking on fresh media in order to recover the greatest number of morphologically different colony types. If no growth was observed after 4 weeks, the plates were autoclaved and discarded.

Table 3. General and selective culture media used to enrich and maintain microorganisms.

Medium	**Abbr.**	**Enriches**	**Contents**
Marine Agar 2216	MA	Marine heterotrophic microbes	High nutrient, 1.9% NaCl
Trypticase Soy Agar	TSA	Heterotrophic microbes	High nutrient, 0.5% NaCl
Reasoner's 2A Agar	R2A	Freshwater microbes	Low nutrient, no salt
Sulfate API Broth and Agar	SAPI	Sulfate-Reducing Bacteria *Incubated anaerobically	Low nutrient, 1% NaCl
Bushnell Haas Agar	BH	Hydrocarbon-degrading microbes	Contains all nutrients to support microbial growth except a carbon source (added fuel is carbon source)
Potato Dextrose Agar with antibiotics*	PDA	Primarily eukaryotes	*Penicillin G and Streptomycin sulfate

3.5.2 Morphology

Colonies that grew on solid media were selected for purification on the basis of their distinct culture and colony features. Representative colonies were thus streaked to fresh media for purification. Subsamples of turbid liquid media (SAPI broth) were transferred to plates of the same medium in order to provide representative colonies for subsequent transfer. All transferred colonies strains were assigned a subculture name (*e.g.,* AB13; "A" means it was isolated from a 3 day sample bottle, "B" means it appeared to be a bacteria colony opposed to "F" for fungal colony, and the number means it was the 13th unique colony type to be transferred from the 3 day samples); transfers were repeated until pure cultures, determined through consistency of colony characteristics and Gram staining.

When observing each plate upon which microbial growth was evident, colonies were compared to those which had previously been transferred. If colonies appeared identical to any which appeared to have been previously selected for purification, a notation was made that that sample bottle probably contained the same organism, so the colony was not transferred anew. The converse applied, however, when a colony appeared different from any previously described and transferred. Not all transfers yielded viable/axenic cultures, especially fungal cultures.

3.5.3 Putative taxonomic group assignment (16S and 18S rRNA sequencing)

Genomic DNA was extracted from pure cultures in the PowerLyzer UltraClean Microbial DNA Isolation Kit (Mo-Bio, Carlsbad, CA, USA), per the manufacturer's instructions, and stored at -20°C until used as template in polymerase chain reactions (PCR). Partial 16S or 18S rRNA gene sequences in *Bacteria* and *Eucarya*, respectively, were amplified by PCR in 25 µl reactions containing 1 µl genomic DNA, 9 µl nuclease-free water, 12.5 µl GoTaq® G2 Hot Start Green Master Mix (Promega, WI, USA), and 1.25 µl per primer (Table 4Table 4. Primer set description used for culture-dependent microbial isolate identification.). A Fungi-specific 18S set of primers was used in PCRs to amplify template DNA from fungal isolates. Colonies growing on PDA plates with antibiotics were assumed to be those of eukaryotic microbes. The PCR cycle was as follows: 94°C (hot start) 5 min, followed by 35 cycles of denaturation (94°C, 30 sec), annealing (cf. Table 4, 30 sec), extension (72°C, 45 sec), and a final extension step (72°C, 5 min). PCR products were visualized on a 1% agarose gel with EZVision® In-Gel Solution (Amresco, OH,

USA). Samples that showed a band at ~800bp were cleaned in the Ultraclean PCR Clean-Up Kit (Mo-Bio, Carlsbad, CA, USA) and then sequenced in the Greenwood Molecular Biology Core Facility at the University of Hawai‘i at Mānoa. Sequences were compared with others in GenBank at the NCBI through BLAST comparisons (Altschul et al., 1997) of sequences from type material.

Table 4. Primer set description used for culture-dependent microbial isolate identification.

Target Gene	Primer name	Source	Annealing temp.	Sequence
***Bacteria*/*Archaea* 16S rRNA**	519F	Pace, Stahl, & David J. Lane, 1986	55°C	CAGCMGCCGCGGTAATWC
	1392R			ACGGGCGGTGTGTRC
***Eukarya* 18S rRNA**	18SL0001	Mahdi, Statzell-Tallman, Fell, Brown, & Donachie, 2008	58°C	TACCTGGTTGATCCTGCCAGT
	18SR0532			TTGATCCTTCTGCAGGTTCACCTAC

3.6 Culture-independent analysis of microbial communities

3.6.1 Community DNA extraction

Upon completing transfer of sub-samples to media for cultivation, the remaining interface material from the 176 selected samples (one of each triplicate, plus those showing uncommon corrosion products, Appendix 1), were filtered through a 0.22 µm pore size, 47 mm diameter, MCE filter (GSW G047S6, Millipore, Bedford, MA, USA). DNA was extracted separately from both halves of the filter in two commercial kits (PowerWater [Mo-Bio, Carlsbad, CA, USA] and NucleoSpin Microbial DNA [Macherney Nagel, Bethlehem, PA, USA]) per half, following the manufacturer’s instructions. Since some of the bottles in each triplicate were considered ‘abiotic’, they were also considered to be negative-controls. Subsamples of 38 such negative-control bottles were filtered, and genomic DNA extracted for microbial community analysis.

3.6.2 Illumina MiSeq next generation sequencing

DNA from each sample extracted in the two kits described above was pooled (5 µl each) and used in community PCR; if the PCR failed, separate PCRs were then run using DNA extracted through each kit.

These PCRs targeted the nuclear ITS1 region in eukaryotes and the V4 region of the *Bacteria/Archaea* 16S rRNA gene (O'Rorke et al., 2015; Smith & Peay, 2014). The Illumina barcoded 16S PCR primers were contaminated, thus a special step[4] was used to clean the PCR master mix prior to adding community DNA extracts. DNA was amplified using fusion primers with a locus specific priming site at the 3' end, the 'a' or 'b' Illumina adapter at the 5' end, and an error-correcting Golay barcode is in the reverse primer (O'Rorke et al., 2015; Smith & Peay, 2014). PCRs were run in 25 µl reactions comprising 3 µl pooled community DNA, 7.5 µl nuclease-free water, 12.5 µl GoTaq® G2 Hot Start Green Master Mix (Promega, WI, USA), 1.5 µl primer A (final reaction concentration 0.2 µM), and 0.5 µl primer B (final reaction concentration 0.192 µM). Positive controls in PCRs comprised DNA extracted from bacterial or fungal samples, and negative controls contained molecular biology grade nuclease-free water. Thermocycler parameters were: 98°C (hot start for 2 min), followed by 45 cycles for ITS primers and 38 cycles for 16S primers of denaturation (98°C, 30 sec), annealing (50°C, 15 sec), extension (72°C, 30 sec), and final extension step (72°C, 5 min). PCR products were visualized on 1.6% agarose gels stained with Gel Red (Biotium, Inc., Fremont, CA, USA).

Samples (15 µl each PCR product) were adjusted to equimolarity using SequalPrep™ Normalization Plates (Invitrogen, NY, USA) and pooled into one multiplexed bacterial 16S library, and one multiplexed fungal ITS library. Each library was pooled in a ~1:2 ratio of bacteria:fungi (Smith & Peay, 2014), and 2 ml of the final pooled libraries were cleaned and concentrated in the MoBio UltraClean PCR Clean-Up kit. DNA in the purified sample was quantified in a Qubit fluorometer (Invitrogen, NY, USA) using the double-stranded DNA high sensitivity assay, and then passed through a final quality control check on a Bioanalyzer Expert 2100 High Sensitivity chip (Agilent Technologies, CA, USA). The final pooled DNA was sequenced in the Genomic Services Laboratory (GSL) at HudsonAlpha (Huntsville, AL, USA), in a 250 base pair paired-end sequencing run on an Illumina MiSeq (San Diego, CA, USA). Three custom primers were used for each sequenced amplicon, one for each sequenced direction, and one for the sample index ID (O'Rorke et al., 2015; Smith & Peay, 2014).

[4]Ethidium monoazide (EMA) at 2.74M/PCR was used to eliminate contaminating DNA in PCR master mix according to Rueckert & Morgan (2007).

The resulting data sets were de-multiplexed by GSL based on the multiplexed barcode ID using MiSeq and Illumina software. The 16S data set was run through the 16S Metagenomics pipeline (https://basespace.illumina.com/apps/593593/16S-Metagenomics) on BaseSpace (Illumina, San Diego, CA, USA) referencing the GreenGenes database (DeSantis et al., 2006; McDonald et al., 2012). The ITS data was analyzed with the QIIME analysis pipeline developed at Juniata College (Brislawn, 2014; Caporaso et al., 2010) referencing the UNITE 2015 database (Kõljalg et al., 2013).

Chapter 4. Results

4.1 Physiological and chemical analyses

4.1.1 Measurements

4.1.1.1 Temperature and relative humidity

Per the Ocean Atlas of Hawai‘i surface water temperature website (“Pacific Islands Ocean Observing System,” 2012), the average surface water temperature around O‘ahu is between 24 to 27 °C. MadgeTech sensor data (Table 5) showed a smaller range in exposure temperature for the long-term bottles stored on top of the shipping container (Figure 3b). However, short-term sample bottles experienced a greater temperature range between day and night due to their direct exposure to the sun.

Table 5. Air temperature and relative humidity data

	Temperature (°C)			Relative Humidity (%)		
Sensor Location	**Average**	**Max**	**Min**	**Average**	**Max**	**Min**
0-1 month August 2012	26.1	45.7	22.5	64.7	82.0	28.5
0-6 month Aug 2012-Mar 2013	24.4	28.6	15.8	70.9	90.5	51.5
6-12 month upper Mar– Aug 2013	23.1	28.2	16.8	70.6	91.0	50.5

4.1.1.2 pH

The pH of seawater collected at Station ALOHA was 8.07. The pH of the ASTM seawater was adjusted to 8.2 before the start of the experiment. The pH of all samples fell to 7 within 3 days of the experiment starting, with that in those containing HRD then falling to pH 6 by the 10th day (Figure 5). By the end of the first month, the pH in all samples averaged ~6, and by 6 months averaged close to pH 7. The pH in all samples after 12 months of exposure was 4 or lower.

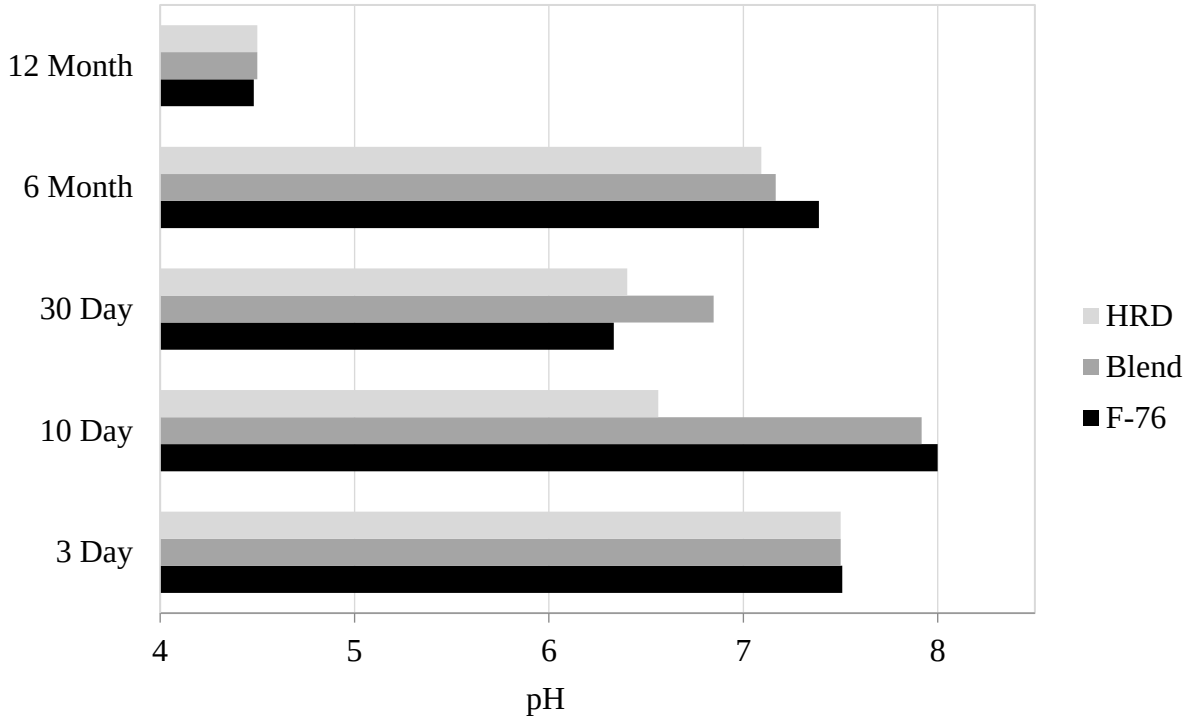

Figure 5. Change in pH of natural seawater when overlain with one of three different diesel fuels in sample bottles containing a steel coupon at 5 exposure periods. Data sorted based on type of fuel in sample bottle (no ASTM samples in this data set).

Minimal pH changes were detected in a fuel/seawater mixture that did not contain a metal coupon (Figure 6). pH was determined with a pH meter/probe, and with pH indicator strips to ensure agreement between measurements taken from samples with coupons using only the pH strips. After removal of the overlaying diesel, the pH of the ASTM seawater was 7.7 - 8.3 according to the pH meter/probe, but was pH 5 according to the 4-square color comparison indicator strips. A second brand of pH test strips with a single square color comparison indicator was used on the 12 month seawater layer samples, and pH in all was 8. The brand of pH strip used for the measurement was determined to be the cause of unexpected 12 month readings from experimental sample bottles.

The one-way ANOVA of pH probe measurements showed statistically significant differences in the change of pH between F-76 and HRD [$F(1, 28) = 21.94$, $p = 6.58 \times 10^{-5}$). The rate of pH change in the HRD samples, which became increasingly acidic over the course of one year, was significantly greater than the pH change in F-76 samples over the same period.

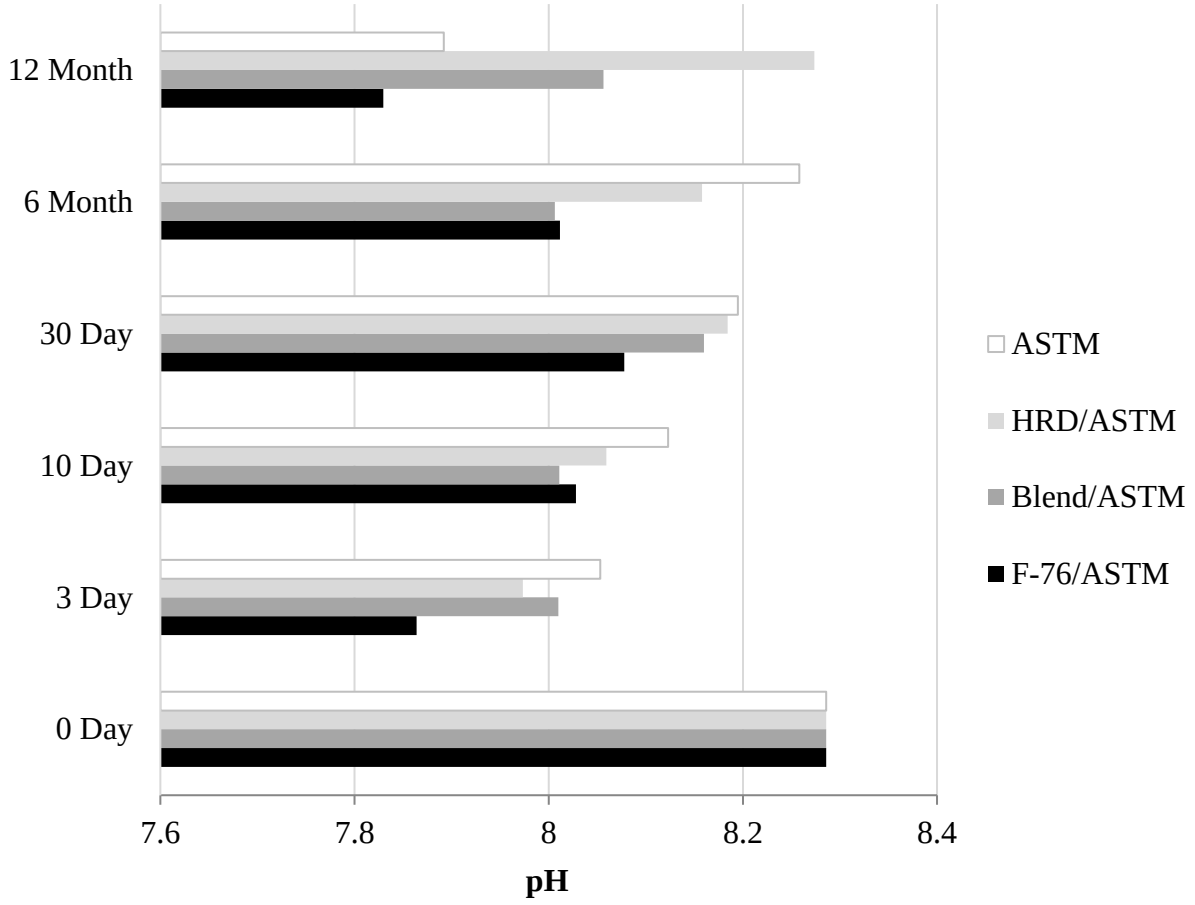

Figure 6. Change in pH of ASTM seawater when overlain with one of three diesel fuels in sample bottles not containing a steel coupon

4.1.1.3 Dissolved oxygen

The concentration of oxygen in water beneath 1 cm of fuel was below 5% (0.3 mg O_2/L) in all samples before the gas was switched from nitrogen to compressed air. Within 10 min of the start of aeration, the oxygen concentration in HRD samples was at 7% (Figure 7), well over the 3% corrosion control threshold. Oxygen concentrations in blended fuel samples were at 5%, and in F-76 were at the 3% threshold. After 35 min, the lowest average oxygen saturation of 19% was measured in F-76, while that in the 50:50 blend and HRD averaged approx. 28%. The greatest difference in oxygen concentrations after 100 min of aeration was in F-76 with 13% less oxygen concentration than the blended fuel in which the oxygen concentration was 80%. A trend was apparent in these data, but the differences were not significant (one-way ANOVA [$F(2, 6) = 1.484$, $p = 0.299$).

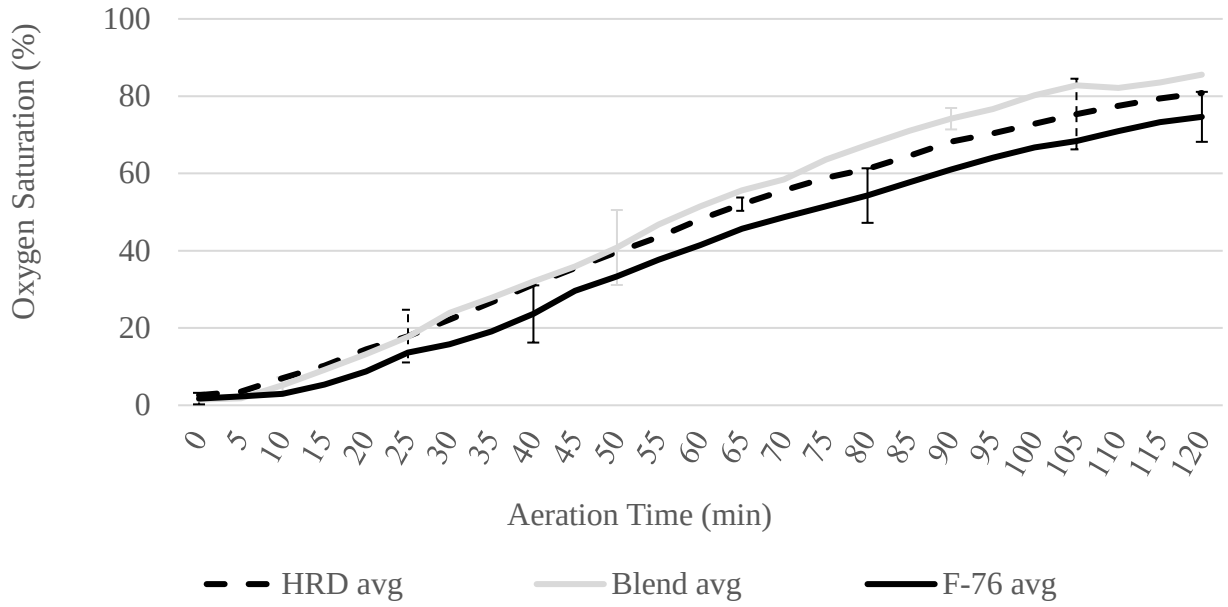

Figure 7. Oxygen concentration (%) in 1 cm ASTM seawater overlain by 1 cm diesel fuel and exposed to air at 30°C after initial deaeration with 99.9% nitrogen gas.

4.1.1.4 TAN

The initial TAN values of both fuel batches from the Naval Fuels & Lubricants Cross Functional Team, AIR-4.4.5.1 in Maryland, before they were shipped to Hawai‘i, were F-76 0.12 mg KOH/g & HRD 0.008 mg KOH/g.

TAN values were determined for samples from the 1 month, 6 month and 12 month exposure periods (Appendix 3). Filtered aerobic (vented) bottles typically had lower TAN values than those maintained in other conditions. However, 53 of the 221 samples were too acidic to be read by the commercially available kit used in this study. Placeholder values of -1.00 were entered for the sample when the reagents in the kit were of insufficient volume to neutralize the amount of acid in the fuel sample.

4.1.1.5 HydroScout

One hundred and twenty-two HydroScout measurements were determined in the 1 month, 6 month and 12 month samples. Measurements were not taken of all samples, however, because not enough fuel was saved from each bottle (5ml fuel is needed to run HS test). Samples were not pooled within the triplicates because variation amongst the triplicates was often observed. Data were inconclusive (Appendix 4).

4.1.1.6 Mass loss / Corrosion rate

Corrosion rates for 1018 steel exposed to various combinations of filtered and nonfiltered seawater and fuel in anaerobic and aerobic conditions were determined. The rate of corrosion decreased as a function of the length of time the samples were exposed, due to the formation of protective oxide layers. According to NACE SP0775 guidelines of General Corrosion Category: six of 648 coupons had corrosion rates categorized as "High"; 400 coupons categorized as "Moderate"; and 242 had "Low" corrosion rates (Table 6).

Table 6. Number of coupons per time trial assigned to General Corrosion Category (NACE, 2013)

Corrosion Category	mm/year	3 d	10 d	1 m	6 m	12 m
Low	<0.025	0	0	17	114	111
Moderate	0.025-0.126	102	108	91	48	51
High	0.127-0.254	6	0	0	0	0
Severe	>0.255	0	0	0	0	0

Filtration of the seawater and fuels before the commencement of incubation did not have a significant role in the subsequent corrosion rate (Figure 8a, Table 7-Table 8).

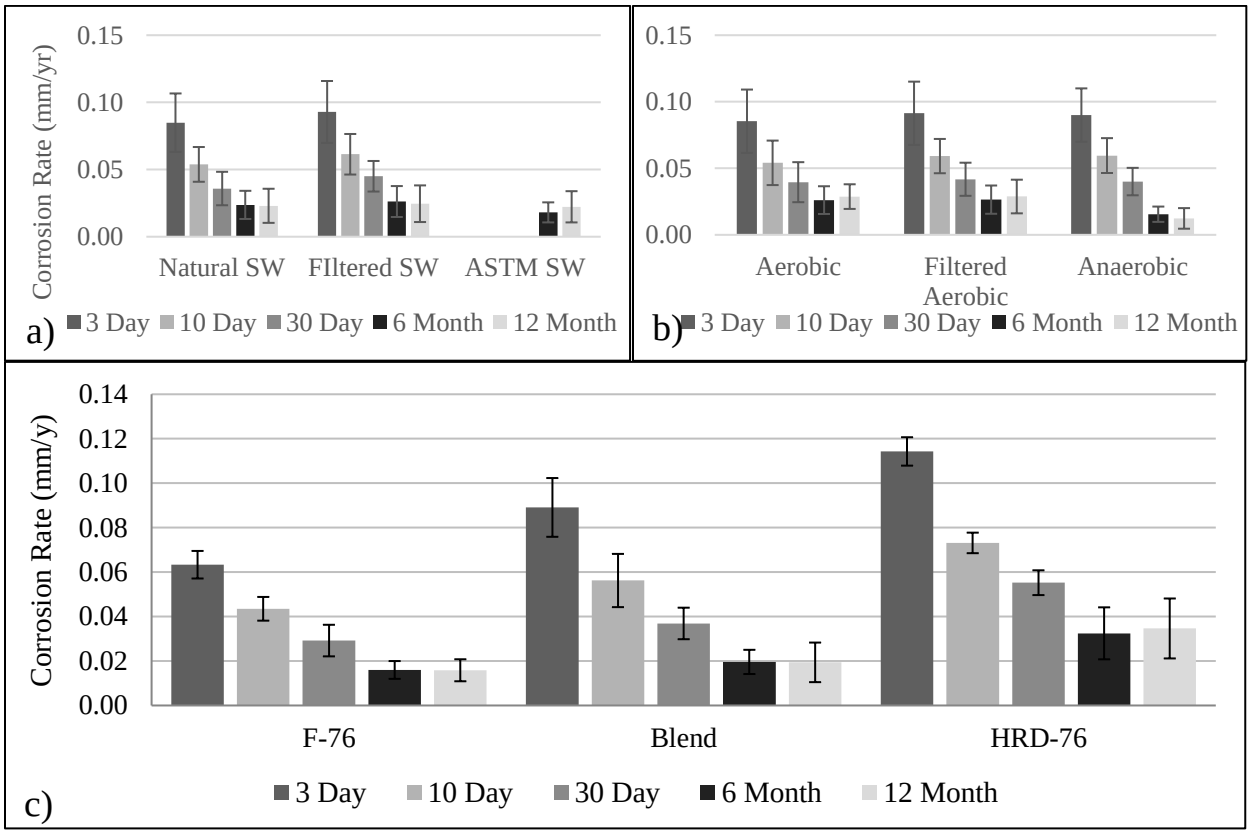

Figure 8. Corrosion rate as a function of a) seawater type b) environmental condition c) fuel type

Corrosion rates among all samples were generally highest in the HRD, with as much as 0.051 mm/year difference between the HRD and F-76 after 3 days, and a difference of 0.019 mm/year after one year. The most corrosive sample condition comprised filtered seawater and filtered HRD in a filter capped bottle, in which the corrosion rate was 0.073 mm/year over the five exposure periods. In contrast, the corrosion rate in the F-76 fuel under the same conditions was 0.038 mm/year. Faster diffusion of available oxygen through the less viscous HRD fuel, discussed in 4.1.3, is considered the likely cause of the higher corrosion rates.

Table 7. Evaluation of variables pertaining to 6 and 12 month incubations, in terms of steel corrosion rate in ASTM seawater overlain with F-76 and HRD only (blended fuel samples not included in this analyses). *p* values < 0.05 indicates a significant difference between the outcomes compared.

Constant Parameters	**Variable**	**n**	**6 m**		**12 m**	
			Stat. Diff.	***p***	**Stat. Diff.**	***p***
Open cap, ASTM	N *vs.* S F-76	3	-	0.848	-	0.354
Vented cap, ASTM		3	-	0.346	-	0.636
Tight cap, ASTM		3	✓	0.006	-	0.596
Open cap, ASTM	N *vs.* S HRD	3	-	0.244	-	0.432
Vented cap, ASTM		3	-	0.319	-	0.308
Tight cap, ASTM		3	-	0.592	-	0.533
N F-76, ASTM	Open *vs.* Vented	3	-	0.725	-	0.849
S F-76, ASTM		3	-	0.537	✓	0.006
N HRD, ASTM		3	-	0.950	-	0.528
S HRD, ASTM		3	-	0.932	-	0.380
F-76, ASTM		6	-	0.739	-	0.483
HRD, ASTM		6	-	0.687	-	0.053
Aerobic, ASTM	N *vs.* S F-76	6	-	0.444	-	0.247
Aerobic, ASTM	N *vs.* S HRD	6	-	0.095	-	0.231
F-76, ASTM	Aer. *vs.* Anaer.	12	✓	1.10E-03	-	0.708
HRD, ASTM		12	✓	2.12E-08	✓	1.16E-03
Aerobic, ASTM	F-76 *vs.* HRD	12	✓	6.38E-08	✓	1.76E-12
Anaerobic, ASTM		6	-	0.558	-	0.053
N F-76, Aerobic	SW *vs.* ASTM	12	✓	0.050	-	0.665
S F-76, Aerobic		12	-	0.705	-	0.333
N F-76, Anaerobic		6	-	0.103	-	0.085
S F-76, Anaerobic		6	✓	4.06E-05	✓	0.021
N HRD, Aerobic		12	✓	2.15E-08	✓	0.020
S HRD, Aerobic		12	✓	6.33E-06	✓	0.005
N HRD, Anaerobic		6	✓	0.034	-	0.184
S HRD, Anaerobic		6	-	0.191	-	0.252

Statistical analysis of the corrosion rate of 1018 steel coupons in different conditions in Pacific Ocean seawater (Table 8) or ASTM (Table 7) showed the rates varied significantly between aerobic HRD samples and anaerobic F-76 samples. However, the corrosion rates in seawater and ASTM seawater were within approximately 10% of each other. As expected, oxygen is necessary for increased rates of corrosion; samples incubated anaerobically showed the lowest rates of corrosion after 12 months (Figure 8b). In the two longest incubations, corrosion rates in aerobic conditions were always statistically greater than in anaerobic conditions, when F-76 was compared to HRD samples. Fuel type, whether filtered or nonfiltered, was the most significant factor in influencing corrosion rate (Figure 8c).

Table 8. Statistical evaluation of variables from 3 days to 12 months as related to steel corrosion rate in Pacific Ocean seawater (SW). *p* values < 0.05 indicates the variable made a significant difference

			3 d		10 d		1 m		6 m		12 m	
Constant Parameters	**Variable**	**n**	**Stat. Diff.**	***p***	**Stat. Diff.**	***p***	**Stat. Diff.**	***p***	**Stat. Diff.**	***p***	**Stat. Diff.**	***p***
Open cap, N SW	N *vs.* S F-76	3	-	0.341	-	0.056	-	0.614	-	0.111	-	0.652
Open cap, S SW		3	-	0.721	-	0.406	-	0.089	-	0.621	-	0.478
Open cap, N SW	N *vs.* S HRD	3	-	0.375	-	0.185	-	0.731	-	0.105	-	0.674
Open cap, S SW		3	-	0.829	-	0.329	✓	0.032	-	0.936	-	0.947
Vented cap, N SW	N *vs.* S F-76	3	-	0.327	-	0.095	-	0.117	✓	0.019	✓	2.64E-04
Vented cap, S SW		3	-	0.686	-	0.942	-	0.080	-	0.284	-	0.179
Vented cap, N SW	N *vs.* S HRD	3	-	0.329	-	0.334	-	0.666	✓	6.31E-03	-	0.241
Vented cap, S SW		3	-	0.504	-	0.068	-	0.558	-	0.211	-	0.802
Tight cap, N SW	N *vs.* S F-76	3	-	0.240	-	0.455	✓	0.004	-	0.984	-	0.058
Tight cap, S SW		3	-	0.672	-	0.901	-	0.298	✓	9.40E-04	-	0.057
Tight cap, N SW	N *vs.* S HRD	3	-	0.707	✓	0.040	-	0.966	-	0.717	-	0.998
Tight cap, S SW		3	-	0.330	-	0.979	-	0.887	-	0.396	-	0.651
F-76, N SW	Open *vs.* Vented	6	-	0.054	✓	0.041	-	0.263	-	0.891	-	0.761
F-76, S SW		6	-	0.692	✓	0.002	-	0.094	✓	0.007	-	0.510
HRD, N SW		6	-	0.365	-	0.292	-	0.349	-	0.949	✓	0.003
HRD, S SW		6	-	0.316	-	0.537	-	0.231	-	0.438	-	0.055
Anaerobic F-76	N *vs.* S SW	6	-	0.474	-	0.531	✓	0.014	-	0.737	✓	0.045
Aerobic F-76		12	-	0.605	-	0.274	✓	0.005	✓	0.024	-	0.117
Anaerobic HRD		6	-	0.379	-	0.451	✓	0.005	-	0.681	-	0.059
Aerobic HRD		12	-	0.148	✓	0.016	✓	0.046	✓	0.037	-	0.956
F-76, N SW	Aer. *vs.* Anaer.	12	-	0.211	✓	2.12E-03	✓	0.005	✓	0.045	✓	0.001
F-76, S SW		12	-	0.407	-	0.069	-	0.485	✓	0.001	✓	2.45E-05
HRD, N SW		12	-	0.745	-	0.078	-	0.104	✓	3.90E-05	✓	1.00E-08
HRD, S SW		12	-	0.278	-	0.546	✓	0.003	✓	3.21E-06	✓	1.39E-07
Aerobic, SW	F-76 *vs.* HRD	24	✓	8.27E-20	✓	3.68E-22	✓	1.48E-20	✓	6.34E-29	✓	4.54E-21
Anaerobic, SW		12	✓	1.47E-09	✓	1.26E-09	✓	1.50E-05	✓	0.027	-	0.658

4.1.2 Corrosion product characterization

4.1.2.1 Visual observations

Visual observations were based on corrosion product color and texture. Identification of corrosion products beyond color are discussed later (4.1.2.2-5).

Based on visual inspection of coupons, which provided a percentage coverage of each coupon, an orange rust was the dominant corrosion product the seawater phase on 96% of coupons (Figure 9a), regardless of sample bottle contents. Many of the samples incubated up to 12 months hosted a fragile exterior orange rust layer over a black rust that was more adherent to the metal surface (Figure 9b). Coupons in the 6 and 12 month anaerobic bottles had the least amount of orange rust in the seawater layer. Some coupons in bottles exposed longer had no orange product, but were rather covered with just a blackened surface in the seawater layer.

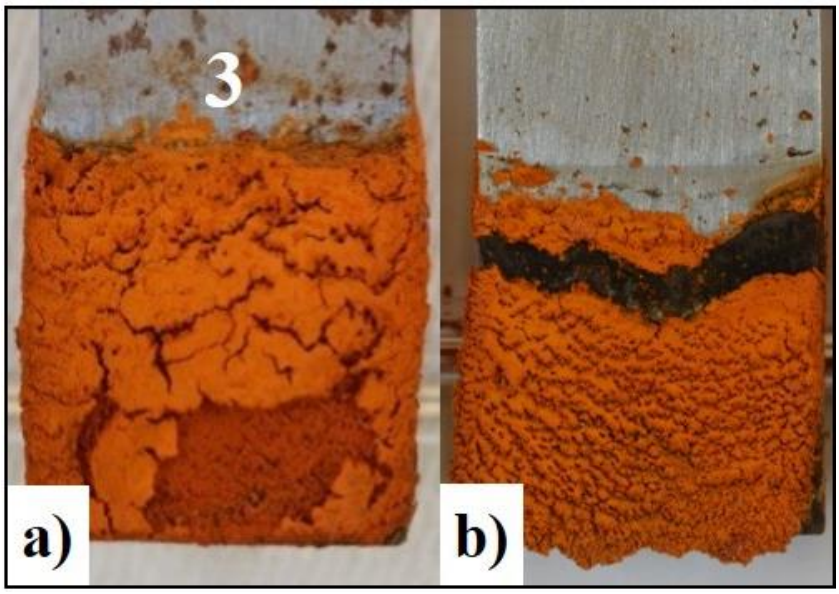

Figure 9. a) Sample coupon 3: >75% coverage by an orange corrosion product in the seawater layer; b) superficial orange rust layer sliding off to reveal inner black rust layer.

In the fuel phase, a reddish-brown rust adhering tightly to the surface of the coupon was observed on 62% of all exposed coupons (Figure 10a). Red rust formed in small amounts (>0-25%) on coupons within the early 3-30 day incubations containing both filtered and non-filtered versions of HRD and Pacific Ocean seawater combinations. Conversely, the F-76 samples typically had no red rust present this early on. In the longer exposures (6 and 12 month), more

coupons in the F-76 and blended fuel were covered in the range of 25-75% by red rust. Samples containing ASTM seawater in the longer exposures, had more red rust than natural seawater samples, implying some differences in corrosion could be attributable to a difference or differences between the ASTM and Pacific Ocean seawaters. Aerobic conditions had the highest percent coverage of red rust, as expected since rust is an iron oxide.

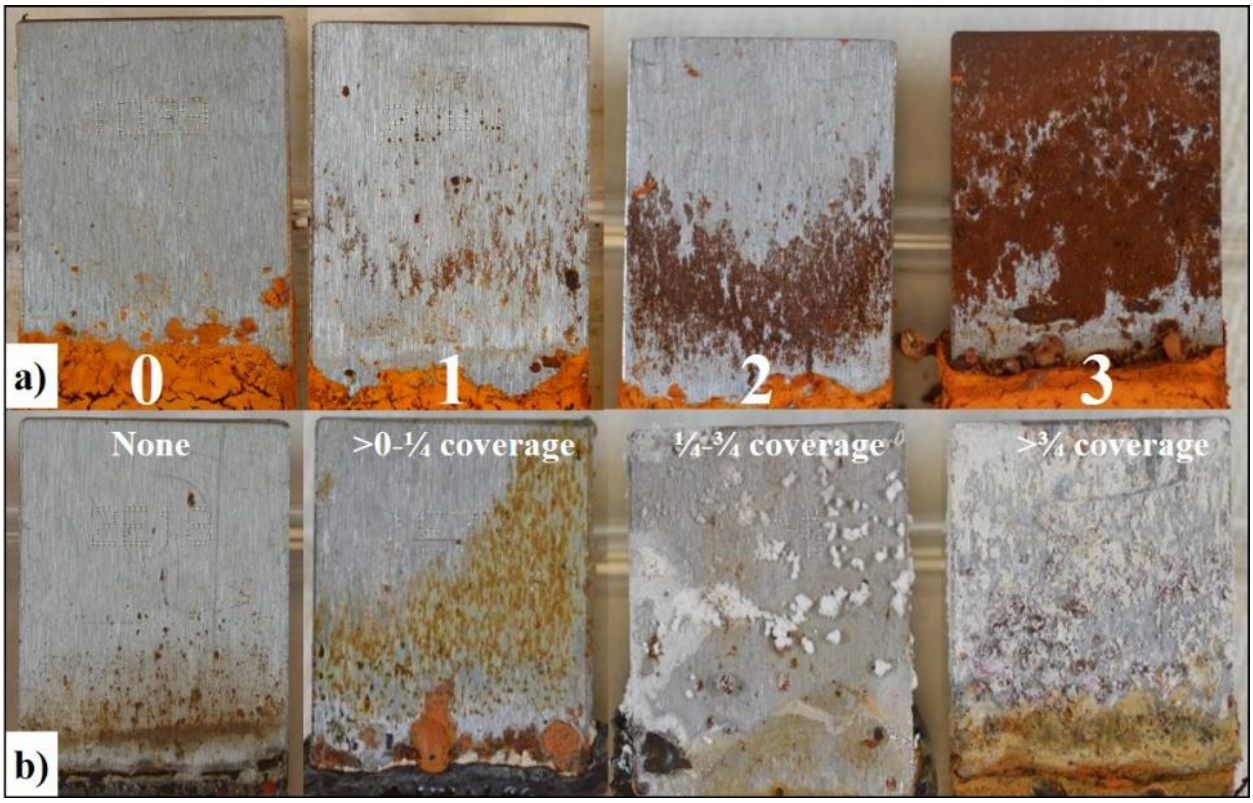

Figure 10. Representative sample coupons showing 0: No coverage; 1: >0-25% coverage, 2: 25-75% coverage, 3: >75% coverage of the coupon surface in the fuel phase of a) red rust; b) white precipitates.

White precipitates (Figure 10b) spread from the fuel/seawater interface up into the fuel layer in 87% of the samples containing HRD. These samples also had the highest corrosion rates (Figure 11). These white precipitates were present on only 9% of all coupons in F-76, and on 27% of coupons in the blended fuel. Samples with the highest amounts of coverage by white precipitates were either in aerobic or filtered aerobic bottles, implicating oxygen in the formation of the white material (Figure 10b category 3 = >75% coverage). This precipitate differed in size and texture from the fuel/seawater interface to the top of the coupon, and furthest into the fuel phase, indicating potential differences in its chemical composition. Various white precipitates examined in detail using spectrographic techniques are described below.

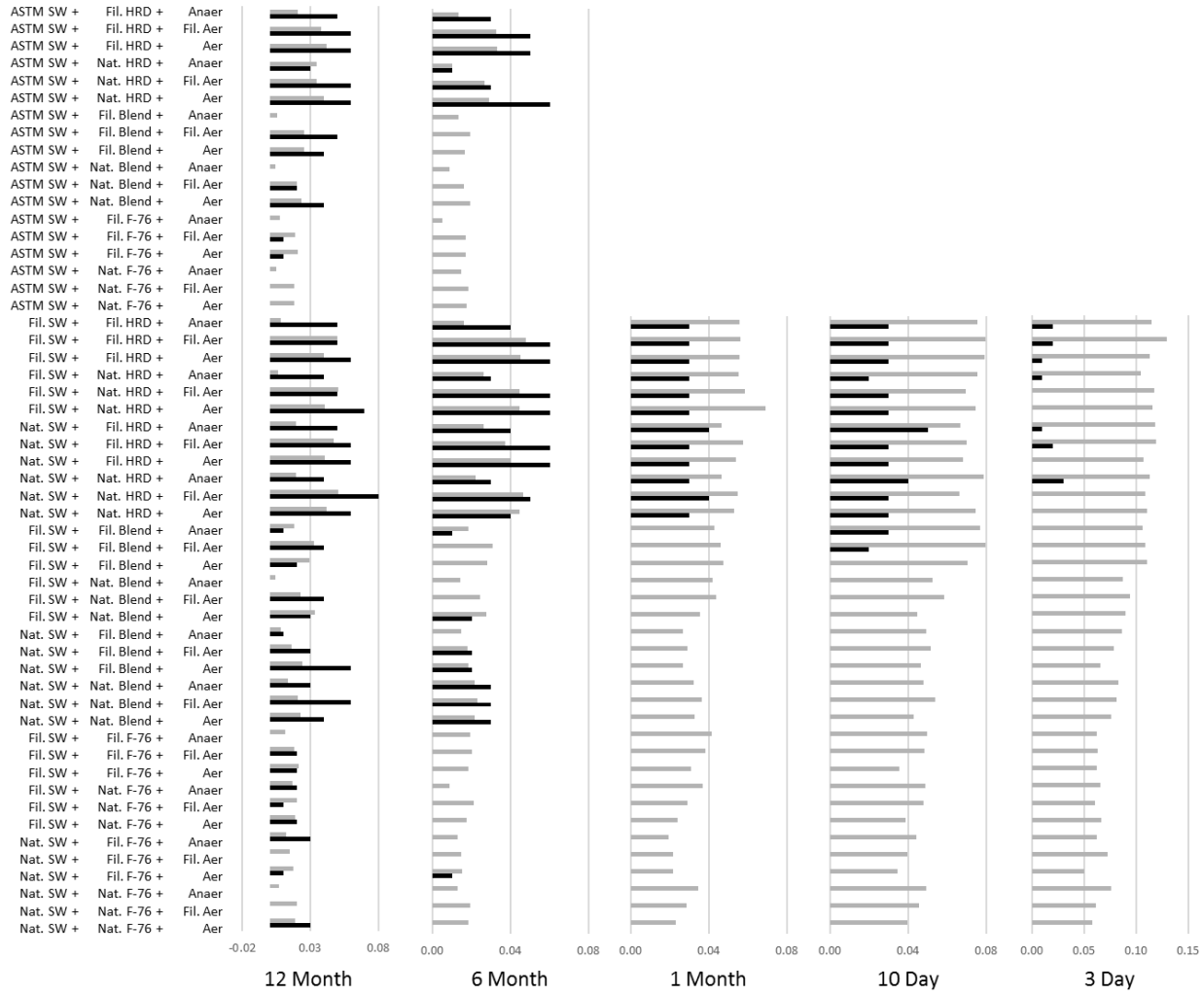

Figure 11. Comparison of corrosion rate (black) and surface coverage of coupon in fuel layer by white precipitates (grey) for the 5 exposure periods. Y-axis describes the 54 sample conditions tested. X-axis shows both corrosion rate (mm/yr) and percentage of coupon surface covered by white precipitate: 0: No coverage; 1: >0-25% coverage, 2: 25-75% coverage, 3: >75% coverage (white precipitate data was divided by 100 to adjust it to the same scale as the corrosion rate).

*Abbreviations: Nat. = Natural unfiltered; Fil. = 0.22 µm filtered; SW = seawater; ASTM SW = ASTM D1141-98 seawater; Blend = 50:50 F-76 and HRD-76 diesel blend; Aer. = aerobic; Anaer. = anaerobic

Coupons incubated anaerobically through 6 and 12 months showed lower corrosion rates and percent coverage by white particles compared to those in aerobic, and filtered aerobic conditions. There was little difference in the percent coverage by white particles between the 3 to 30 day incubated samples, regardless of whether or not they were incubated aerobically or anaerobically, most likely due to the fact that the starting solutions were not de-aerated before being put in the sample bottles. Lack of de-aeration allowed white precipitate formation until sample bottles became anaerobic sometime between 1 and 6 months of incubation. Subsequent

persistence of precipitates may explain why the white particles whose formation is oxygen-dependent were present on coupons incubated anaerobically.

Rust tubercles formed in the fuel layer of 59% of sample coupons. Cleaning revealed a corrosion pit under each tubercle (Figure 12b). Tubercles were observed even after the shortest exposure period (3 days), and although no pits were formed by this time, discoloration of the underlying metal indicated the environment in the tubercle likely differed from that in the bulk solution.

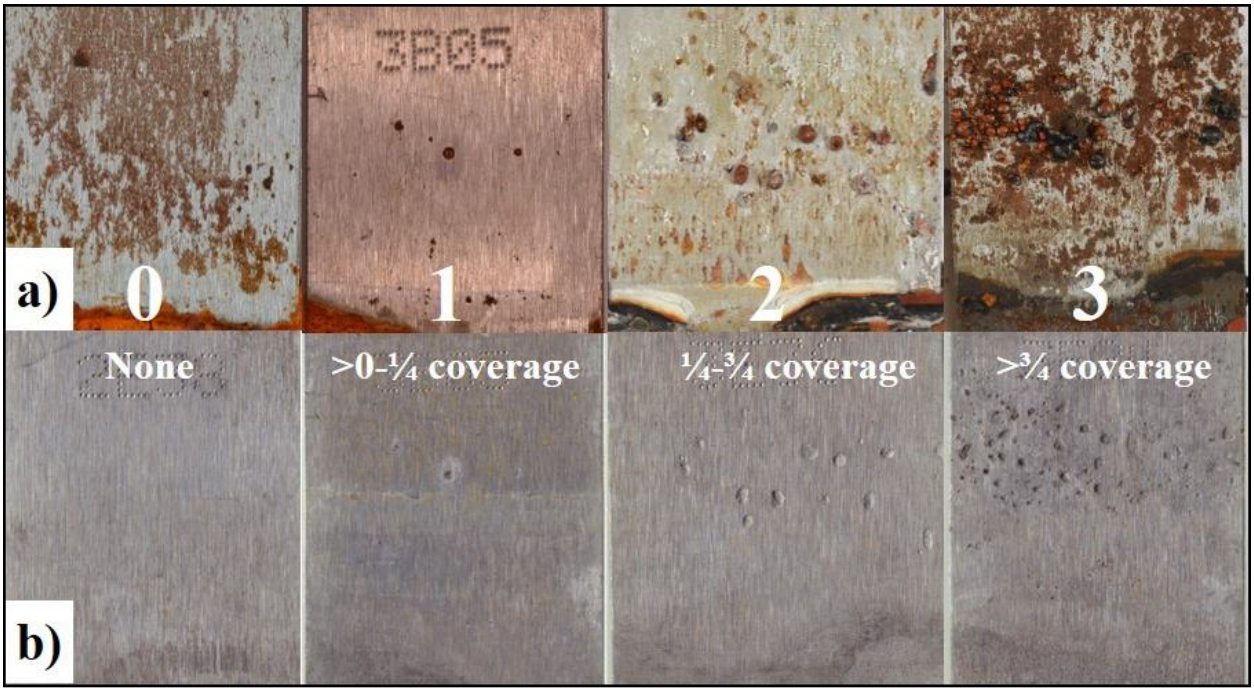

Figure 12. Representative sample coupons showing 0: No coverage; 1: >0-25% coverage, 2: 25-75% coverage, 3: >75% coverage of a) tubercles on coupon in fuel layer; b) cleaned coupons showing pits under each tubercle.

Steel coupons incubated in filtered seawater plus filtered blended fuel had the highest number/coverage of tubercles at all incubation times except 30 days. In this respect, there was an 18-day period during which the 30 day samples experienced greater temperature fluctuations during the day, and this may have contributed to this difference. Coupons in bottles incubated aerobically had more tubercle formation. Higher prevalence of rust tubercles, regardless of exposure time, was determined in HRD and blended fuel samples, suggesting increased oxygen penetration through HRD enabled more corrosion.

4.1.2.2 XRD

XRD analysis (Li, Kealoha, & Hihara, 2015) of coupon regions immersed in fuel layers determined the red rust to comprise lepidocrocite and goethite (**Error! Reference source not found.**). The white deposits examined in the 6 month HRD samples were identified as thermonatrite ($Na_2CO_3 \cdot H_2O$) and trona ($Na_3H(CO_3)_2)(H_2O)_2$). Analysis of coupon regions in the seawater layer all showed similar corrosion products, with an inner black magnetite layer and an outer orange lepidocrocite layer.

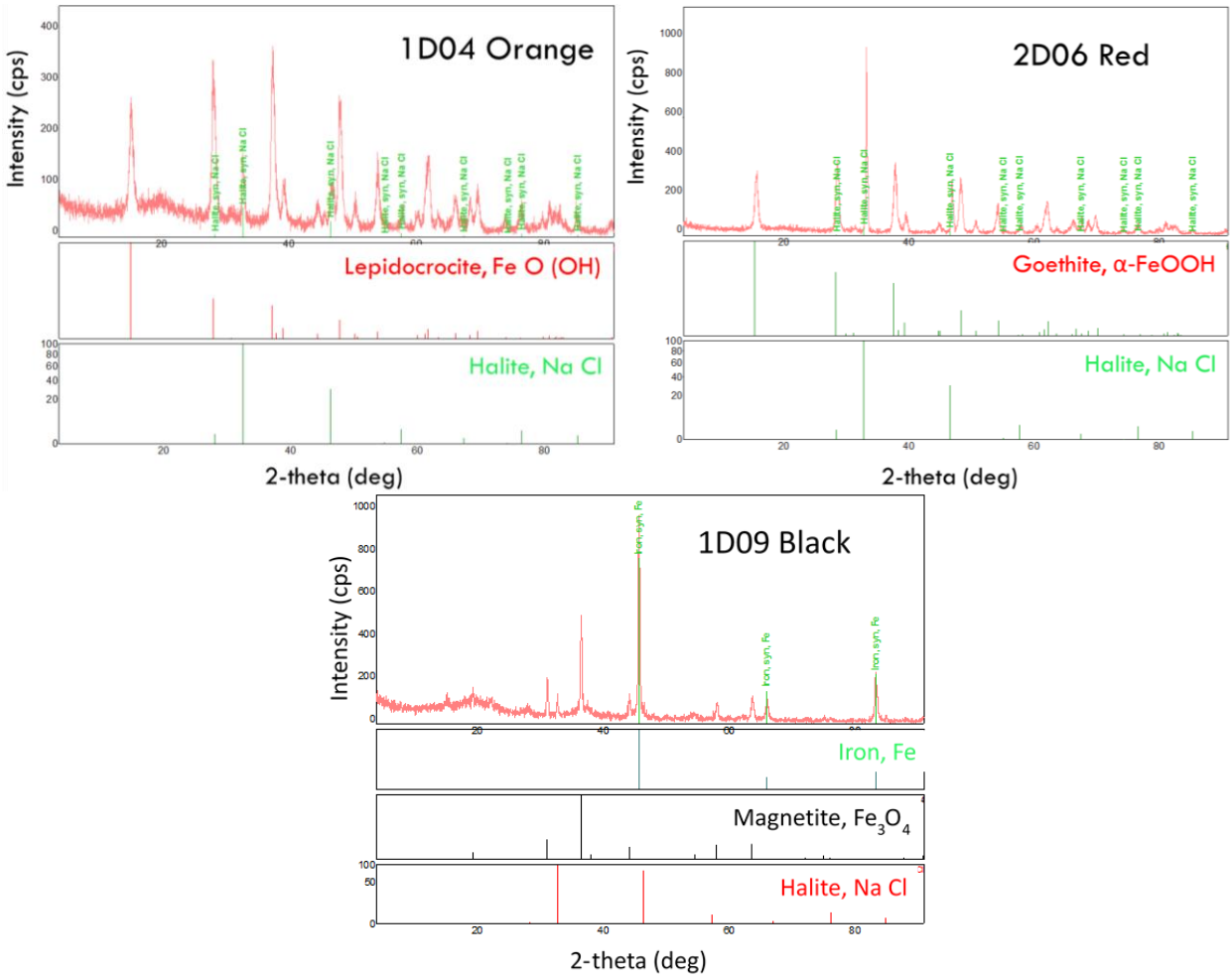

Figure 13. XRD spectra identifying colored corrosion products, a) orange is lepidocrocite, b) Red is goethite, c) black is magnetite, Y-axis units, 'cps' is 'counts per second'

4.1.2.3 Raman spectroscopy

Raman analysis was conducted on at least one coupon from each triplicate set incubated in each environmental condition (Li et al., 2015).

Orange rust (Figure 9a) was confirmed through Raman spectroscopy to be lepidocrocite, with strong signals at 248, 303 370, 520 cm^{-1}. The red rust (Figure 10a) was weakly confirmed by the same technique to be goethite, with signals at 306 and 384 cm^{-1}.

Signal analysis of the white crystalline deposits indicated the presence of mainly calcium and sodium carbonates. However, a smooth white deposit was often seen at the fuel/seawater interface (Figure 15a); this was identified as magnesium hydroxide ($Mg(OH_2)$), a.k.a. brucite, or milk of magnesia, with a relatively weak and broad peak at 448 cm^{-1} (Figure 14a). Small round crystals immediately above the white strip (Figure 14b & Figure 15b) were identified as calcium carbonate ($CaCO_3$), a.k.a. calcite or aragonite. Larger white particles dominated further up the coupon and into the fuel layer. These round and irregular-shaped crystals showed a Raman signal at 1083 cm^{-1} and were identified as sodium carbonate (Na_2CO_3) (Figure 14c-d and Figure 15c). Columnar crystals dominating at the top of the coupon furthest from the seawater, were identified as trisodium hydrogendicarbonate dehydrate ($Na_3H(CO_3)\cdot(H_2O)_2$, at 1064 and 3440 cm^{-1}, a.k.a. trona (Figure 14e-f & Figure 15d), which matched the XRD results.

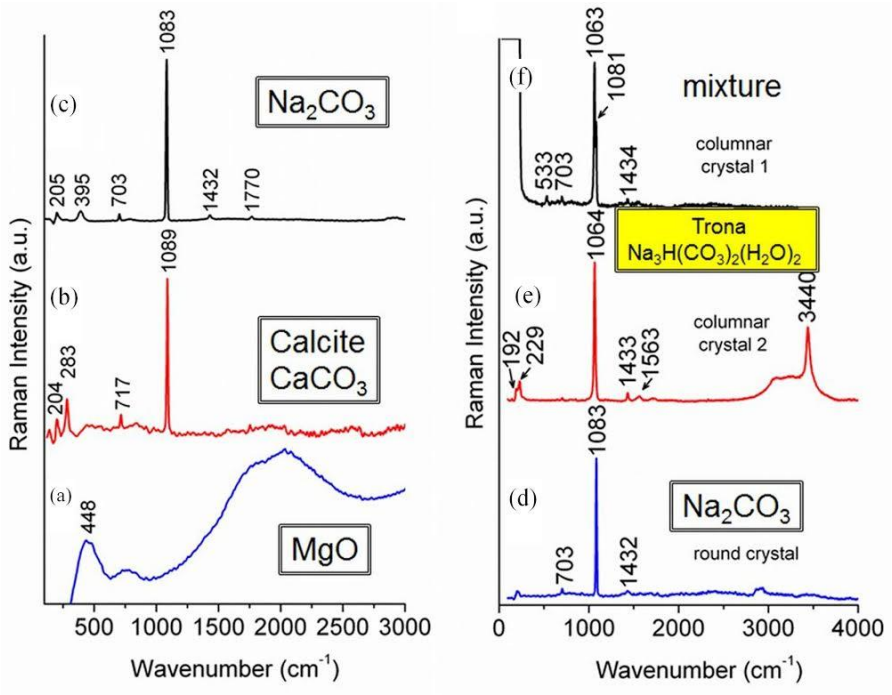

Figure 14. Raman spectra of white deposits formed on sample 3D35 incubated 6 months in seawater/HRD-76 in 'filtered' aerobic conditions: a) from smooth white deposit at fuel/seawater interface; b) from small round white particles in fuel layer; c) from larger white crystal in fuel layer; d) different large white crystal in fuel layer; e) columnar white crystals at top of coupon in fuel layer; f) mixture of different columnar crystal at top of fuel layer (Li et al., 2015).

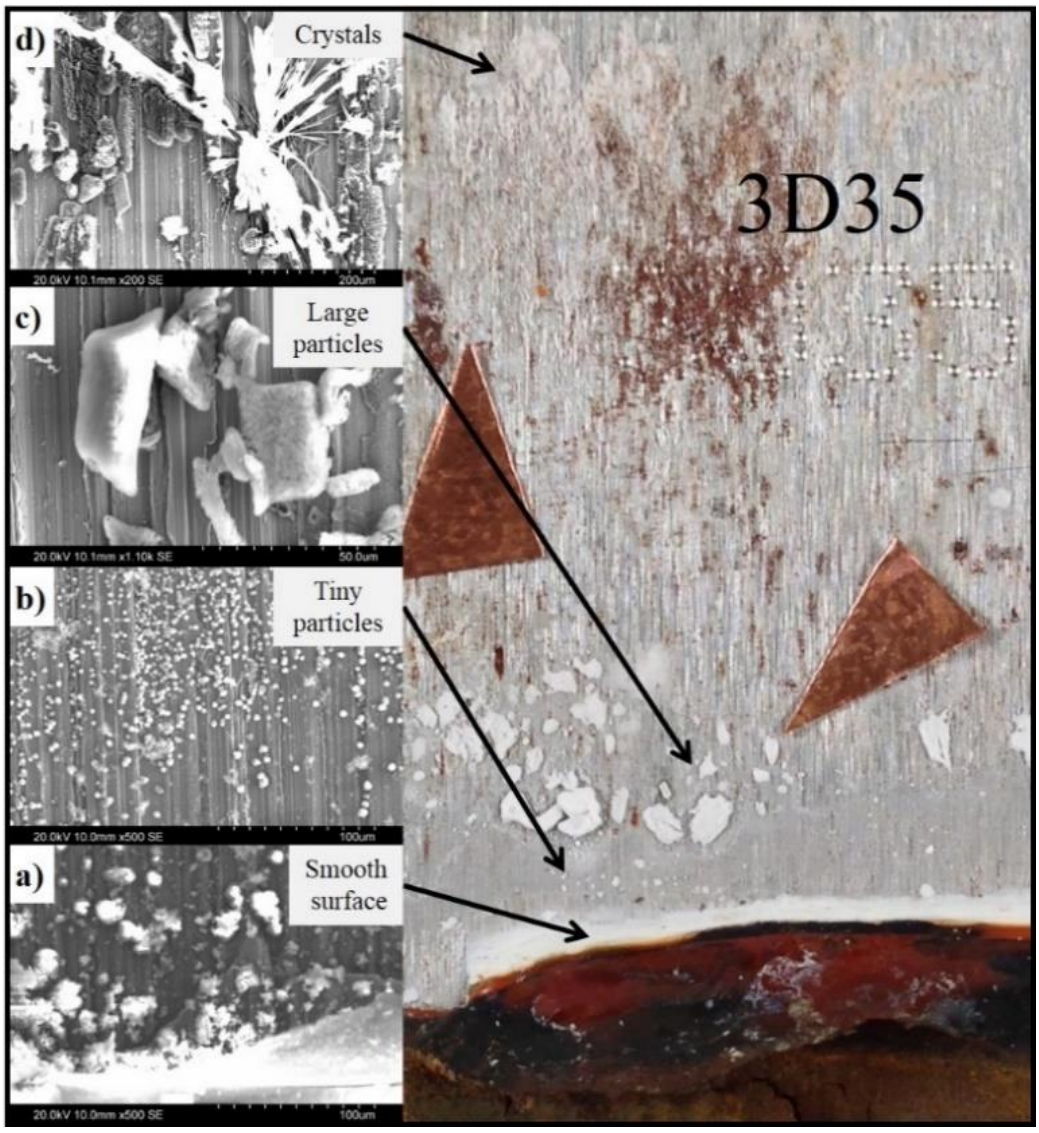

Figure 15. SEM images of representative white carbonate particles from sample coupon 3D35 incubated 6 months in seawater/HRD, 'filtered' aerobic conditions: a) magnesium hydroxide; b) calcium carbonate; c) sodium carbonate; d) trona. Copper tape triangles were used to orient the stage during SEM analysis (Li et al., 2015).

4.1.2.4 SEM with EDXA

SEM micrographs and elemental composition (obtained using EDXA, Figure 16) were acquired for orange, black, and red rust samples (Li et al., 2015).

EDXA analysis (Li et al., 2015) of the orange rust (Figure 16a) showed the most pure formation of rust with 26.78% atomic iron and 63.91% atomic oxygen content, *i.e.*, iron (III) oxide-hydroxide, γ-FeO(OH), confirming lepidocrocite. The minimal amount of other atoms present was presumed to be from seawater. The black magnetite corrosion products contained much

higher concentrations of sodium and magnesium (Figure 16b), indicating that the chloride components of the salts in the seawater have migrated to the steel/rust interface during the corrosion process. The red rust that formed in the fuel layer (Figure 16c) was typically observed in F-76 containing samples. These had a larger sodium signal (3.95 atomic %) indicating that cathodic regions resided in the fuel layer and the anodic regions were in the seawater layer. Most of the base metal corrosion occurred in the anodic seawater layer. There was a very high carbon signal during red rust examination, *i.e.*, 42.8% C, which was likely fuel residue. When analyzing the differently shaped white particles deposited on different regions of the coupon in the fuel layer (Figure 15), EDXA results supported XRD and Raman findings.

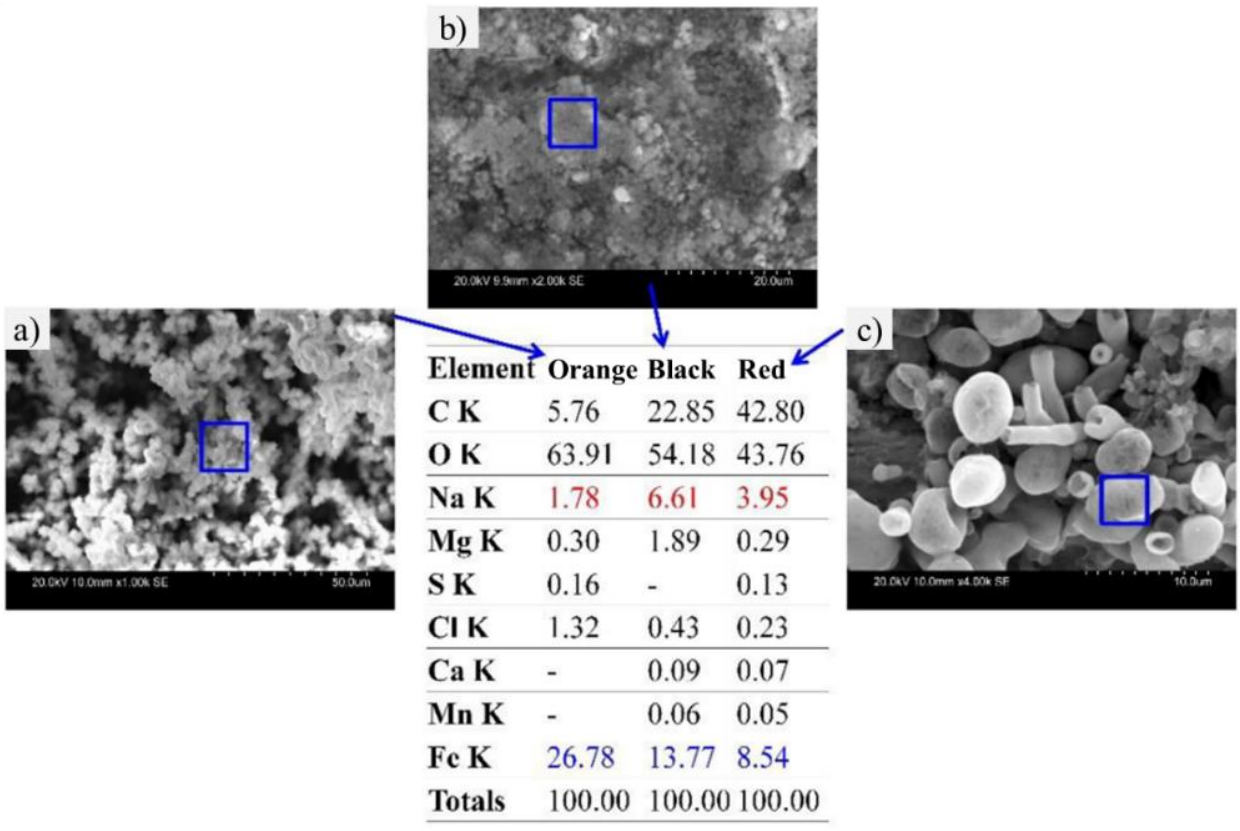

Element	Orange	Black	Red
C K	5.76	22.85	42.80
O K	63.91	54.18	43.76
Na K	1.78	6.61	3.95
Mg K	0.30	1.89	0.29
S K	0.16	-	0.13
Cl K	1.32	0.43	0.23
Ca K	-	0.09	0.07
Mn K	-	0.06	0.05
Fe K	26.78	13.77	8.54
Totals	100.00	100.00	100.00

Figure 16. SEM images with EDXA results of morphological and elemental analysis of corrosion products formed on steel immersed in seawater/F-76 for 6 months: a) orange lepidocrocite corrosion; b) black magnetite corrosion; c) red goethite corrosion (Li et al., 2015).

4.2 Biological analysis

4.2.1 Identification of cultivated microbes

4.2.1.1 General & selective media

Of all 3882 inoculated media plates/tubes, 1779 (46%) showed growth. The total number of plates with growth did not significantly decrease over time (Table 9). However more of the slower-growing organisms were recovered from R2A, BH, and PDA at after the longer incubation periods. Nutrient-rich culture media (MA & TSA) had the highest numbers of plates with growth per sample. Although much time and effort were needed to complete the cultivation-based approaches, visually distinct microbes did grow on different media (Figure 17).

Table 9. Number and percentage of inoculated culture media showing microbial growth from all samples

Media	3 d	10 d	1 m	6 m	12 m
MA	93 (31.1)	87 (26.6)	71 (23.8)	90 (20.0)	86 (21.3)
TSA	59 (19.7)	67 (20.5)	62 (20.8)	83 (18.4)	72 (17.8)
R2A	47 (15.7)	42 (2.8)	61 (20.5)	87 (19.3)	77 (19.1)
BH	28 (9.4)	42 (12.8)	42 (14.1)	53 (11.8)	61 (15.1)
PDA	20 (6.7)	50 (15.3)	33 (11.1)	83 (18.4)	63 (15.6)
SAPI	52 (17.4)	39 (11.9)	29 (9.7)	55 (12.2)	45 (11.1)

4.2.1.2 Morphology

Approximately 500 subcultures were prepared from the six different culture media on the basis of visual observations of colony characteristics. Of those, 248 were from aerobic (open cap) bottles that were later disregarded since the surroundings at the outdoor exposure site were likely to have introduced allochthonous material not representative of what would enter a ship's ballast tank. Colony isolation and subsequent identification therefore focused on those from the anaerobic and filtered aerobic bottles, which yielded 85 putatively unique *Bacteria* isolates and 40 unique microbial eukaryotes.

It was often difficult to distinguish unique subcultures based on their morphology alone, especially since most looked different depending on which medium they were grown on, or at was the growth stage of the culture. The visually unique cultivated microbes offered a glimpse

into microbial community diversity present at the end of each incubation period. Natural unfiltered seawater yielded the greatest colony diversity, cf. number of colonies, whether in anaerobic or filtered aerobic growth conditions. Filtered seawater samples yielded significantly fewer unique colony types, all of which were presumed to have come from microbes present in the fuel. Cultivation approaches using filtered seawater negative control bottles after each of the five exposure times resulted in 1-2 unique colonies on MA plates. Presumably, filtering seawater through 0.22 µm pore size membranes could not remove all marine microbes; future work in this field should employ no larger than 0.1 µm pore size filters.

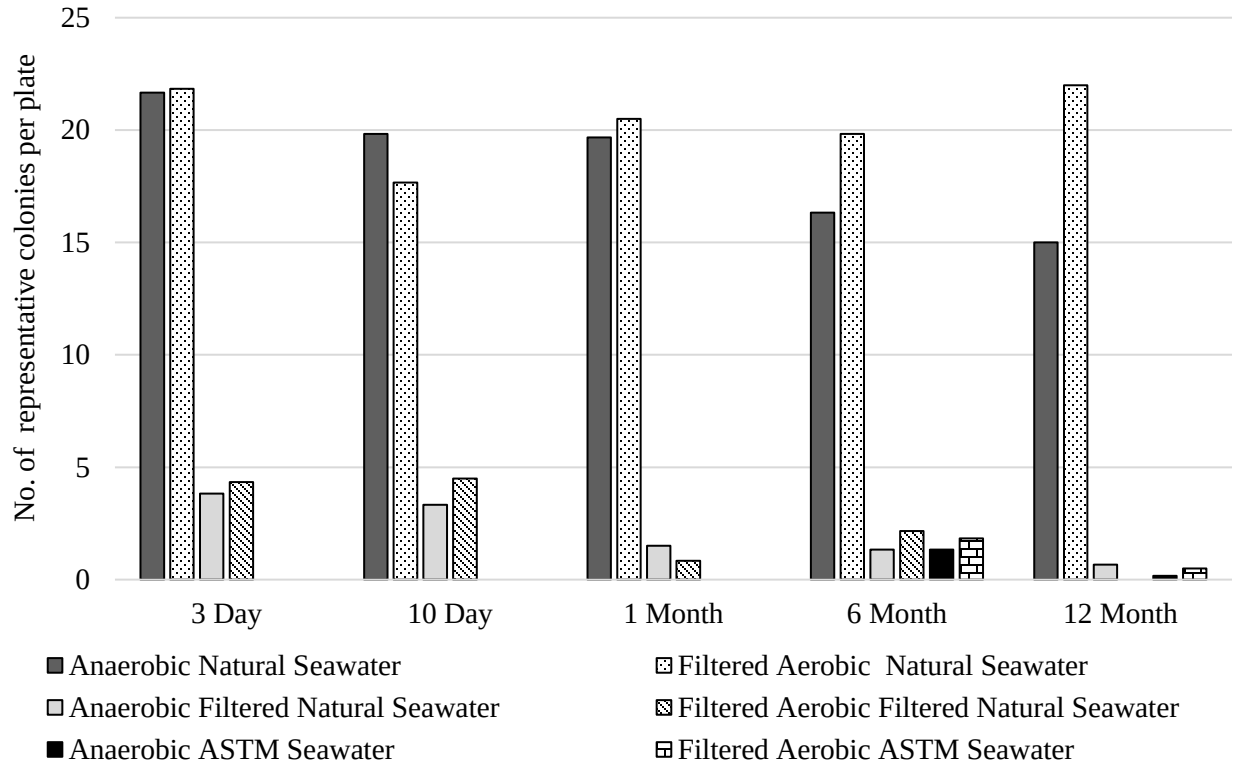

Figure 17. Mean number of unique colony types identified per water source

4.2.1.1 Isolate identification through ribosomal gene sequencing

Sanger sequencing of the 16S and 18S rRNA enabled putative genus-level identification of 25 bacteria (Table 10) and 27 fungi (Table 11) cultivated from the simulated environments. Isolates belonged to the *Actinobacteria* (15%), *Firmicutes* (6%), *Proteobacteria* (22%), *Ascomycota* (50%), and *Basidiomycota* (6%). This sequencing helped sort the cultures and reduce duplication, and provide insights into which were the most dominant culturable microbes in the samples.

Table 10. Putative identification of *Bacteria* cultures based on BLAST analysis

Subculture	BLAST result 16S ribosomal RNA	Accession #	% sequence identity	Sequence length
AB20	*Mycobacterium anyangense* QIA-38 *Mycobacterium iranicum* M05 *Mycobacterium pallens* czh-8 *Mycobacterium duvalii* ATCC 43910	NR_136492 NR_117909 NR_043760 NR_026073	99.9	820
BB100	*Mycobacterium poriferae* ATCC 35087	NR_025235	99.7	628
SW19			99.9	701
SW14			99.6	825
EB20	*Terracoccus luteus* DSM 44267	NR_026412	99.3	440
HRD01	*Methylobacterium hispanicum* DSM 16372	NR_112613	99.4	812
EB06	*Rhizobium azibense* 23C2	NR_133841	97.1	795
BB101	*Stappia indica* B106	NR_116431	99.9	799
BB102	*Thalassospira xiamenensis* M-5 = DSM 17429 *Thalassospira permensis* SMB34	CP004388 NR_116841	99.8	805
SW12	*Novosphingobium malaysiense* MUSC 273	NR_126280	99.9	771
EF10	*Novosphingobium indicum* H25	NR_044277	99.9	792
AB86	*Alteromonas macleodii* ATCC 27126	NR_114053	99.0	403
CB13	*Alcanivorax xenomutans* JC109	NR_133958	99.9	812
EB17			99.9	697
EB18			99.7	308
BB02	*Alcanivorax gelatiniphagus* MEBiC08158	NR_136483	99.9	813
BB45	*Alcanivorax borkumensis* SK2	NR_074890	99.1	114
SW16			99.7	328
SW23			99.5	798
SW24			99.7	674
SW25			99.5	812
SW27b			99.5	825
BB103	*Halomonas meridiana* NBRC 15608 *Halomonas johnsoniae* T68687 *Halomonas hamiltonii* W1025 *Halomonas axialensis* Althf1 *Halomonas meridiana* DSM 5425 *Halomonas aquamarina* DSM 30161	NR_113779 NR_115090 NR_115089 NR_027219 NR_042066 NR_042063	100	710
AB18	*Bermanella marisrubri* RED65	NR_042750	97.0	635

Table 11. Putative identification of microbial eukaryotes based on BLAST analysis

Subculture	BLAST result 18S ribosomal RNA	Accession #	% Sequence identity	Sequence length
EF14	*Cladosporium velox* CBS:119417	DQ780937	99.8	967
DF32	*Aureobasidium pullulans* CBS 584.75	EU682922	99.9	870
DF33			99.9	870
DF38	*Alternaria malorum var. polymorpha* STE-U 4570	AY251129	99.4	837
DF13	*Eurotium herbariorum*	AB008402	100	263
DF47	*Aspergillus proliferans* WB1908	AB002083	99.7	867
EF16			99.7	922
BF46			99.2	851
BF48	*Emericella nidulans*	AB008403	99.6	901
BF08			99.2	476
DF45			99.4	908
CF05	*Penicillium roqueforti* ATCC 10110	GQ458035	100	152
AF15			100	777
DF46	*Penicillium limosum*	EF411061	99.8	902
EF09	*Talaromyces viridis* CBS 114.72	AB024587	99.2	911
DF43			99.2	922
EF08	*Pichia philogaea* NRRL Y-7813 *Candida diddensiae*, JCM 9598	JQ698914 AB013508	98.4	761
DF22	*Clitopilus brunnescens*	JF706314	94.5	767
BF24	*Flavodon cf. flavus* Hulcr 6853	KR119078	99.0	913
DF29	*Resinicium mutabile* FP102989	DQ834917	95.3	872
DF39			98.1	933
DF44			97.7	925
ASTM01	*Sporidiobolus salmonicolor*	AB021697	99.5	655
AB101			99.8	497
CB14			99.7	773
BF34	*Wallemia canadensis* MUCL-15061	KJ494582	99.7	760
DF35			99.7	813

One such isolate, HRD01, identified as Alphaproteobacterium *Methylobacterium hispanicum* (99.39% sequence identity), was cultivated directly from HRD after fuel shipment was received.

4.2.2 Culture-independent analysis of the microbial community

4.2.2.1 DNA extraction

Community DNA was extracted from 214 of 648 experimental samples, comprising 176 sample bottles and 38 negative control bottles (Appendix 1).

4.2.2.2 Illumina MiSeq next generation sequencing

4.2.2.2.1 BaseSpace analysis of 16S rRNA gene sequence data

BaseSpace 16S Metagenomics software identified 21,122,267 reads, of which 20,051,310 passed quality control filtering; 77.8% of filtered reads were assigned to unique OTUs. Microbial community taxonomic composition in the 246 sequenced samples is shown in Table 12.

Table 12. 16S-based assignment of sequences per exposure period

***Archaea*/*Bacteria* taxonomic level**	**3 d**	**10 d**	**1 m**	**6 m**	**12 m**
Phylum	23	23	22	18	19
Class	38	42	37	32	32
Order	80	86	72	64	63
Family	178	196	145	148	132
Genus	411	440	313	348	299

At the Class level, Gammaproteobacteria affiliated sequences dominated the shorter incubation periods up to 1 month (Figure 18). Thereafter, Alphaproteobacteria and Bacilli 16S rRNA gene fragment abundance increased in the longer incubations. The 16S rRNA gene sequence read count comprised 45 *Bacteria* and *Archaea* classes per incubation period (Table 13).

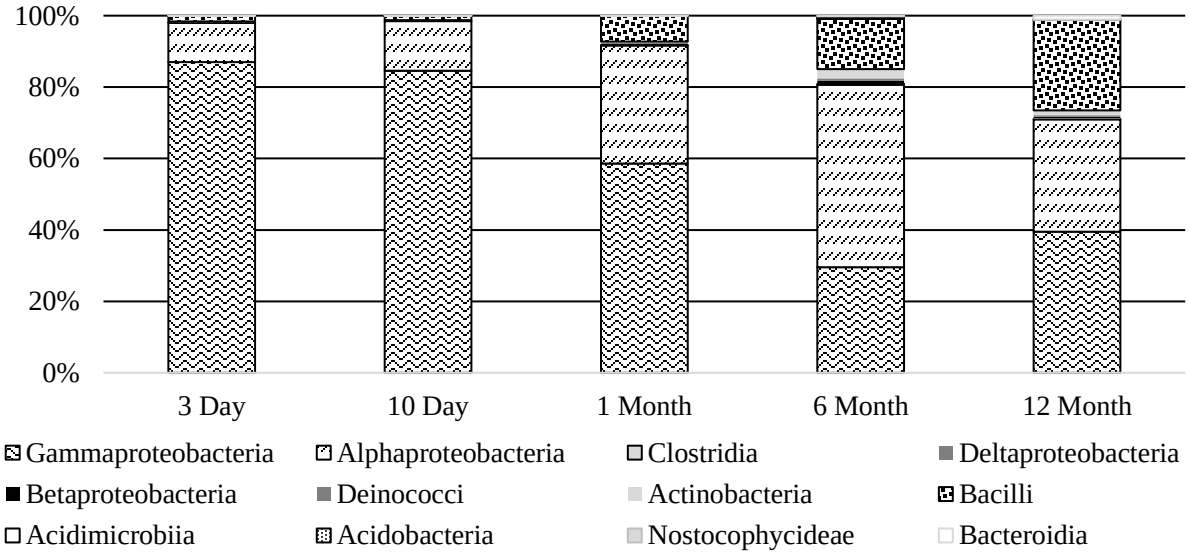

Figure 18. Taxonomic Class distribution of 16S V6 reads from each incubation period. Only classes with >0.1% of amplicons in a single incubation period are displayed.

Table 13. Sequences per taxonomic class per incubation period detected by BaseSpace 16S Metagenomics analysis. Numbers represent abundance of 16S genes identified to the class level.

Class	3 d	10 d	1 m	6 m	12 m
Acidimicrobiia	137	7	2	473	1
Acidobacteria	43	52	6	488	19
Actinobacteria	2,285	1,428	785	3,855	2,115
Alphaproteobacteria	159,681	269,202	78,185	76,181	49,817
Anaerolineae		5	1		
*Archaea*_Halobacteria	70	137	200	687	305
*Archaea*_Thaumarchaeota	3	5	1		
Bacilli	22,776	24,628	17,167	21,044	40,289
Bacteroidia	108	16	62	79	1,668
Betaproteobacteria	1,821	1,324	984	1,341	596
Brocadiae		1			1
Caldithrixae	13	15	3	72	2
Chlamydiia	4	6	1		
Chlorobia	4	7		74	1
Chrysiogenetes	3		1		
Chthonomonadetes					5
Clostridia	398	588	108	322	227
Deferribacteres	4	3	1		1
Deinococci	735	410	516	851	727
Deltaproteobacteria	293	478	32	106	361
Epsilonproteobacteria	6	12	4	93	5
Erysipelotrichi		1		98	3
Flavobacteriia	694	176	108	114	121
Fusobacteria		5	1		
Gammaproteobacteria	1,264,732	1,637,610	138,617	44,192	62,591
Ktedonobacteria	3	9	1		2
Leptospirae	34	33	1	2	
Mollicutes	20	24	3	9	4
Nitriliruptoria	11				
Nitrospira	14	8	2	1	
Nostocophycideae	43	29	1	221	67
Opitutae	365	540	50	24	35
Oscillatoriophycideae	27	57	3	2	3
Pedosphaerae	1	4			
Planctomycetia	6	6	18	2	
Rubrobacteria		25		6	3
Sphingobacteriia	812	1,043	105	60	142
Spirochaetes	7	7	8		2
Synechococcophycideae	108	79	14	2	4
Synergistia	24	8	3	4	2
Thermobacula	1	2	1	1	
Thermodesulfobacteria	2	1			
Thermoleophilia		21	7	14	
Thermotogae	3	12	2	2	1
Verrucomicrobiae	119	150	25	11	11
Virus_Group II	3,175	4,378	514	293	365
% Total Class Count	**37%**	**49%**	**6%**	**4%**	**4%**

Five hundred and sixty-two genera were identified by the Illumina 16S Metagenomics analysis pipeline (Appendix 5-Appendix 9). One hundred and ninety of 299 genera persisted in samples for the duration of the experiment, meaning they were detected at all 5 exposure periods (Table 14).

Table 14. Number of genera that only persisted until the specified incubation duration

***Archaea*/*Bacteria* genera present**	**3 d**	**10 d**	**1 m**	**6 m**	**12 m**
Detected after only one incubation period	27	41	12	30	15
Two incubation periods	85				
Three incubation periods	76				
Four incubation periods	85				
All five incubation periods	190				

Oleispira-affiliated sequences numerically dominated filtered seawater samples at the end of the three-day incubation period, regardless of fuel type, or whether the samples had vented or tightened caps (Figure 19, Table 15). These sequences continued to dominate in the 10-day samples (Figure 20), but by 30 days *Bacillus*-affiliated sequences dominated six of the 12 filtered seawater samples, while *Oleispira* dominated the other six (Figure 21). Five of the aforementioned six *Oleispira* samples were incubated anaerobically, which in itself presents quite a conundrum given *Oleispira* is considered an aerobe, and one of the two known species in the genus is not mesophilic (Yakimov et al., 2003). At the end of the 6-month incubation, *Oleispira*-affiliated sequences were only dominant in two of 48 samples; both samples were anaerobic (Figure 22). In contrast, *Bacillus* dominated 23 of 48 samples, nearly all of which were either filtered seawater or ASTM. At 12 months, *Bacillus* continued to dominate the filtered and ASTM seawater samples, whereas *Oleispira* was only dominant in one sample, which again was anaerobic (Figure 23).

In natural seawater, *Alteromonas* and *Oleibacter* dominated the 3 and 10 day samples. There was more community diversity in the 1 month samples than in shorter incubations; dominant genera in terms of number of sequences detected in those samples were *Parvibaculum*, *Alteromonas* and *Jannaschia* (Table 15). At the end of the 6-month incubation, *Parvibaculum*-affiliated sequences were numerically dominant in 10 of 17 natural seawater samples, regardless of fuel type. By 12 months, *Parvibaculum* (7) and *Bacillus* (6) dominated the communities of the 16 natural seawater samples.

Table 15. 16S rRNA gene copy counts of the top 25 most abundant genera among the 190 genera detected of all five incubation periods

3 d		10 d		1 m		6 m		12 m	
Alteromonas	475,460	*Alteromonas*	546,733	*Oleispira*	108,976	*Parvibaculum*	71,882	*Parvibaculum*	67,164
Oleibacter	351,399	*Oleispira*	396,099	*Microbulbifer*	37,448	*Alcanivorax*	64,167	*Marinobacter*	45,096
Oleispira	219,657	*Oleibacter*	352,728	*Hyphomonas*	21,207	*Bacillus*	21,609	*Bacillus*	27,018
Jannaschia	82,863	*Microbulbifer*	146,438	*Jannaschia*	17,848	*Thalassospira*	18,471	*Paracoccus*	7,417
Microbulbifer	81,031	*Jannaschia*	138,074	*Alteromonas*	17,171	*Acinetobacter*	8,213	*Halomonas*	7,114
Alcanivorax	32,826	*Candidatus Endobugula*	48,927	*Bacillus*	16,378	*Paracoccus*	7,387	*Anoxybacillus*	4,945
Candidatus Endobugula	28,946	*Alcanivorax*	32,934	*Phyllobacterium*	12,659	*Halomonas*	7,005	*Pseudomonas*	3,504
Hyphomonas	14,564	*Hyphomonas*	25,634	*Alcanivorax*	8,438	*Rhodovulum*	6,440	*Acinetobacter*	2,619
Bacillus	13,510	*Bacillus*	14,111	*Oleibacter*	8,159	*Phyllobacterium*	5,162	*Staphylococcus*	2,340
Halomonas	9,579	*Ruegeria*	12,468	*Halomonas*	5,615	*Telmatospirillum*	4,206	*Corynebacterium*	1,920
Maricaulis	7,472	*Halomonas*	8,599	*Thalassospira*	3,550	*Amaricoccus*	3,420	*Prevotella*	1,657
Pseudomonas	4,912	*Phyllobacterium*	7,697	*Anoxybacillus*	3,119	*Hyphomonas*	3,320	*Roseospira*	1,619
Ruegeria	4,109	*Marinobacter*	7,496	*Amaricoccus*	3,047	*Anoxybacillus*	3,044	*Oleispira*	1,479
Ochrobactrum	3,834	*Phaeobacter*	7,391	*Pseudomonas*	2,370	*Oleispira*	2,095	*Hyphomicrobium*	1,312
Phyllobacterium	3,668	*Pseudomonas*	5,470	*Hirschia*	2,295	*Pseudomonas*	2,048	*Virgibacillus*	1,184
Saccharospirillum	3,593	*Dinoroseobacter*	5,157	*Parvibaculum*	2,100	*Alicyclobacillus*	2,037	*Paenibacillus*	1,168
Acinetobacter	2,975	*Vibrio*	4,690	*Sphingomonas*	2,013	*Mesorhizobium*	2,024	*Alcanivorax*	1,074
Anoxybacillus	2,286	*Maricaulis*	4,626	*Ruegeria*	1,990	*Roseospira*	1,845	*Jannaschia*	1,045
Thalassospira	2,004	*Sphingomonas*	4,237	*Acinetobacter*	1,652	*Thermus*	1,528	*Thermus*	880
Vibrio	1,804	*Thalassospira*	3,988	*Telmatospirillum*	1,525	*Corynebacterium*	1,359	*Phenylobacterium*	870
Marinobacter	1,728	*Anoxybacillus*	3,406	*Stenotrophomonas*	1,303	*Jannaschia*	1,312	*Hyphomonas*	780
Rhodovulum	1,700	*Octadecabacter*	2,949	*Marinobacter*	1,050	*Virgibacillus*	1,297	*Pontibacillus*	761
Corynebacterium	1,679	*Acinetobacter*	2,773	*Virgibacillus*	728	*Staphylococcus*	1,264	*Telmatospirillum*	650
Hirschia	1,500	*Anaerospora*	2,692	*Thermus*	638	*Pontibacillus*	1,054	*Alicyclobacillus*	559
Anaerospora	1,475	*Rhodovulum*	2,507	*Anaerospora*	629	*Phycicoccus*	1,039	*Marinibacillus*	515

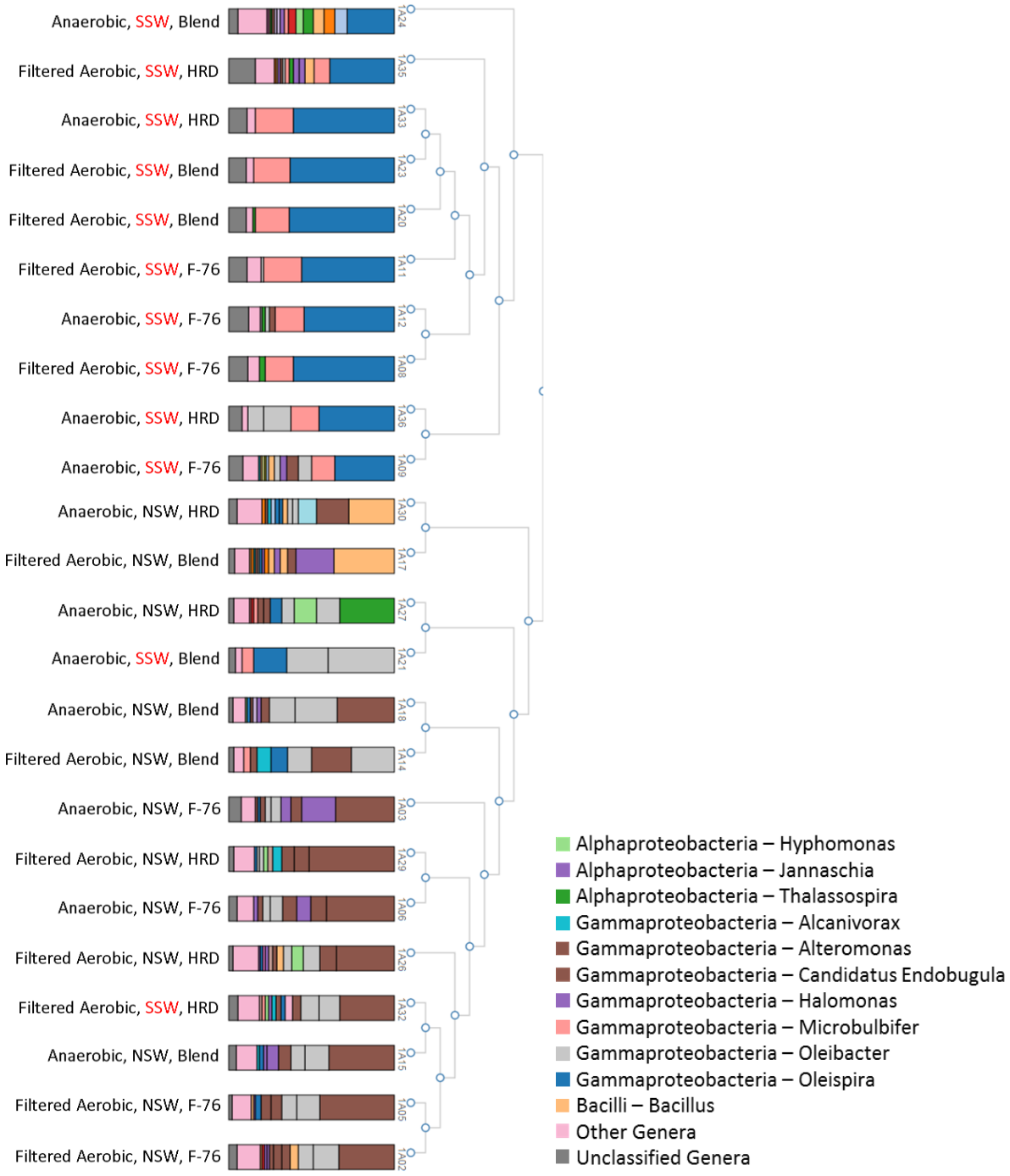

Figure 19. Dendrogram of BaseSpace 16S Metagenomics analysis of 3 day samples with top 11 genera displayed in color key

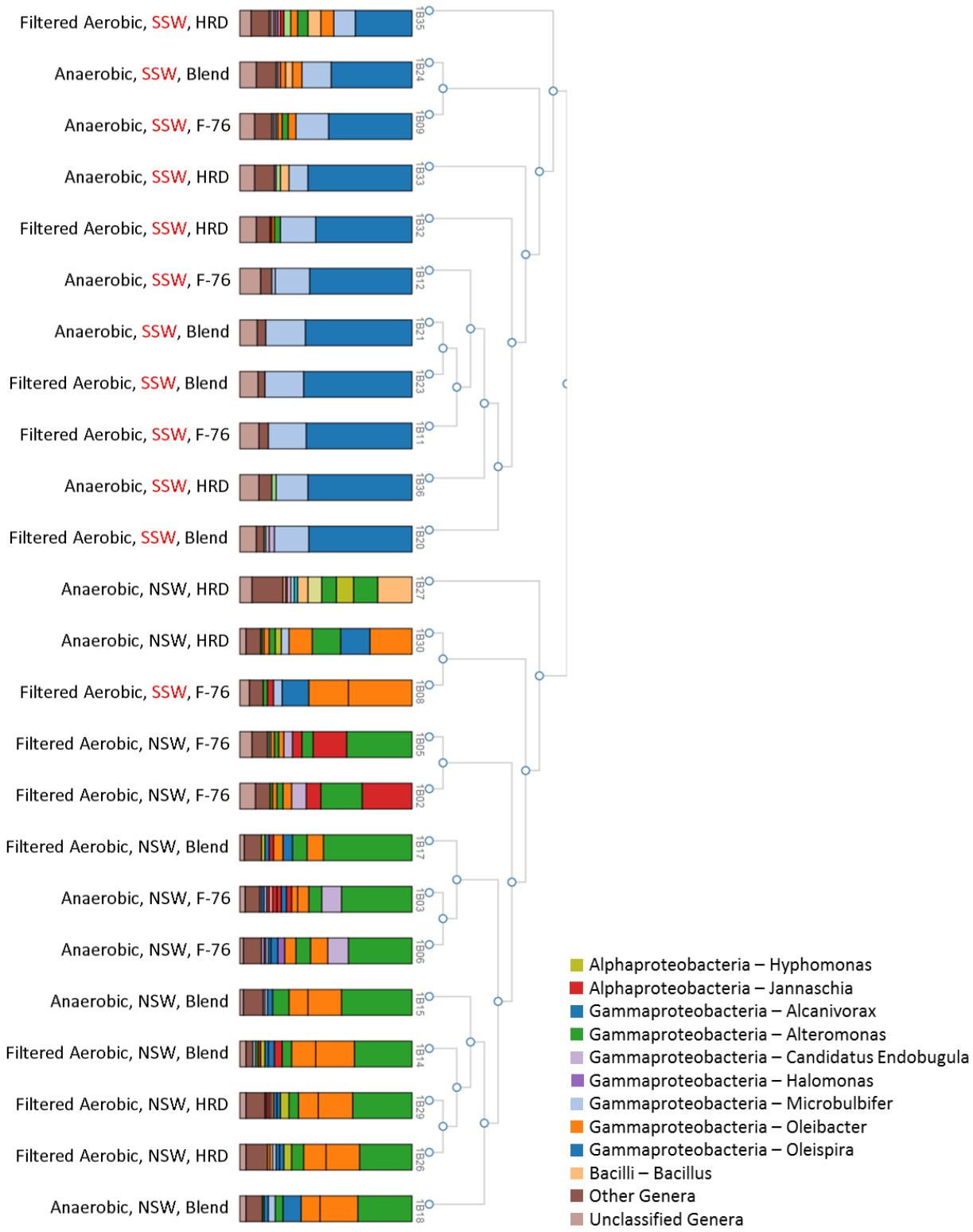

Figure 20. Dendrogram of BaseSpace 16S Metagenomics analysis of 10 day samples with top 10 genera displayed in color key

Figure 21. Dendrogram of BaseSpace 16S Metagenomics analysis of 1 month samples with top 11 genera displayed in color key

Figure 22. Dendrogram of BaseSpace 16S Metagenomics analysis of 6 month samples with top 12 genera displayed in color key

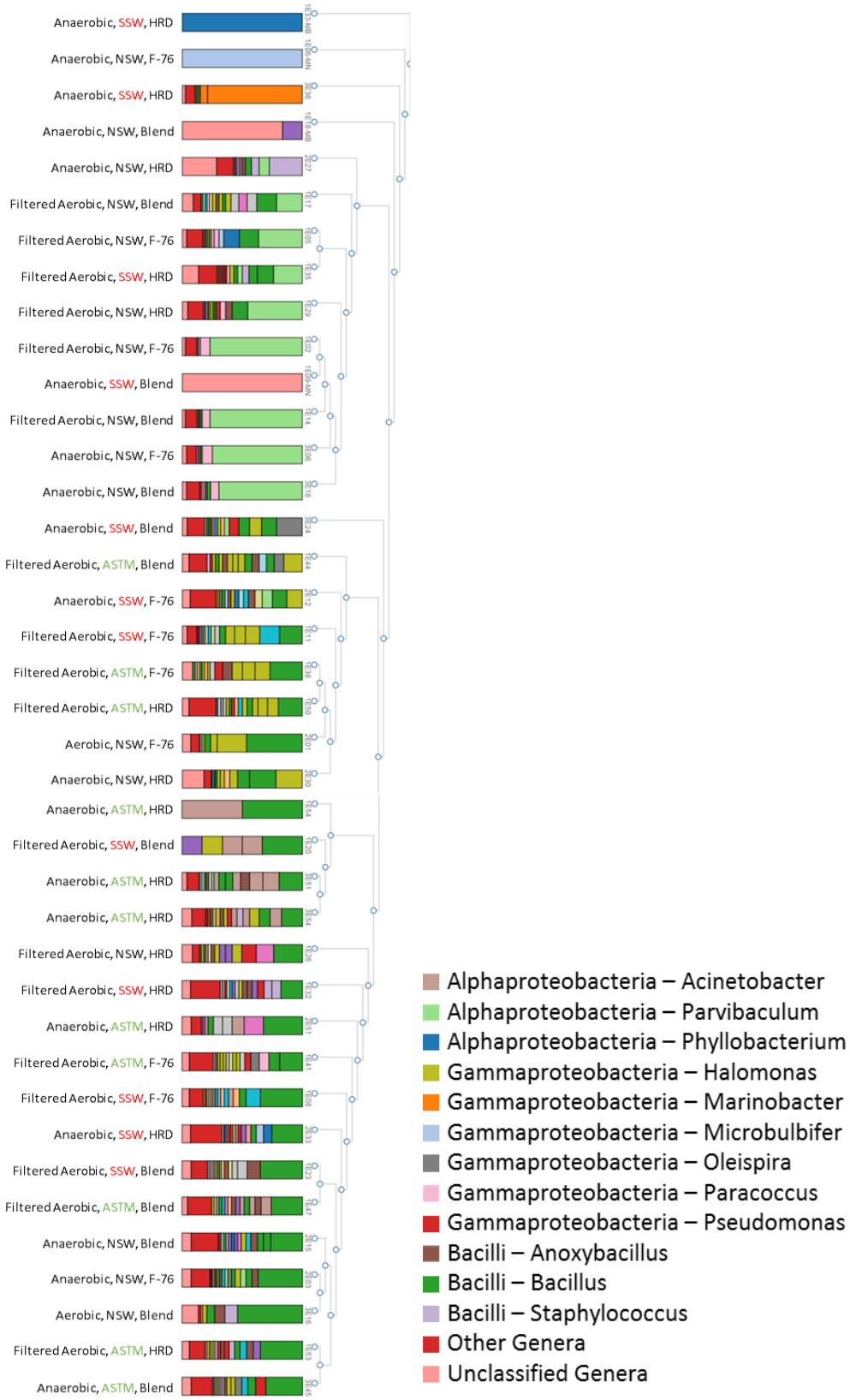

Figure 23. Dendrogram of BaseSpace 16S Metagenomics analysis of 12 month samples with top 12 genera displayed in color key

Genera detected in samples between 3 days and 12 months incubation were predominantly those reported as hydrocarbon degraders and iron-oxidizing bacteria (Table 16 -Table 17). The numbers of sequences so affiliated, such as with hydrocarbon degraders, increased over time, while the number of IOB/IRB-affiliated sequences decreased.

Table 16. Abundance of 16S rRNA gene fragments affiliated with major microbial metabolic groups at the end of each incubation period.

	Hydrocarbon Degrader		**Sulfur Bacteria**		**Iron Bacteria**		**Nitrate Reducing**		**Acid Producing**		**Others**	
	Count	**% Total**	**Count**	**% Total**	**Count**	**% Total**	**Count**	**% Total**	**Count**	**% Total**	**Count**	**% Total**
3 d	776,341	55.81	327	0.02	477,012	34.29	2,596	0.19	2,992	0.22	595,461	42.81
10 d	1,032,409	56.35	538	0.03	547,771	29.90	8,105	0.44	2,862	0.16	767,885	41.91
1 m	170,436	57.64	48	0.02	19,992	6.76	1,871	0.63	1,671	0.57	100,148	33.87
6 m	188,044	71.55	68	0.03	74,466	28.33	2,063	0.78	8,222	3.13	56,019	21.31
12 m	164,636	84.00	444	0.23	68,466	34.93	46,139	23.54	2,636	1.34	22,059	11.25

Table 17. Genera in major microbial metabolic groups based on metabolism

Hydrocarbon degraders (94)		**Sulfur bacteria (20)**	**Iron bacteria (14)**	**Nitrate Reducing Bacteria (10)**	**Acid Producing Bacteria (4)**
Acetobacterium	*Legionella*	*Acidiphilium*	*Acidovorax*	*Acidovorax*	*Acinetobacter*
Acholeplasma	*Lutibacterium*	*Arcobacter*	*Alteromonas*	*Aquabacterium*	*Bacteroides*
Achromobacter	*Marinobacter*	*Desulfacinum*	*Aquabacterium*	*Dechloromonas*	*Clostridium*
Acidovorax	*Marinobacterium*	*Desulfobacter*	*Deferribacter*	*Geobacter*	*Thiobacillus*
Acinetobacter	*Marinomonas*	*Desulfomonile*	*Gallionella*	*Marinobacter*	
Aerococcus	*Mesorhizobium*	*Desulfonatronum*	*Geobacter*	*Nitrobacter*	
Afipia	*Methylobacterium*	*Desulfosarcina*	*Leptothrix*	*Rhodovulum*	
Agrobacterium	*Microbacterium*	*Desulfosporosinus*	*Paracoccus*	*Thauera*	
Alcanivorax	*Micrococcus*	*Desulfotomaculum*	*Rhodobacter*	*Thermomonas*	
Alteromonas	*Moraxella*	*Desulfovibrio*	*Sediminibacterium*	*Thiobacillus*	
Arthrobacter	*Mycobacterium*	*Desulfuromonas*	*Shewanella*		
Azospirillum	*Neptunomonas*	*Paracoccus*	*Sulfobacillus*		
Bacillus	*Nocardia*	*Rhodovulum*	*Thermomonas*		
Bacteroides	*Nocardioides*	*Shewanella*	*Thiobacillus*		
Beijerinckia	*Nostoc*	*Thermodesulfatator*			
Blastochloris	*Novosphingobium*	*Thermodesulfovibrio*			
Brachybacterium	*Ochrobactrum*	*Thiobacillus*			
Brevibacterium	*Oleispira*	*Thiomicrospira*			
Brevundimonas	*Oscillatoria*	*Thiomonas*			
Burkholderia	*Paenibacillus*				
Carnobacterium	*Parvibaculum*				
Chelatococcus	*Peptococcus*				
Citrobacter	*Planococcus*				
Clostridium	*Polaromonas*				
Comamonas	*Providencia*				
Corynebacterium	*Pseudidiomarina*				
Cupriavidus	*Pseudomonas*				
Cycloclasticus	*Ralstonia*				
Dechloromonas	*Rhizobium*				
Delftia	*Rhodococcus*				
Desulfosarcina	*Salinisphaera*				
Desulfovibrio	*Sarcina*				
Dietzia	*Serratia*				
Enterobacter	*Shewanella*				
Enterococcus	*Sphingobium*				
Erwinia	*Sphingomonas*				
Erythrobacter	*Staphylococcus*				
Escherichia	*Stenotrophomonas*				
Flavobacterium	*Streptomyces*				
Fusibacter	*Thauera*				
Geobacillus	*Thermus*				
Geobacter	*Vibrio*				
Geotoga	*Xanthobacter*				
Gordonia	*Xanthomonas*				
Halanaerobium					
Halomonas					
Hirschia					
Hyphomonas					
Klebsiella					
Lactobacillus					

4.2.2.2.2 QIIME Analysis of ITS Data

QIIME analysis pipeline of ITS 1 sequences identified 78,991 total reads, of which 77,754 reads passed quality control filtering. Taxonomic breakdown of the 103 OTUs from the 135 sequenced community DNA samples is shown in Table 18.

Table 18. Distribution of eukaryotes at five taxonomic levels identified by QIIME analysis of ITS1 gene at the end of particular incubation periods

***Eucarya* taxonomic level**	**3 d**	**10 d**	**1 m**	**6 m**	**12 m**
Phylum	2	2	2	3	2
Class	3	2	2	4	3
Order	5	3	1	6	2
Family	4	3	1	7	2
Genus	4	3	1	8	2

At the class level, Eurotiomycetes and Dothideomycetes were only present at the end of the three-day incubation period (Figure 24). The number of Agaricomycetes-affiliated sequences increased between 10 days and 6 months. By the end of the 12-month incubation period, however, only 3 sequences affiliated with the *Eucarya* were detected.

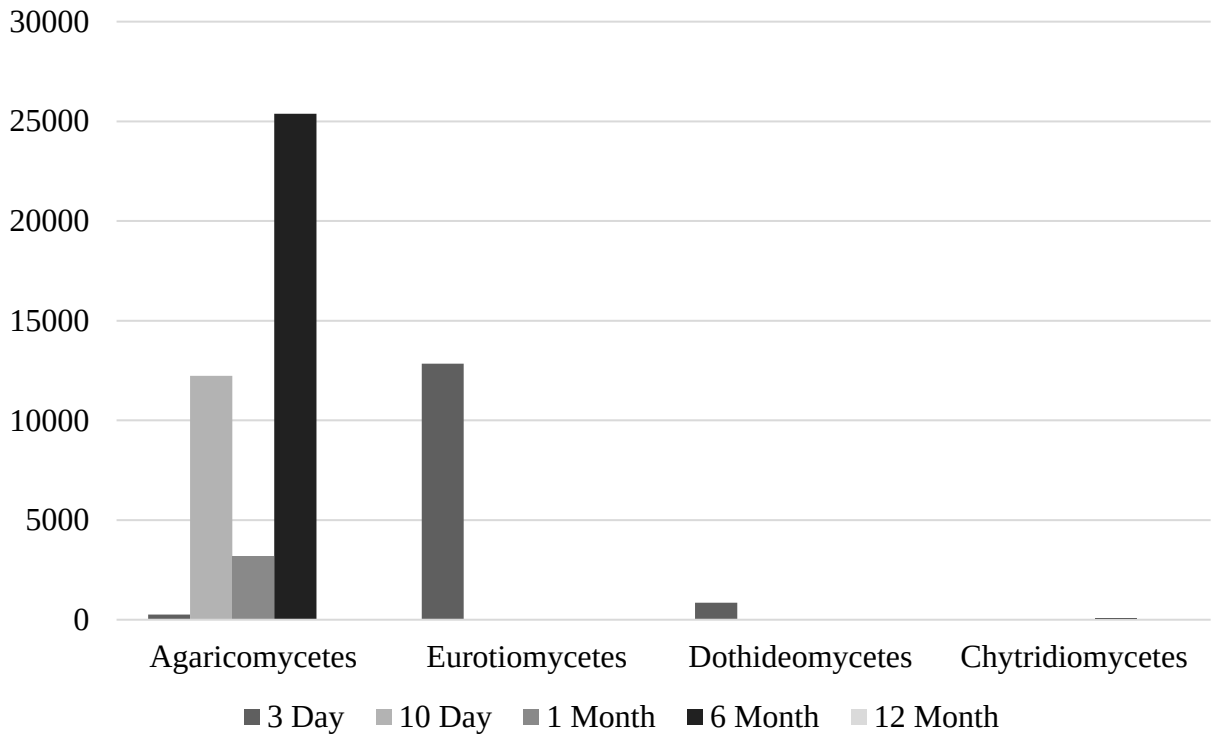

Figure 24. Distribution of eukaryotic classes based on QIIME analysis of ITS reads recovered at the end of each incubation period

Some 75% of the *Eucarya* genera-level sequences were not assigned to a genus by QIIME analysis. Of those assigned, however, two were overwhelmingly abundant (*Verrucaria* and *Fuscoporia*). At the end of the three-day incubation, *Verrucaria*-affiliated sequences accounted for 57% of the total, while those affiliated with *Fuscoporia* comprised only 1% (Figure 25). Thereafter, *Verrucaria*-affiliated sequences were essentially absent or in very low numbers at the end of later incubation periods, while those of *Fuscoporia* were dominant, comprising as much as 90% of the total reads at the end of the six-month incubation. At the end of the 12-month incubation, 1226 of 1229 reads were not assigned at the genus level.

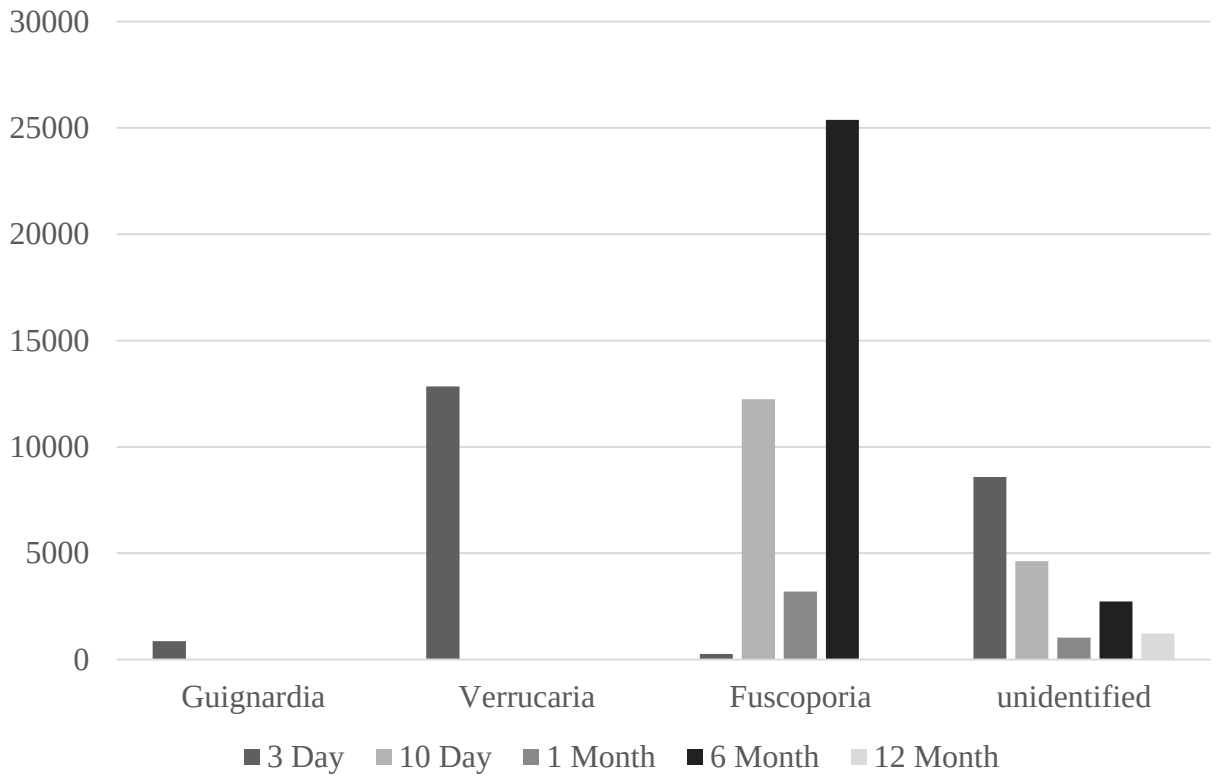

Figure 25. Prevalent *Eucarya* genera identified by QIIME analysis at the end of five incubation periods

Chapter 5. Discussion

A range of electrochemical and microbiological tests were performed to determine if evidence of MIC existed i) in natural and synthetic seawaters; ii) under aerobic and anaerobic conditions; and iii) with and without naturally-occurring microbes.

5.1 Physiological and electrochemical parameters

5.1.1 pH of fuel-seawater mixtures

Corrosion rate variations between fuels is likely not caused by the chemical effects of the fuels. The long-term 12-month exposure of ASTM seawater to the various fuels showed that ASTM seawater pH values ranked from highest to lowest according to the fuel: HRD, F-76:HRD blend, and F-76. Higher pH values generally slow the corrosion rate of steels due to passivation. Thus, corrosion rates should have been lowest in HRD, followed by the F-76:HRD blend, and then F-76. The trend in corrosion rates, however, was opposite to that expected, since corrosion rates were highest in HRD, followed by the F-76:HRD blend, and then F-76. In addition, when steel coupons are added to the seawater-fuel mixtures, the rust precipitation will generally buffer the solution, resulting in only small pH variation. Hence, there was little indication that pH was related to corrosion rates of steel in the different fuels. The data described here align well with literature reports that the corrosion rate of mild steel is independent of pH between 4.5-9.5, but at pH 4.0 or below, hydrogen evolution occurs and corrosion increases rapidly (Little, Staehle, & Davis, 2001).

5.1.2 Oxygen diffusion in fuels

Variation in corrosion rates was most likely caused by the diffusion of dissolved oxygen through the fuel layer. The higher corrosion rates in the aerated samples indicated that oxygen reduction was the primary cathodic reaction for corrosion, and that hydrogen evolution was a secondary mechanism. In the experimental setup, the steel coupons were immersed in a seawater-fuel mixture wherein the fuel layer floated on the water layer. Therefore, in order for the cathodic reaction to occur at the steel-water interface, dissolved oxygen has to diffuse through the fuel layer to regions of water in contact with the steel surface. Hence, higher corrosion rates indicate higher oxygen diffusion rates through the fuel. This can be corroborated by calculating the

oxygen diffusion coefficient (23) based on the dynamic viscosity η of the fuels:

$$Diffusion\ Coefficient\ (D) = \frac{kT}{6\pi\eta r^2} \quad (23)$$

k = Boltzmann constant (8.617 x 10^{-5} eV/K)

T = Temperature (°K)

η = Dynamic viscosity (density [ρ] x kinematic viscosity [υ]) (Fu & Turn, 2015)

r = Radius of particle (dissolved oxygen)

The ranking of the fuels from the highest to lowest dynamic viscosity (η = υ x ρ) was as follows: HRD, F-76:HRD blend, F-76.

5.1.3 Corrosion morphology

Steel samples with the highest corrosion rates had the greatest coverage of white precipitate in the fuel layer. These carbonates and hydroxides likely precipitated by OH^- that was generated by O_2 reduction in the vicinity of water on the steel surface (*i.e.*, cathodic regions). Oxygen must diffuse through fuel to reach the cathode, and Ca^{2+}, Na^{2+}, and Mg^{2+} must migrate from the seawater into the fuel layer to form calcium and sodium carbonates and magnesium hydroxide (Figure 26). The formation of the white precipitates as an indicator of high corrosion rate was confirmed by data showing that the highest amount of corrosion occurred in HRD, followed by the F-76:HRD blend, and then F-76. This also accords with the rate of corrosion increasing with the rate of oxygen diffusion through the fuels. Previous studies have shown carbonate "scale" deposition over cathodic surfaces, especially when the electrolyte contains high levels of calcium and magnesium ions (Petersen & Melchers, 2012). It has been a longstanding belief that waters containing high levels of Ca and Mg (*i.e.*, "hard" water) are less corrosive than those containing low Ca and Mg levels (*i.e.*, "soft") since the carbonates would add to the iron oxides, creating a protective layer and reducing the long-term corrosion rate (Revie & Uhlig, 2008). It this case, however, the carbonates and hydroxide precipitated primarily on the cathodic sites in the fuel layer and did not form a continuous protective layer over the entire coupon. Samples with carbonate scales in the fuel layer consistently had the highest corrosion rates, and scales typically occurred in HRD samples (Figure 11).

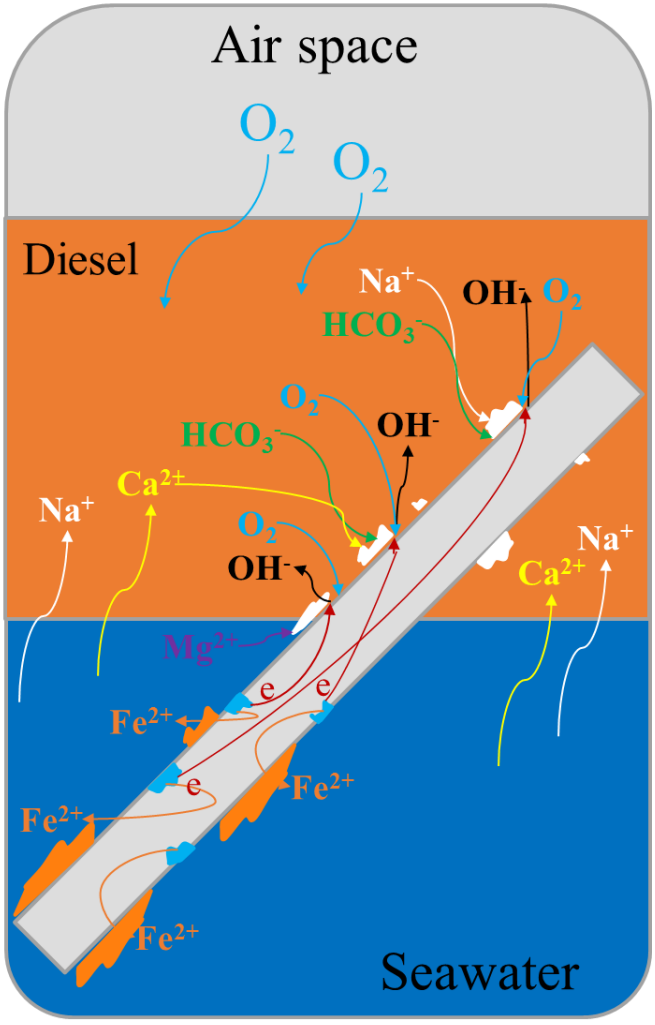

Figure 26. Schematic of white carbonate and hydroxide precipitation on steel coupon when oxygen is present in a diesel/seawater system

5.2 Microbial communities

5.2.1 Sampling

Rust tubercle microbial communities were not studied with the methods employed in this study since biofilms on the coupon and corrosion product surfaces were not adequately captured and extracted. Only planktonic microbes were collected, based on the assumption/observation that planktonic communities will be reflected in the biofilm (Baird, Ogles, & Baldwin, 2016). The findings here do not fully support this assumption however, given that SRB were not detected in this metagenomics study above 0.24% of the total community read counts in any of the 5 incubations

Low read counts of SRB-affiliated sequences in the Illumina data contrasted with the highest read counts of microaerophilic IOB and aerobic hydrocarbon-degraders. The development of methods to extract community DNA directly from corrosion products should be a first step in further characterizing this corrosive community. Current DNA extraction and PCR methods are inhibited by excess iron (Marty, Ghiglione, Païssé, & Gueuné, 2012).

5.2.2 Diversity of microbes

It has been reported that almost 200 microbial genera, representing more than 500 species and strains, are known to thrive on hydrocarbons, and that oil-degrading bacteria are probably present in each milliliter of pelagic seawater (Wang, Wang, Lai, & Shao, 2010). Ninety-four genera, comprising almost 50% of the known hydrocarbonoclastic genera, were detected in this study. For example, *Alcanivorax dieselolei* is a Gammaproteobacterium identified as an obligate hydrocarbonoclastic bacteria (Hassanshahian, Emtiazi, & Cappello, 2012), and cultured from sample bottles containing F-76 and blended diesel. As expected, reduction in microbial community complexity did not occur over the course of this year-long study, according to the Illumina data. Diversity of cultured microbes after a one year incubation averaged 15 unique representative colony types per plate, whereas after 3 days plates averaged 22 unique colonies. Putative genus-level identification of cultured isolates belonged to the *Bacteria* Classes *Actinobacteria* (15%), *Firmicutes* (6%), *Proteobacteria* (22%); and *Eukarya* Classes *Ascomycota* (50%), and *Basidiomycota* (6%). The majority of cultured *Bacteria* and *Eukarya* isolates are known to belong in hydrocarbonoclastic genera (Bento, Beech, Gaylarde, Englert, & Muller, 2005; Elshafie, AlKindi, Al-Busaidi, Bakheit, & Albahry, 2007; Geissler, Keller-schultz, & Keasler, 2015; Harayama, Kasai, & Hara, 2004; Hassanshahian et al., 2012; Little et al., 2001; Magot, 2005; Prince, 2005; Rabus, 2005; van Beilen & Witholt, 2005; Wang et al., 2010; Zhu, Lubeck, & Kilbane, 2003).

The Illumina metagenomics data also shows a reduction in community diversity of 112 total *Bacteria/Archaea* genera detected between those detected from the 3 day samples until one year. Of the 562 total *Bacteria/Archaea* genera detected from the samples, 299 were still detected after one year of incubation. *Eucarya* detected *via* metagenomics were less phylogenetically diverse, with reads only assigned to 9 unique genera.

Also, only 78% of microbes cultured from the diesel/seawater interface layers in the sample bottles and putatively identified by 16S rRNA gene sequencing were also represented in the Illumina data.

5.3 Conclusions

This is the first study to compare steel coupon corrosion rates in terms of microbial community structure through both cultivation and molecular analyses over both time and fuel composition in a diesel fuel seawater system. Key findings for future work in MIC:

- Corrosion rates of 1018 steel in ASTM seawater D1141 were statistically different from samples immersed in natural (*i.e.*, Pacific Ocean) seawater. Furthermore, the amount of white precipitates deposited on steel coupons in the fuel layer differed between the natural and synthetic seawaters, and was an indicator of higher corrosion rates.
- Corrosion rates of steel coupons in open and vented-cap bottles did not differ significantly, and therefore such a comparison would be redundant in future studies. This would be particularly so if the incubation environment contains airborne microbes that differ from those expected under normal operating conditions.
- Filtering the seawater and fuels did not significantly impact the corrosion rate of the steel coupons, most likely due to the water and salts being equally corrosive in all samples. However, filtering natural seawater through a 0.22 µm pore size filter was not sufficient to remove all microbes; a 0.1 µm or smaller pore size filter should be used in future studies.
- Methods to capture sessile biofilm communities among corrosion products for metagenomics analysis should be developed, and would enable time-series changes in tubercle community structure to be determined.

Expanding the knowledge-base of which microbial communities contribute to corrosion, and not just those that are easy to culture in the laboratory, will enhance understanding of how such microbes affect industry and guide the way to better control and mitigation of corrosion of metal infrastructure.

Summary

Microbiologically Influenced Corrosion (MIC) of steel coupons was compared to electrochemical corrosion of the same steel in an alternative fuel and seawater combination. Corrosion behavior of UNS G10180 plain-carbon steel in blended seawater-fuel mixtures was evaluated at various intervals for one year: i) with and without naturally-occurring microbes; ii) under aerobic and anaerobic conditions; and iii) in natural and synthetic seawaters. Fuels were petroleum-diesel F-76, green-diesel HRD-76, and a 50/50 blend of F-76 and HRD-76. Immersion tests were conducted and corrosion products were visually assessed for extent of steel coupon surface coverage; products were characterized and identified by surface analytical techniques including energy dispersive x-ray analysis, x-ray diffraction, and Raman spectroscopy. Corrosion rates were calculated based on mass-loss data for each coupon. Microbes present were putatively identified by Illumina MiSeq next generation sequencing, and Sanger sequencing of rRNA genes in cultivated microbes.

Corrosion rates of 1018 carbon steel were driven by oxygen reduction and were highest in HRD, followed by the F-76:HRD blend, and then F-76. White carbonate and hydroxide precipitates formation in the fuel layer was shown to be a consistent visual indicator for a high corrosion rate of steel, which conflicts with previous studies. Tested conditions that did not statistically impact corrosion rates were filtering natural seawater and having open both and vented sample bottles. However, filtering natural seawater through a 0.22 μm pore size filter was not sufficient to remove all microbes; a 0.1 μm or smaller pore size filter should be used in future studies. Also, ASTM seawater had statistically different corrosion rates (~10%) than samples containing Pacific Ocean seawater. Ships that transverse the world's oceans would need to take into account the differences in potential corrosivity of natural waters and mitigation steps based solely on ASTM seawater trials may account for some premature failures due to corrosion.

Appendices

Appendix 1. Samples from which community genomic DNA was extracted for Illumina MiSeq next generation sequencing and BaseSpace 16S metagenomics analysis.

Water	Fuel	Env. Cond.	3 d			10 d			1 m			6 m			12 m		
Natural Seawater	Natural F-76	Aerobic														2E01	
	Filtered F-76																
Filtered Seawater	Natural F-76																
	Filtered F-76																
Natural Seawater	Natural Blend																
	Filtered Blend																3E16
Filtered Seawater	Natural Blend																
	Filtered Blend																
Natural Seawater	Natural HRD																
	Filtered HRD												2D28				
Filtered Seawater	Natural HRD																
	Filtered HRD													3D34			
ASTM Seawater	Natural F-76																
	Filtered F-76																
	Natural Blend																
	Filtered Blend																
	Natural HRD																
	Filtered HRD																
Natural Seawater	Natural F-76	Filtered Aerobic	1A02			1B02			1C02			1D02			1E02		
	Filtered F-76		1A05			1B05			1C05			1D05			1E05		
Filtered Seawater	Natural F-76		1A08			1B08			1C08			1D08			1E08		
	Filtered F-76		1A11			1B11			1C11			1D11			1E11		
Natural Seawater	Natural Blend		1A14			1B14			1C14			1D14			1E14		
	Filtered Blend		1A17			1B17			1C17			1D17			1E17		
Filtered Seawater	Natural Blend		1A20			1B20			1C20			1D20			1E20		
	Filtered Blend		1A23			1B23			1C23			1D23			1E23		
Natural Seawater	Natural HRD		1A26			1B26			1C26			1D26			1E26		
	Filtered HRD		1A29			1B29			1C29			1D29			1E29		
Filtered Seawater	Natural HRD		1A32			1B32			1C32			1D32			1E32		
	Filtered HRD		1A35			1B35			1C35			1D35			1E35		
ASTM Seawater	Natural F-76											1D38			1E38		
	Filtered F-76											1D41			1E41		
	Natural Blend											1D44			1E44		
	Filtered Blend											1D47			1E47		
	Natural HRD											1D50			1E50		
	Filtered HRD											1D53			1E53		
Natural Seawater	Natural F-76	Anaerobic	1A03			1B03			1C03			1D03	2D03	3D03	1E03	2E03	
	Filtered F-76		1A06			1B06			1C06			1D06			1E06		3E06
Filtered Seawater	Natural F-76		1A09			1B09			1C09			1D09			1E09		
	Filtered F-76		1A12			1B12			1C12			1D12			1E12	2E12	
Natural Seawater	Natural Blend		1A15			1B15			1C15			1D15			1E15	2E15	
	Filtered Blend		1A18			1B18			1C18			1D18	2D18		1E18		3E18
Filtered Seawater	Natural Blend		1A21			1B21			1C21			1D21	2D21		1E21		
	Filtered Blend		1A24			1B24			1C24		3C24	1D24		3D24	1E24		3E24
Natural Seawater	Natural HRD		1A27			1B27			1C27		3C27	1D27		3D27	1E27	2E27	
	Filtered HRD		1A30			1B30			1C30			1D30	2D30		1E30	2E30	
Filtered Seawater	Natural HRD		1A33			1B33			1C33			1D33	2D33		1E33	2E33	
	Filtered HRD		1A36			1B36			1C36			1D36		3D36	1E36		3E36
ASTM Seawater	Natural F-76											1D39			1E39		
	Filtered F-76											1D42			1E42		
	Natural Blend											1D45		3D45	1E45		3E45
	Filtered Blend											1D48			1E48		
	Natural HRD											1D51	2D51		1E51	2E51	3E51
	Filtered HRD											1D54		3D54	1E54		3E54

Appendix 1 (continued). Samples from which community genomic DNA was extracted for Illumina MiSeq Next Generation Sequencing and BaseSpace 16S metagenomics analysis.

Water	Fuel	Env. Cond.	0 d	3 d	10 d	1 m	6 m	12 m
Natural Seawater	N/A	Anaerobic	NSW 000	NSW 003	NSW 010	NSW 030	NSW 182	NSW 365
Filtered Seawater	N/A	Anaerobic	SSW 000	SSW 003	SSW 010	SSW 030	SSW 182	SSW 365
ASTM Seawater	N/A	Anaerobic	ASTM 000				ASTM 182	ASTM 365
N/A	Natural F-76	Anaerobic	NDA 000	NDA 003	NDA 010	NDA 030	NDA 182	NDA 365
N/A	Filtered F-76	Anaerobic	SDA 000	SDA 003	SDA 010	SDA 030	SDA 182	SDA 365
N/A	Natural Blend	Anaerobic	NDB 000	NDB 003	NDB 010	NDB 030	NDB 182	NDB 365
N/A	Filtered Blend	Anaerobic	SDB 000	SDB 003	SDB 010	SDB 030	SDB 182	SDB 365
N/A	Natural HRD	Anaerobic	NDC 000	NDC 003	NDC 010	NDC 030	NDC 182	NDC 365
N/A	Filtered HRD	Anaerobic	SDC 000	SDC 003	SDC 010	SDC 030	SDC 182	SDC 365

Appendix 2. Ethidium monoazide treatment of contaminated Illumina sequencing primers

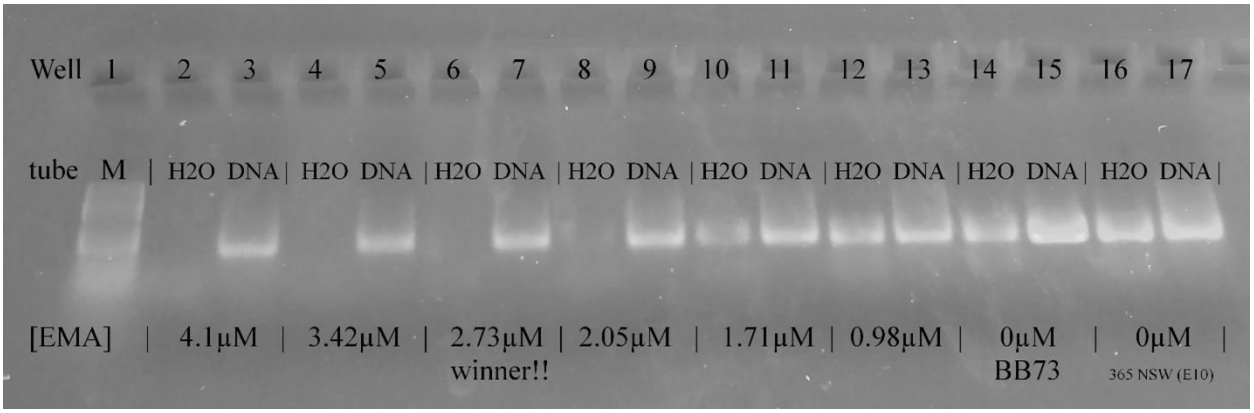

Appendix 3. TAN results reported in g KOH/g fuel. "-1.00" means sample was more acidic than the test kit's range.

				1 Month			6 Month			12 Month		
Fuel	**Water**	**C**	**EC**	**1C**	**2C**	**3C**	**1D**	**2D**	**3D**	**1E**	**2E**	**3E**
N F-76	N SW	O	1	0.00	0.40	0.10	-1.00	0.10	0.10	0.30		
		V	2	-1.00	0.10	-1.00	-1.00			0.10		
		T	3	-1.00			0.10			0.00	0.00	0.10
S F-76		O	4	0.20	0.20	0.20	0.00	0.10	0.10	0.30		
		V	5	-1.00			0.10	0.00	-1.00	0.10		
		T	6	0.20			0.00			0.10	0.00	0.20
N F-76	S SW	O	7	0.40			0.10			0.30		
		V	8	0.00			0.20			0.50		
		T	9	0.20	0.10	0.20	0.10	0.10	-1.00	0.10		
S F-76		O	10	0.40			0.10			-1.00		
		V	11	0.10	0.10	0.20	0.10			-1.00		
		T	12	-1.00			0.10			0.10		
N Blend	N SW	O	13	0.40			-1.00			-1.00		
		V	14	0.00			0.20			0.00		
		T	15	-1.00			-1.00			-1.00	0.20	-1.00
S Blend		O	16	0.00			-1.00			-1.00		
		V	17	-1.00			-1.00			-1.00		
		T	18	-1.00			-1.00			-1.00		
N Blend	S SW	O	19	-1.00	0.10	0.10	-1.00			-1.00		
		V	20	0.30			-1.00			0.00		
		T	21	0.20			-1.00	0.10	0.10	0.30	0.00	0.00
S Blend		O	22	0.30	0.00	0.00	0.05			-1.00		
		V	23	-1.00			0.00	0.00	0.00	-1.00		
		T	24	0.30				0.10	0.10	0.00		
N HRD	N SW	O	25	0.10	0.10	0.10	0.10	0.00	0.10	0.00		
		V	26	0.00			0.10			-1.00		
		T	27	0.10	0.40	0.10	0.10	0.10	0.10	0.10	-1.00	-1.00
S HRD		O	28	0.20			0.20			0.20		
		V	29	0.00			-1.00			0.20	0.10	0.00
		T	30	0.10	0.10	0.00	0.00	0.00	-1.00	0.10		
N HRD	S SW	O	31	0.00			0.20			0.10	-1.00	0.10
		V	32	0.50			0.20			0.10		
		T	33	0.00			0.00	-1.00	-1.00	0.20		
S HRD		O	34	0.00			0.10	0.00	0.10	0.00		
		V	35	0.30			0.10			-1.00		
		T	36	-1.00			0.20		0.00	-1.00		
N F-76	ASTM SW	O	37				0.00			-1.00		
		V	38				0.00			0.10		
		T	39				0.20	0.20	0.10	-1.00	-1.00	0.10
S F-76		O	40				0.00			0.15		
		V	41				-1.00			0.15	0.10	0.10
		T	42				0.05			0.10	0.10	0.00
N Blend		O	43				0.00			0.20		
		V	44				0.10			0.20		
		T	45				0.10	0.00	0.10	0.10		
S Blend		O	46				0.10			0.10		
		V	47				-1.00			0.20		
		T	48				0.00	-1.00	0.00	0.20		
N HRD		O	49				0.10			0.30		
		V	50				-1.00			0.20		
		T	51				0.10	0.40	-1.00	0.10		
S HRD		O	52				0.30			0.30		
		V	53				0.00			0.20		
		T	54				0.10	-1.00	0.00	0.10	0.00	0.00
N F-76	n/a	T	NCB		0.00			0.00			0.00	
N Blend	n/a	T	NCB		0.10			0.20			0.10	
N HRD	n/a	T	NCB		0.00						0.10	

Abbreviations: C - Cap type; EC - Environmental Condition 1-54; N - "Natural" unfiltered; S - "Sterile" 0.22µm filtered; Blend - 50:50 F-76:HRD-76 diesel mixture; ASTM – American Standard Testing Method D1141-98 seawater; O - aerobic condition; V - 0.22µm filtered aerobic; T - anaerobic

Appendix 4. HydroSCOUT results (ppm water in oil).

				1 Month			6 Month			12 Month		
Fuel	**Water**	**C**	**EC**	**1C**	**2C**	**3C**	**1D**	**2D**	**3D**	**1E**	**2E**	**3E**
N F-76	N SW	O	1	65			-98	42				
		V	2									
		T	3				78					
S F-76		O	4					83	51			
		V	5					63				
		T	6							75	50	54
N F-76	S SW	O	7				53					
		V	8				89			120		
		T	9		53		71		63	320		
S F-76		O	10				174			110		
		V	11	134		30	54			48		
		T	12				99					
N Blend	N SW	O	13				56					
		V	14							113		
		T	15				-62			74		
S Blend		O	16				-155			68		
		V	17				237					
		T	18				-48					
N Blend	S SW	O	19	249		74						
		V	20				65			300		
		T	21				48	51		45	48	
S Blend		O	22		71	62	-228					
		V	23	41			75		87			
		T	24	41		35		62	51			
N HRD	N SW	O	25				65			62		
		V	26				5					
		T	27				42					41
S HRD		O	28					38				
		V	29				24					
		T	30					68				
N HRD	S SW	O	31	17			230					
		V	32	44								
		T	33					339		63		
S HRD		O	34					15				
		V	35				0					
		T	36					27				
N F-76	ASTM SW	O	37							143		
		V	38				107			33		
		T	39				183	86	102	93		1569
S F-76		O	40				65			27		
		V	41				56					36
		T	42				69				66	0
N Blend		O	43				59					
		V	44				18			93		
		T	45				69	23		48		
S Blend		O	46				155			174		
		V	47				48			71		
		T	48				86					
N HRD		O	49				48					
		V	50					83	72	126		
		T	51							147		
S HRD		O	52									
		V	53						48			
		T	54				1470		140	29	20	

Abbreviations: C - Cap type; EC - Environmental Condition 1-54; N - "Natural" unfiltered; S - "Sterile" 0.22µm filtered; Blend - 50:50 F-76 : HRD-76 diesel mixture; ASTM – American Standard Testing Method D1141-98 seawater; O - aerobic condition; V - 0.22µm filtered aerobic; T - anaerobic

Appendix 5. Genera and 16S rRNA copy counts only detected in the 3 day incubation samples

Gene copy count	277	0	0	0	0
Genera count	27	0	0	0	0
Genera	**3 d**	**10 d**	**1 m**	**6 m**	**12 m**
Actinoplanes	1				
Algibacter	16				
Anaeromyxobacter	36				
Azorhizophilus	1				
Bifidobacterium	1				
Chromobacterium	2				
Desulfacinum	1				
Desulfonauticus	3				
Dolichospermum	1				
Euzebya	11				
Filifactor	15				
Gloeotrichia	1				
Kitasatospora	1				
Lutibacterium	2				
Methylocaldum	1				
Micromonospora	2				
Negativicoccus	2				
Olleya	149				
Psychroserpens	11				
Rhodoferax	3				
Sphingobacterium	9				
Spongiibacter	1				
Sulfobacillus	1				
Syntrophobacter	2				
Terriglobus	1				
Trichodesmium	1				
Ulvibacter	2				

Appendix 6. Genera and 16S rRNA copy counts detected in the 10 day incubation samples

Gene copy count	686	1201	0	0	0
Genera count	37	78	0	0	0
Genera	**3 d**	**10 d**	**1 m**	**6 m**	**12 m**
Acidimicrobium		1			
Acidiphilium	1	1			
Actinomadura		1			
Actinopolyspora		3			
Anaerobranca	5	2			
Anaerococcus	4	2			
Anaeromusa		1			
Balneimonas		388			
Bellilinea		1			
Blastococcus		9			
Blautia		4			
Brevibacterium	3	9			
Burkholderia	2	3			
Caldanaerobacter		1			
Caldilinea		3			
Candidatus Regiella	5	4			
Candidatus Rhabdochlamydia		1			
Chondromyces	27	19			
Citromicrobium		1			
Colwellia		11			
Conexibacter		4			
Crenothrix		2			
Cyanobacterium		2			
Deinococcus	2	9			
Desulfonatronovibrio	4	3			
Desulfotalea		1			
Dickeya	2	3			
Erysipelothrix		1			
Faecalibacterium		1			
Frankia		1			
Fulvivirga	1	245			
Gallionella	1	1			
Geobacter	4	10			
Hahella	1	3			
Haliscomenobacter		1			
Herbaspirillum	2	35			
Hylemonella		2			
Jeotgalicoccus	1	1			
Kaistella	5	2			
Leptolyngbya	3	35			
Leptothrix		1			
Leptotrichia		4			
Leucothrix		3			

Genera continued	**3 d**	**10 d**	**1 m**	**6 m**	**12 m**
Longilinea		1			
Marichromatium	10	19			
Meiothermus		1			
Methylobacillus	3	1			
Methylomicrobium	3	5			
Microbispora		16			
Morganella		1			
Moritella	2	3			
Oceanibulbus	120	140			
Olivibacter		2			
Oscillospira	1	1			
Parascardovia		6			
Patulibacter		16			
Pediococcus		25			
Pedosphaera	1	4			
Planctomyces	4	5			
Planifilum		1			
Polaromonas	1	12			
Pseudoxanthomonas		1			
Roseivirga	290	1			
Roseobacter	1	1			
Runella		1			
Salinivibrio	2	6			
Sarcina		2			
Sporotomaculum	1	1			
Sutterella	1	6			
Symploca	3	2			
Teredinibacter	164	8			
Tetragenococcus	2	6			
Thermodesulfatator	2	1			
Thiobacillus		3			
Thiocystis	2	3			
Thiomicrospira		1			
Tindallia		5			
Xanthomonas		59			

Appendix 7. Genera and 16S rRNA copy counts detected in the 1 month incubation samples

Gene copy count	1006	1755	131	0	0
Genera count	25	27	44	0	0
Genera	**3 d**	**10 d**	**1 m**	**6 m**	**12 m**
Agrobacterium			15		
Arsenophonus	13	12	1		
Arthrospira	1		16		
Asticcacaulis		1	1		
Candidatus Amoebophilus	1	1	1		
Candidatus Entotheonella	2		1		
Candidatus Phlomobacter	2	1	1		
Candidatus Protochlamydia	2	3	1		
Cerasicoccus		3	1		
Chitinophaga		4	5		
Denitratisoma	1		1		
Desulfurispirillum	3		1		
Desulfurispora		8	2		
Ferrimonas	187	171	2		
Finegoldia			9		
Francisella	3	2	1		
Fusobacterium		1	1		
Haererehalobacter			1		
Halanaerobacter	2	1	1		
Heliorestis	2	3	1		
Laceyella	1	1	1		
Lautropia		4	3		
Limnobacter			2		
Litoricola	52	52	7		
Methylomonas	4	3	2		
Nitrosopumilus	3	5	1		
Oceanisphaera	26	38	4		
Ornithinicoccus			8		
Phaeospirillum			1		
Pontibacter			12		
Reinekea	9	9	3		
Salegentibacter	8	7	3		
Salinisphaera	12	12	2		
Salisaeta		1	1		
Thalassomonas	653	1400	6		
Thermicanus	3	2	1		
Thermomonas			2		
Thiohalorhabdus	9	8	2		
Vagococcus			1		
Virgisporangium			1		
Waddlia	2	2	1		
Winogradskyella	5		2		
Xanthobacter			1		
Xylella			1		

Appendix 8. Genera and 16S rRNA copy counts detected in the 6 month incubation samples

Gene copy count	699	916	556	2157	0
Genera count	63	66	43	113	0
Genera	**3 d**	**10 d**	**1 m**	**6 m**	**12 m**
Acholeplasma				2	
Acidisoma	3	3	1	9	
Acidovorax	17	22	65	251	
Aerococcus		1		52	
Aggregatibacter	1			151	
Agrococcus				2	
Agromyces	8	9	2	6	
Alishewanella	65	43	4	3	
Allochromatium	49	61	9	1	
Aminiphilus		1		2	
Antarctobacter	33	3	1	36	
Arcobacter				17	
Arsenicicoccus			1	1	
Aurantimonas	2	2		769	
Azohydromonas	1			1	
Bartonella	7	7	2	11	
Bergeyella	1			13	
Bizionia	14	5		1	
Bulleidia				12	
Candidatus Contubernalis	1			2	
Carboxydocella				3	
Carnobacterium				1	
Caulobacter	48	298	186	5	
Cellulomonas	1	10	1	2	
Chelativorans		4	1	52	
Chelatococcus				4	
Chromohalobacter	1	30		244	
Cystobacter	4	6		2	
Dactylosporangium			1	2	
Demequina		1	2	8	
Desulfomonile	3	2		1	
Desulfosarcina	9	7	2	2	
Desulfosporosinus	1	2		1	
Desulfuromonas	3		1	3	
Diaphorobacter		4	7	2	
Dietzia		6	91	16	
Dysgonomonas				4	
Edaphobacter	7	9	1	2	
Escherichia				1	
Gallibacterium	1			5	

Genera continued	**3 d**	**10 d**	**1 m**	**6 m**	**12 m**
Georgenia		1		3	
Giesbergeria	1		1	2	
Gramella	5	4	1	1	
Granulicatella	16	34		4	
Haladaptatus		2		15	
Halanaerobium				1	
Haloferax				1	
Halomicronema	2	3		2	
Halopelagius				7	
Halorhodospira	2	7		1	
Haloterrigena	1	4	2	2	
Halothiobacillus	6	6		1	
Herpetosiphon				17	
Knoellia				4	
Kocuria		4		7	
Labrys	4	7	1	2	
Lactobacillus	23	34	4	7	
Leptospira	34	33	2	3	
Listeria				2	
Lysinibacillus	4	1		2	
Magnetospirillum	1			1	
Megasphaera	1	1		1	
Methylocella				1	
Methylopila	1	2		1	
Methyloversatilis				8	
Mycoplasma	2	2	1	7	
Natronomonas		9	36	1	
Nocardia				4	
Nocardiopsis				1	
Opitutus				1	
Oxalobacter	27	1		1	
Pedobacter	10	11		4	
Pirellula	2	1		1	
Pleomorphomonas	4			6	
Polaribacter	189	8		3	
Polynucleobacter				1	
Porphyromonas		6		3	
Promicromonospora				1	
Propionivibrio				1	
Providencia	10	24	3	2	

Appendix 8 (continued). Genera and 16S rRNA copy counts detected in the 6 month samples

Genera	3 d	10 d	1 m	6 m	12 m
Pseudochrobactrum				3	
Pullulanibacillus		1		1	
Rarobacter				1	
Rathayibacter	1	1	27	1	
Rhodococcus	2	68	5	7	
Rhodocyclus	1			5	
Rhodoplanes	1	1		27	
Rickettsiella	10	12	2	1	
Rothia	1			55	
Rubrivivax		17		18	
Sagittula	6	11	2	2	
Salimicrobium				1	
Schlegelella		1	11	33	
Shimia	5	9	1	3	
Singulisphaera			35	1	
Sinomonas				12	
Snowella	3	4	1	1	
Soehngenia			17	42	
Solirubrobacter		1	13	27	
Sporichthya				19	
Streptosporangium	2	1		1	
Syntrophomonas	3	5	1	2	
Thermoactinomyces	2	1		1	
Thermobaculum	1	2	1	1	
Thermodesulfovibrio	14	8	2	1	
Thermovenabulum				2	
Thiomonas	1			1	
Thiothrix	12	15	5	2	
Trabulsiella		5	1	2	
Variovorax	1	4		4	
Verrucomicrobium	6	8	3	1	
Vogesella	2			1	
Zoogloea				43	

Appendix 9. Genera and 16S rRNA copy counts detected in the 12 month incubation samples

Gene copy count	1385078	1823819	294302	260122	195535
Genera count	259	269	226	235	299
Genera	**3 d**	**10 d**	**1 m**	**6 m**	**12 m**
Acetobacterium	2	10	3		2
Achromobacter	37	180	7	110	30
Acinetobacter	2975	2773	1652	8213	2619
Actinobacillus	84	1	5		231
Actinocatenispora	106	151	18	13	18
Actinomyces					1
Actinomycetospora	1	14		1	34
Aeromicrobium	1	1			1
Afipia		2		1	2
Alcanivorax	32826	32934	8438	64167	1074
Alicycliphilus	1	21	24	24	1
Alicyclobacillus	914	1152	626	2037	559
Alkalibacillus	9	23	7	17	15
Alkalibacterium	6	2	1	2	1
Alkaliphilus	2	6	2		2
Alloiococcus		8		6	6
Alteromonas	475460	546733	17171	791	371
Amaricoccus	593	341	3047	3420	367
Aminobacter	25	23	6	25	11
Ammonifex	7	7		1	2
Ammoniphilus		25	2	7	2
Amphritea	81	109	10	3	4
Amycolatopsis				254	2
Anaerospora	1475	2692	629	27	3
Ancylobacter	15	24	1	18	2
Aneurinibacillus	10	19	17	16	22
Anoxybacillus	2286	3406	3119	3044	4945
Aquabacterium	119	269	51	12	4
Aquimarina	80	16	4	2	1
Arenimonas	19			32	4
Arthrobacter	1	1			1
Azomonas	4	6		1	3
Azospirillum	628	334	52	137	98
Bacillus	13510	14111	16378	21609	27018
Bacteroides	8		14		11
Balneola	63	69	15	6	14
Beijerinckia	4	2		193	1
Blastochloris	299	58	77	37	4
Bosea		3	1	2	1
Brachybacterium	55	127	20	9	28
Bradyrhizobium	136	520	146	320	219
Brevibacillus	18	1	76	10	2
Brevundimonas			3		24
Brochothrix	3	4	3	1	1
Caldicellulosiruptor	70	46	6	7	45
Caldithrix	13	15	4	2	2

Appendix 9 (continued). Genera and 16S rRNA copy counts detected in the 12 month samples

Genera	3 d	10 d	1 m	6 m	12 m
Caloramator	26	56	15	2	4
Calothrix	29	13		301	64
Campylobacter	6	12	2	1	2
Candidatus Blochmannia	242	201	43	12	9
Candidatus Endobugula	28946	48927	577	146	140
Candidatus Liberibacter	34	71	9	23	3
Candidatus Phytoplasma	18	22	3	3	5
Candidatus Portiera	25	124	2	2	2
Candidatus Scalindua		1			1
Cellvibrio	194	412	116	2	2
Chlorobaculum	4	7		1	1
Chromatium	81	93	6	5	5
Chroococcidiopsis	3	7	1		1
Chroococcus	6	33	2	1	1
Chryseobacterium	20	38	90	4	42
Chthonomonas					5
Citricoccus					2
Citrobacter		2			3
Clostridium	9	86	5	9	6
Cohaesibacter	66	84			1
Cohnella	28	31	42	14	27
Comamonas	320	18	131	23	1
Coprobacillus					3
Coraliomargarita	30	43	1	6	3
Corynebacterium	1679	547	507	1359	1920
Coxiella	23	37	3		3
Cupriavidus	147			34	3
Curtobacterium				349	25
Curvibacter	150	4	2		2
Cycloclasticus	254	339	52	70	20
Dechloromonas	5				2
Deferribacter	4	3	1		1
Delftia	169	139	361	366	401
Dermacoccus				26	1
Desulfobacter	4	3	2		1
Desulfofrigus	18	22	1		1
Desulfonatronum	74	124	27	6	6
Desulfotomaculum	3	6	1	37	39
Desulfovibrio	60	231	5	13	349
Desulfuromusa	1	2		3	1
Dethiosulfovibrio	24	7	3	2	3
Devosia	163	30	7	24	6
Dialister					33
Dinoroseobacter	967	5157	523	16	16
Dokdonella	5	1	1	1	23
Ectothiorhodospira	351	524	110	17	22
Ehrlichia	953	82	181	13	12

Appendix 9 (continued). Genera and 16S rRNA copy counts detected from the 12 month samples

Genera	3 d	10 d	1 m	6 m	12 m
Ekhidna	66	69	10	7	5
Enhydrobacter		24	11	11	66
Enterobacter	41	154	158	133	262
Enterococcus		8		37	1
Erwinia	21	335	7	441	3
Erythrobacter		60			1
Exiguobacterium	7	33	8		1
Ferrimicrobium	136	5	2	1	1
Fervidobacterium	3	12	2	2	1
Flammeovirga	2	7	3	1	3
Flavisolibacter		142		28	18
Flavobacterium		1			140
Gardnerella					1
Gemella	2	2		1	1
Geobacillus	291	425	386	505	323
Geodermatophilus				6	15
Glaciecola	1307	1107	229	5	6
Gluconobacter	38	17		1	4
Gordonia	2	1		1	1
Granulicella	1	1			19
Haemophilus	294	3	7		421
Haliangium	1	1			1
Archaea_Haloarcula		7		31	13
Archaea_Halobaculum					2
Halochromatium	6	10	3	1	1
Halomonas	9579	8599	5615	7005	7114
Halonotius	13	13		193	4
Archaea_Haloquadratum	5	12		74	18
Archaea_Halorhabdus	2	54	65	3	46
Archaea_Halorubrum	23	30	135	690	266
Hirschia	1500	1272	2295	783	134
Hydrocarboniphaga	94	130	20	14	11
Hydrogenophaga	1		1	4	14
Hydrogenophilus	445	25	228	133	87
Hymenobacter	59	82	17	8	61
Hyphomicrobium	75	394	40	169	1312
Hyphomonas	14564	25634	21207	3320	780
Inquilinus	14	24	3	10	10
Isoptericola	64	13	71	104	13
Janibacter		28		249	3
Jannaschia	82863	138074	17848	1312	1045
Janthinobacterium	1			1	14
Jiangella					1
Kaistobacter	11	20	2	7	18
Klebsiella	1	34	18	16	26
Kushneria	12	17	2	4	1
Kytococcus					2

Appendix 9 (continued). Genera and 16S rRNA copy counts detected in the 12 month samples

Genera	3 d	10 d	1 m	6 m	12 m
Legionella	82	99	6	14	8
Lentibacillus	16	13	17	15	21
Lewinella	112	148	23	15	14
Loktanella	152	411	68	20	8
Luteibacter	176	199	11		2
Luteimonas		3		1	1
Luteolibacter	16	28	7	2	1
Lysobacter	1				1
Macrococcus	4	6	2	1	30
Mannheimia	31	1	1	17	70
Maricaulis	7472	4626	185	112	108
Marinibacillus	394	261	435	842	515
Marinobacter	1728	7496	1050	173	45096
Marinobacterium	19	27	2		1
Marinomonas	105	236	33	3	9
Marinospirillum	273	343	27	4	1
Marivita	370	588	92	33	13
Mesorhizobium	35	51	1	2024	9
Methylibium	9	5	3	3	1
Methylobacterium	6	87	100	38	458
Methylonatrum	109	145	26	9	5
Methylophaga	250	346	56	8	4
Methylosinus	7	6	1	2	148
Microbulbifer	81031	146438	37448	772	353
Micrococcus	236	32	1	45	6
Moorella	29	41	4	125	12
Moraxella	1	4			343
Muricauda	31	39	4	1	4
Mycetocola					6
Mycobacterium	10	213	2	374	58
Nannocystis	5	10		3	1
Natronincola					1
Natronococcus	25	5	12	230	28
Nautella	138	72	62	3	2
Neisseria	5	50	4	54	1
Neorickettsia	1	4	1	1	3
Neptunomonas	611	1604	3		1
Nesterenkonia	8	53	3	6	13
Niabella	57	97	9	8	6
Nisaea	33	58	7	266	18
Nitrincola	593	1082	227	5	8
Nitrobacter	19	141	91	72	87
Nitrosococcus	32	30	7	6	1
Nocardioides	47	14	51	1	1
Nostoc	8	11	1	3	2
Novispirillum					1
Novosphingobium	1106	401	47	300	203

Appendix 9 (continued). Genera and 16S rRNA copy counts detected in the 12 month samples

Genera	3 d	10 d	1 m	6 m	12 m
Ochrobactrum	3834	135	313	249	2
Octadecabacter	299	2949	112	952	43
Oenococcus	1			2	2
Oleibacter	351399	352728	8159	39	235
Oleispira	219657	396099	108976	2095	1479
Oleomonas	7	7	4	29	32
Oscillatoria	4	1			1
Paenibacillus	72	85	33	99	1168
Paenisporosarcina	13	19	2	10	3
Paracoccus	1294	2093	584	7387	7417
Parvibaculum	559	364	2100	71882	67164
Paucibacter	6	5	25	77	5
Pectinatus	5	10		25	24
Pedomicrobium	9	48		148	82
Pelagibaca	714	4	9	204	1
Pelagicoccus	335	493	66	37	48
Pelomonas	29	20	266	558	9
Pelotomaculum	4	3			3
Peptococcus	18	10	6	29	5
Peptoniphilus	1	51	2		1
Phaeobacter	689	7391	252	29	12
Phenylobacterium	61	710	86	118	870
Photobacterium	1	15	1		1
Phycicoccus	1	1		1039	2
Phyllobacterium	3668	7697	12659	5162	27
Pilimelia				91	1
Piscibacillus	21	15	72	385	32
Planococcus	69	10	10	13	51
Planomicrobium	239	12	8	10	13
Plesiomonas	47	145	17		206
Pontibacillus	735	331	553	1054	761
Prevotella	99	5	48	2	1657
Prochlorococcus	103	40	14		4
Pseudaminobacter	5	18	2	8	1
Pseudidiomarina	71	106	25	1	6
Pseudoalteromonas	1015	1330	8	3	1
Pseudoclavibacter					1
Pseudomonas	4912	5470	2370	2048	3504
Pseudonocardia			115		5
Psychrobacter	19	33	1	1	2
Psychromonas	28	65	21		13
Ralstonia	53	308	24	64	21
Rheinheimera	2	4	1	7	212
Rhizobium	4	6	41	174	36
Rhodobacter	38	42	6	29	15
Rhodobium	94	147	26	27	19
Rhodospirillum	91	104	26	150	129
Rhodothalassium	82	61	15	61	53

Appendix 9 (continued). Genera and 16S rRNA copy counts detected in the 12 month samples

Genera	3 d	10 d	1 m	6 m	12 m
Rhodothermus	12	18	1	1	2
Rhodovibrio	5	7		2	3
Rhodovulum	1700	2507	587	6440	54
Rickettsia	2	4	1		3
Roseivivax	228	451	108	20	23
Roseomonas	100	62	12	11	9
Roseospira	605	678	297	1845	1619
Roseovarius	130	256	45	5	2
Rubellimicrobium	16	19	4	4	7
Rubritalea	16	14	4	1	1
Rubrobacter		25		5	3
Ruegeria	4109	12468	1990	770	365
Saccharopolyspora	22	14	2	42	66
Saccharospirillum	3593	2495	394	143	30
Salinibacter	38	13	21	1	1
Salinicoccus		3			2
Salinimonas	337	480	20	2	1
Sediminibacillus	239	148	150	266	179
Segetibacter	1	7			1
Selenomonas	3	1		2	1
Serinicoccus	3	13		6	51
Serratia	117	137	8	4	4
Shewanella	141	138	6	4	49
Shinella		3	1	199	3
Sinorhizobium		4		16	1
Sphingobium	22	40	9	17	142
Sphingomonas	661	4237	2013	172	81
Spirosoma					13
Sporolactobacillus	7	12		39	119
Sporosarcina	17	71	19	9	20
Staphylococcus	745	940	191	1264	2340
Stenotrophomonas	177	220	1303	125	398
Steroidobacter	167	198	36	16	9
Streptococcus	29	276	146	32	27
Streptomyces	1	2		9	1
Symbiobacterium	3	4		1	1
Telmatospirillum	556	393	1525	4206	650
Tenacibaculum	23	5	2		1
Tepidanaerobacter	2	2			2
Tepidimonas	8	21	5	145	83
Thalassobius	240	508	43	32	41
Thalassospira	2004	3988	3550	18471	274
Thauera	10	17	23	37	73
Thermoanaerobacterium	2	22	7		1
Thermobacillus	164	22	107	35	221
Thermogemmatispora	3	9	1		2
Thermus	733	400	638	1528	880
Thioalkalimicrobium	15	20	2	2	1

Appendix 9 (continued). Genera and 16S rRNA copy counts detected in the 12 month samples

Genera	3 d	10 d	1 m	6 m	12 m
Thioalkalivibrio	8	7	2		1
Thiocapsa	141	167	20	16	15
Thiorhodococcus	10	15	1		1
Thiorhodospira	106	167	31	5	4
Tolumonas	9	26	6	6	23
Treponema	7	7	8		2
Trichococcus	1	2	2	2	3
Turicibacter					1
Uliginosibacterium	7	4	1	1	1
Umboniibacter	14	22	4		1
Veillonella	2	6	1	159	23
Vibrio	1804	4690	125	3	3
Virgibacillus	618	687	728	1297	1184
Viridibacillus	1	1			1
Zhouia	4	5	1		1

References

Advanced Materials Association. (n.d.). What are microbiologically influenced corrosion (MIC) mechanisms and processes? Retrieved from http://www.advancedmaterialsassoc.com/faq-metals-corrosion-13.html

Altschul, S. F., Madden, T. L., Schäffer, A. A., Zhang, J., Zhang, Z., Miller, W., & Lipman, D. J. (1997). Gapped BLAST and PSI-BLAST: A new generation of protein database search programs. *Nucleic Acids Research*, *25*(17), 3389–3402. http://doi.org/10.1093/nar/25.17.3389

ASTM International. (1999). Standard Practice for Preparing, Cleaning, and Evaluating Corrosion Test Specimens. *Annual Book of ASTM Standards*, 15–21. http://doi.org/10.1520/G0001-03

Baird, C., Ogles, D., & Baldwin, B. R. (2016). Molecular microbiological methods to investigate microbial influenced corrosion in fully integrated kraft pulp and paper mills. In *Corrosion* (pp. 1–11). NACE International.

Bartis, J., & Lawrence Van Bibber. (2011). *Alternative fuels for military applications*. *RAND Corporation*. Retrieved from http://oai.dtic.mil/oai/oai?verb=getRecord&metadataPrefix=html&identifier=ADA536540

Bento, F. M., Beech, I. B., Gaylarde, C. C., Englert, G. E., & Muller, I. L. (2005). Degradation and corrosive activities of fungi in a diesel-mild steel-aqueous system. *World Journal of Microbiology and Biotechnology*, *21*(2), 135–142. http://doi.org/10.1007/s11274-004-3042-2

Bingham, F. M., & Lukas, R. (1996). Seasonal cycles of temperature, salinity and dissolved oxygen observed in the Hawaii Ocean Time-series. *Deep-Sea Research II*, *43*(3), 19–213. Retrieved from http://cmore.soest.hawaii.edu/members/HOTEL/1996/BinghamandLukas1996.pdf

Brislawn, C. (2014). JC_qiime_pipline. Retrieved January 1, 2014, from https://bitbucket.org/colin_brislawn/jc_qiime_pipeline/src/372d92398ff0?at=master

Brown, M. V, Philip, G. K., Bunge, J. A., Smith, M. C., Bissett, A., Lauro, F. M., … Donachie, S. P. (2009). Microbial community structure in the North Pacific ocean. *The ISME Journal*, *3*(12), 1374–86. http://doi.org/10.1038/ismej.2009.86

Caporaso, J. G., Kuczynski, J., Stombaugh, J., Bittinger, K., Bushman, F. D., Costello, E. K., … Knight, R. (2010). QIIME allows analysis of high-throughput community sequencing data. *Nature Methods*, *7*(5), 335–336. http://doi.org/10.1038/nmeth.f.303

Chavez, F. P., Messié, M., & Pennington, J. T. (2011). Marine primary production in relation to climate variability and change. *Annual Review of Marine Science*, *3*(1), 227–260.

http://doi.org/10.1146/annurev.marine.010908.163917

Craig, B. (2011). Keeping the Navy ’s green fleet from rusting. *CorrDefense Online Magazine*, *7*(1), 1–2.

DeSantis, T. Z., Hugenholtz, P., Larsen, N., Rojas, M., Brodie, E. L., Keller, K., … Andersen, G. L. (2006). Greengenes, a chimera-checked 16S rRNA gene database and workbench compatible with ARB. *Applied and Environmental Microbiology*, *72*(50), 69–72.

Diesel fuel storage and handling guide. (2014). Retrieved from www.cracao.com

Duce, R. A., & Tindale, N. W. (1991). Chemistry and biology of iron and other trace metals in the ocean. *Limnology and Oceanography*, *36*(8), 1715–1726. http://doi.org/10.4319/lo.1991.36.8.1715

Edwards, K. J., Bach, W., McCollom, T. M., & Rogers, D. R. (2004). Neutrophilic iron-oxidizing bacteria in the ocean: Their habitats, diversity, and roles in mineral deposition, rock alteration, and biomass production in the deep-sea. *Geomicrobiology Journal*, *21*(6), 393–404. http://doi.org/10.1080/01490450490485863

Eidsa, G. (1988). Corrosion products from SRB environments. In C. A. C. Sequeira & A. K. Tiller (Eds.), *Microbial Corrosion* (pp. 91–94). Elsevier Applied Science.

Elshafie, A., AlKindi, A. Y., Al-Busaidi, S., Bakheit, C., & Albahry, S. N. (2007). Biodegradation of crude oil and n-alkanes by fungi isolated from Oman. *Marine Pollution Bulletin*, *54*(11), 1692–6. http://doi.org/10.1016/j.marpolbul.2007.06.006

Focht, D. D. (1982). Advances in Microbial Ecology. In K. C. Marshall (Ed.), *Soil Science* (Vol. 134, p. 403). Boston, MA: Springer US. http://doi.org/10.1097/00010694-198212000-00014

Francis, R. (2012). Iron and carbon steel. In *The corrosion performance of metals for the marine environment: a basic guide* (pp. 3–13). Maney Publishing.

Fu, J., & Turn, S. Q. (2015). Effects of biodiesel contamination on oxidation and storage stability of neat and blended hydroprocessed renewable diesel. *Energy and Fuels*, *29*(8), 5176–5186. http://doi.org/10.1021/acs.energyfuels.5b01260

Fuel, Naval Distillate. (2006). Retrieved from http://assist.daps.dla.mil.

Gaylarde, C. C., & Beech, I. B. (1988). Molecular basis of bacterial adhesion to metals. In C. A. C. Sequeira & A. K. Tiller (Eds.), *Microbial Corrosion* (pp. 20–28). Elsevier Applied Science.

Geissler, B., Keller-schultz, C., & Keasler, V. (2015). Don’t just blame the SRBs and APBs for MIC. In *CORROSION2015* (pp. 1–12). Dallas.

Hamilton, W. A. (1998). Sulfate-reducing bacteria: Physiology determines their environmental impact. *Geomicrobiology Journal*, *15*(1), 19–28.

http://doi.org/10.1080/01490459809378059

Harayama, S., Kasai, Y., & Hara, A. (2004). Microbial communities in oil-contaminated seawater. *Current Opinion in Biotechnology*, *15*(3), 205–214. http://doi.org/10.1016/j.copbio.2004.04.002

Hassanshahian, M., Emtiazi, G., & Cappello, S. (2012). Isolation and characterization of crude-oil-degrading bacteria from the Persian Gulf and the Caspian Sea. *Marine Pollution Bulletin*, *64*(1), 7–12. http://doi.org/10.1016/j.marpolbul.2011.11.006

Hawaii Ocean Time-series (HOT). (2015). Retrieved October 8, 2012, from http://hahana.soest.hawaii.edu/hot

Hays, G. F. (2013). Now is the time. Retrieved from http://www.corrosion.org/images_index/nowisthetime.pdf

Herro, H. M. (1998). MIC myths - does pitting cause MIC? *Corrosion98*, (278), 1–20.

Heyer, A., D'Souza, F., Morales, C. F. L., Ferrari, G., Mol, J. M. C., & de Wit, J. H. W. (2013). Ship ballast tanks a review from microbial corrosion and electrochemical point of view. *Ocean Engineering*, *70*, 188–200. http://doi.org/10.1016/j.oceaneng.2013.05.005

Javed, M. A., Marić, D., Mcarthur, S. L., Stoddart, P. R., Palombo, E. A., & Wade, S. A. (2012). Comparison of the corrosion of carbon steel in natural seawaters – Evidence of MIC?, (17), 1–11.

Knothe, G. (2010). Biodiesel and renewable diesel: A comparison. *Progress in Energy and Combustion Science*, *36*(3), 364–373. http://doi.org/10.1016/j.pecs.2009.11.004

Koch, G. H., Brongers, M. P. H., Thompson, N. G., Payer, J. H., & Virmani, P. Y. (2002). *Corrosion costs and preventive strategies in the United States*. *NACE International*. Retrieved from papers2://publication/uuid/4D469A9D-07D6-4543-B217-3A15873793CF

Kõljalg, U., Nilsson, R. H., Abarenkov, K., Tedersoo, L., Taylor, A. F. S., Bahram, M., … Larsson, K.-H. (2013). Towards a unified paradigm for sequence-based identification of fungi. *Molecular Ecology*, *22*(21), 5271–5277. http://doi.org/10.1111/mec.12481

Li, S., Kealoha, J., & Hihara, L. H. (2015). Corrosion of low-carbon steel in seawater/biodiesel mixtures – a study related to the corrosion of fuel tanks in ships. In *Corrosion* (pp. 1–14). Dallas.

Little, B. J., & Lee, J. S. (2007). *Microbiologically Influenced Corrosion*. a John Wiley & Sons, Inc. Retrieved from http://onlinelibrary.wiley.com/doi/10.1002/9783527610426.bard040603/full

Little, B. J., Lee, J. S., & Ray, R. I. (2011). Microbiologically influenced corrosion: Global phenomena, local mechanisms. *Corrosion and Materials*, *36*(1), 46–51.

Little, B. J., Staehle, R., & Davis, R. (2001). Fungal influenced corrosion of post-tensioned cables. *International Biodeterioration and Biodegradation*, *47*(2), 71–77. http://doi.org/10.1016/S0964-8305(01)00039-7

Magot, M. (2005). Indigenous microbial communities in oil fields. In B. Ollivier & M. Magot (Eds.), *Petroleum Microbiology* (pp. 21–34). Washington D.C.: ASM Press.

Mahdi, L. E., Statzell-Tallman, A., Fell, J. W., Brown, M. V, & Donachie, S. P. (2008). *Sympodiomycopsis lanaiensis sp. nov*., a basidiomycetous yeast (Ustilaginomycotina: Microstromatales) from marine driftwood in Hawai'i. *FEMS Yeast Research*, *8*(8), 1357–1363. http://doi.org/10.1111/j.1567-1364.2008.00448.x

Majumder, A., & Singh, R. K. R. (2012). Role of bacteria in corrosion and assisted cracking of mild steel: A review. *Corrosion & Prevention*, *9*, 1–9.

Marty, F., Ghiglione, J.-F., Païssé, S., & Gueuné, H. (2012). Evaluation and optimization of nucleic acid extraction methods for the molecular analysis of bacterial communities associated with corroded carbon steel. *Biofouling*, *28*(April), 37–41. Retrieved from http://www.tandfonline.com/doi/abs/10.1080/08927014.2012.672644

McDonald, D., Price, M., Goodrich, J., Nawrocki, E., DeSantis, T., Probst, A., … Hugenholtz, P. (2012). An improved Greengenes taxonomy with explicit ranks for ecological and evolutionary analyses of bacteria and archaea. *International Society for Microbial Ecology*, *6*(3), 610–618.

Muyzer, G., & Stams, A. A. J. M. (2008). The ecology and biotechnology of sulphate-reducing bacteria. *Nature Reviews Microbiology*, *6*(june). http://doi.org/10.1038/nrmicro1892

NACE. (2013). *Standard Practice: Preparation, installation, analysis, and interpretation of corrosion coupons in oilfield operations* (Vol. SP0775-201).

Nergaard, M., & Grimholt, C. (2010). *An Introduction to scaling causes, problems and solutions*. Trondheim. Retrieved from http://www.ipt.ntnu.no/~jsg/undervisning/naturgass/oppgaver/Oppgaver2010/10Nergaard.pdf

O'Rorke, R., Cobian, G. M., Holland, B. S., Price, M. R., Costello, V., & Amend, A. S. (2015). Dining local: The microbial diet of a snail that grazes microbial communities is geographically structured. *Environmental Microbiology*, *17*(5), 1753–1764. http://doi.org/10.1111/1462-2920.12630

Obuekwe, C. O., Donald, W. S., Cook, F. D., & William, J. (1981). Surface changes in mild steel coupons from the action of corrosion-causing bacteria. *Applied and Environmental Microbiology*, *41*(3), 766–774.

Olsen, E., & Szybalski, W. (1949). Aerobic microbiological corrosion of water pipes. In *Microbioloical Corrosion 1* (pp. 1019–1110).

ONR. (2012). Navy Surges Toward Energy Independence. *Currents*, 1–15.

Pacific Islands Ocean Observing System. (2012). Retrieved October 8, 2012, from http://www.pacioos.hawaii.edu

Passman, F. J. (2013). Microbial contamination and its control in fuels and fuel systems since 1980 - a review. *International Biodeterioration and Biodegradation*, *81*, 88–104. http://doi.org/10.1016/j.ibiod.2012.08.002

Patil, S., Choudhary, L., & Singh, R. K. R. (2012). Influence of sulphate reducing bacteria in stress corrosion cracking of mild steel in aqueous solutions. In *Corrosion & Prevention* (pp. 1–5).

Petersen, R. B., & Melchers, R. E. (2012). Long-term corrosion of cast iron cement lined pipes. In *Corrosion & Prevention* (Vol. 23, pp. 1–12).

Prince, R. C. (2005). The microbiology of marine oil spill bioremediation. In B. Ollivier & M. Magot (Eds.), *Petroleum Microbiology* (pp. 317–336). Washington D.C.: ASM Press.

Rabus, R. (2005). Biodegradation of hydrocarbons under anoxic conditions. In B. Ollivier & M. Magot (Eds.), *Petroleum Microbiology* (pp. 277–300). Washington D.C.: ASM Press.

Ray, R. I., Lee, J. S., & Little, B. J. (2010). Iron-oxidizing bacteria: A review of corrosion mechanisms in fresh water and marine environments. In *Corrosion*. National Association of Corrosion Engineers. Retrieved from http://oai.dtic.mil/oai/oai?verb=getRecord&metadataPrefix=html&identifier=ADA526447

Revie, R. W., & Uhlig, H. H. (2008). *Corrosion and corrosion control: An introduction to corrosion science and engineering*. *British Corrosion Journal* (4th ed., Vol. 7). Hoboken: John Wiley & Sons, Inc. http://doi.org/10.1179/000705972798323134

Riser, S. C., & Johnson, K. S. (2008). Net production of oxygen in the subtropical ocean. *Nature*, *451*(7176), 323–5. http://doi.org/10.1038/nature06441

Rueckert, A., & Morgan, H. W. (2007). Removal of contaminating DNA from polymerase chain reaction using ethidium monoazide. *Journal of Microbiological Methods*, *68*(3), 596–600. http://doi.org/10.1016/j.mimet.2006.11.006

Schwartz, M., Blakeley, K., & O'Rourke, R. (2012). *Department of Defense energy initiatives : Background and issues for Congress*. Retrieved from https://www.fas.org/sgp/crs/natsec/R42558.pdf

Singh, A., Sharma, C., & Lata, S. (2008). Microbial influenced corrosion due to *Desulfovibrio desulfuricans*. *Anti-Corrosion Methods and Materials*, *58*(6), 315–322. http://doi.org/10.1108/00035591111178873

Smith, D. P., & Peay, K. G. (2014). Sequence depth, not PCR replication, improves ecological inference from next generation DNA sequencing. *PLoS ONE*, *9*(2).

http://doi.org/10.1371/journal.pone.0090234

Suflita, J. M. (2013). Biocorrosion in the diesel fuel infrastructure: Impact of ultra low sulfur diesel, fatty acid methyl esters and select alternative fuels. In *Corrosion* (pp. 1–47). Boulder.

Trench, C. J., & Kiefner, J. F. (2001). *Oil pipeline characteristics and risk factors: Illustrations from the decade of construction*.

Usher, K. M., Kaksonen, A. H., Cole, I., & Marney, D. (2014). Critical review: Microbially influenced corrosion of buried carbon steel pipes. *International Biodeterioration and Biodegradation*, *93*, 84–106. http://doi.org/10.1016/j.ibiod.2014.05.007

Usher, K. M., Kaksonen, A. H., & MacLeod, I. D. (2014). Marine rust tubercles harbour iron corroding archaea and sulphate reducing bacteria. *Corrosion Science*, *83*, 189–197. http://doi.org/10.1016/j.corsci.2014.02.014

van Beilen, J. B., & Witholt, B. (2005). Diversity, function, and biocatalytic applications of alkane oxygenases. In B. Ollivier & M. Magot (Eds.), *Petroleum Microbiology* (pp. 259–276). Washington D.C.: ASM Press.

Varnam, A. H., & Malcolm, E. G. (2000). *Enivironmental Microbiology* (Illustrate). CRC Press.

Videla, H. A., & Herrera, L. K. (2005). Microbiologically influenced corrosion: looking to the future. *International Microbiology : The Official Journal of the Spanish Society for Microbiology*, *8*(3), 169–80. Retrieved from http://www.ncbi.nlm.nih.gov/pubmed/16200495

von Wolzogen Kuhr, C. A. H., & van der Vlugt, L. S. (1934). De grafiteering van gietijzer als electro biochemisch proces in anaerobe gronden. *Water*, *18*, 147–165.

Wang, L., Wang, W., Lai, Q., & Shao, Z. (2010). Gene diversity of CYP153A and AlkB alkane hydroxylases in oil-degrading bacteria isolated from the Atlantic Ocean. *Environmental Microbiology*, *12*(5), 1230–1242. http://doi.org/10.1111/j.1462-2920.2010.02165.x

Weinberg, E. D. (1989). Cellular regulation of iron assimilation. *The Quarterly Review of Biology*, *64*(3), 261. http://doi.org/10.1086/416359

Welikala, S. R., Singh, R. K. R., Gates, W. P., & Panter, C. (2012). Role of biofilms of sulfate reducing bacteria in electrochemical corrosion of steel. *NACE International*, 1–10.

Witherby & Co. Ltd. (2002). *Guidelines for Ballast Tank Coating Systems and Surface Preparation*. London.

Yakimov, M. M., Giuliano, L., Gentile, G., Crisafi, E., Chernikova, T. N., Abraham, W. R., … Golyshin, P. N. (2003). *Oleispira antarctica* gen. nov., sp. nov., a novel hydrocarbonoclastic marine bacterium isolated from Antarctic coastal sea water. *International Journal of Systematic and Evolutionary Microbiology*, *53*(3), 779–785.

http://doi.org/10.1099/ijs.0.02366-0

Yoon, J. J. (2009). *What's the difference between biodiesel and renewable (green) diesel*. Advanced Biofuels USA.

Zhu, X., Lubeck, J., & Kilbane, J. (2003). Characterization of microbial communities in gas industry pipelines. *Applied and Environmental …*, *69*(9). http://doi.org/10.1128/AEM.69.9.5354